**Charles University in Prague**

**Faculty of Science**

Program: Immunology


**Mgr. Jan Dobeš**

# Novel Mechanisms Regulating Immune Tolerance and Homeostasis in the Intestine

Nové regulační mechanismy imunitní tolerance a homeostázy ve střevě

Ph. D. Thesis

Supervisor: RNDr. Dominik Filipp, CSc.

Prague, 2015

**Declaration**

I hereby declare that my thesis is a presentation of my original research work. Wherever contribution of others is involved, every effort is made to indicate this clearly, with reference the literature. This thesis contains no material that has been submitted previously, in whole or in part, for the award of any other academic degree or diploma.

Prague, 6th of October, 2015

**Prohlášení**

Prohlašuji, že jsem závěrečnou práci zpracoval samostatně a že jsem uvedl všechny použité informační zdroje a literaturu. Tato práce ani její podstatná část nebyla předložena k získání jiného nebo stejného akademického titulu.

V Praze, 6. 10. 2015

Podpis (Signature):

## ACKNOWLEDGEMENTS

I would like to thank all the people that made accomplishment of this thesis possible. My thanks belongs to Dominik Filipp, my supervisor, for the great opportunity to work in his laboratory on the attractive scientific topic and for his enthusiastic admittance. I would like to acknowledge all members of the Laboratory of Immunology, especially Martina Dobešová, Matouš Vobořil, Jana Balounová and Aleš Neuwirth for their help, suggestions and critical comments. My thanks belongs also to members of Laboratories of Leukocyte Signalling and Cell and Developmental biology, especially to Aleš Drobek, Lucie Tůmová, Jitka Stančíková, Tomáš Brdička and Vladimír Kořínek. I also give my thanks to Zdeněk Cimburek for his excellent FACS sorting assistance. Lastly, but importantly, my deep thanks also go to my wife, parents and family for their love, support and encouragement.

## ABSTRACT

Immune tolerance to host own tissues and cells is the fundamental attribute of properly working immune system. The repertoire of effector T-cells, which possess randomly generated antigen-specific receptors, is during their development shaped by central immune tolerance to retain only those specificities which do not recognize self-antigens. In addition, various mechanisms of peripheral tolerance keep in check potentially self-reactive cells which escaped from the protective mechanism of central tolerance. Thus, a tight regulation of tolerance, operating at several anatomical places in the host body, collectively imposes immune homeostasis and well-being of the organism. The breach of central tolerance can have far reaching consequences, as demonstrated by mutations in *Autoimmune regulator* gene. These mutations lead to the development of severe autoimmune disease, comprising several clinical components, gastrointestinal-associated symptoms including. We have shown, that in the absence of Autoimmune regulator, the occurrence of gastrointestinal symptoms is associated with the loss of thymic-mediated central tolerance to enteric α-defensins, essential antimicrobial peptides produced by intestinal Paneth cells. The loss of tolerance leads to the escape of defensin-specific T-cells to immune periphery and consequently, to their attack on Paneth cells, resulting in their diminishment. This, in turn, impacts the composition of intestinal microbiota, affecting the polarization of T-cells in the gut towards Th17 phenotype which further provides a milieu supporting inflammatory autoimmunity and perturbations in intestinal homeostasis. Moreover, we showed the importance of several members of Wnt signaling cascade in the regulation of intestinal homeostasis and their impact on immune-mediated dysfunction of intestinal epithelia.

# ABSTRAKT

Jednou ze základních vlastností správně fungujícího imunitního systému je udržování tolerance ke tkáním tělu vlastním. Centrální tolerance zabezpečuje odstranění T-buněčných klonů nesoucích antigenně specifické receptory schopné rozeznat antigeny produkované tělu vlastními tkáněmi. Rozličné mechanismy periférní tolerance následně zabezpečují kontrolu nad potenciálně autoreaktivními buňkami, které nebyly v brzlíku odstraněny během ustanovení centrální tolerance. Správné nastavení a regulace tolerogenních procesů je tedy důležitým homeostatickým mechanismem organismu. Narušení centrální tolerance má dalekosáhlé důsledky, což může být dokumentováno mutacemi v genu kódujícím *Autoimunitní regulátor*. Tyto mutace vedou k rozvoji vícesložkového autoimunitního onemocnění, které postihuje i gastrointestinální trakt. Tato práce popisuje spojitost mezi absencí Autoimunitního regulátoru a ztrátou centrální tolerance k antimikrobiálním produktům Panethových buněk – enterickým α-defensinům. Ztráta tolerance vede k úniku defensin-reaktivních T-buněk mimo brzlík a následně k jejich útoku na Panethovy buňky. Tento proces má za následek snížení počtu Panethových buněk, což vede ke změnám ve složení střevní mikroflóry a polarizaci T-buněčné odpovědi ve střevě ve směru k Th17 prozánětlivým buňkám, které mohou dále negativně ovlivňovat střevní homeostázu. Předkládaná práce navíc poukazuje na důležitost několika komponent Wnt signální kaskády v udržování střevní homeostázy a jejich vliv na některé imunitní mechanismy zprostředkované tímto epitelem.

## TABLE OF CONTENTS

## LIST OF ABBREVATIONS

| | |
|---|---|
| Aire | Autoimmune regulator, the most powerful gene in the immune system |
| Axin | Axis inhibitory protein |
| Apc | Adenomatous polyposis coli |
| APC | Antigen presenting cell |
| APECED | Autoimmune polyendocrinopathy-candidiasis-ectodermal dystrophy |
| AMP | Antimicrobial peptide |
| CBC | Crypt base columnar cell |
| Ck1 | Casein kinase 1 |
| cTEC | Cortical thymic epithelial cell |
| DC | Dendritic cell |
| Dll | Delta-like ligand |
| DN | Double negative |
| DP | Double positive |
| Dvl | Dishevelled |
| EEC | Enteroendocrine cell |
| Egf | Epidermal growth factor |
| FRC | Fibroblastic reticular cell |
| GALT | Gut-associated lymphoid tissue |
| GC | Goblet cell |
| Gsk3 | Glycogen synthetase kinase 3 |
| HEL | Hen egg lysozyme |
| Hic1 | Hypermethylated in cancer 1 |
| iAPC | Intestinal antigen presenting cell |

| | |
|---|---|
| IBD | Inflammatory bowel disease |
| ILC | Innate lymphoid cells |
| iSCs | Intestinal stem cells |
| Lgr5 | Leucine-rich repeat containing G-protein 5 |
| LNSC | Lymph node stromal cell |
| Lrp | Lipoprotein receptor-related protein |
| M-cell | Microfold cell |
| mLN | Mesenteric lymph node |
| Mmp7 | Matrix metalloproteinase 7 |
| mTEC | Medullary thymic epithelial cell |
| Nkd1 | Naked cuticle homolog 1 |
| OVA | Ovalbumin |
| PC | Paneth cell |
| pMHC | peptide-major histocompatibility complex |
| SFB | Segmented filamentous bacteria |
| SP | Single positive |
| sIg | Secretory immunoglobulin |
| TC | Tuft cell |
| Tcf | T-cell factor protein |
| TCR | T-cell receptor |
| TRA | Tissue restricted antigen |
| Treg | T-regulatory cell |

# LITERATURE OVERVIEW

## 1. INTRODUCTION

The gastrointestinal tract is an internal organ of our body specialized in digestion of food, uptake of nutrients and re-absorption of water. It forms a physical barrier between its luminal content and the host's own body. The tract itself represents probably the largest surface area capable of a direct contact with foreign particles and pathogens (Mowat and Agace, 2014) as the surface of human small intestine alone is estimated to be larger than 300 $m^2$ (Moog, 1981). Intestine is continuously exposed to a large amount of foreign antigenic material, processing more than one hundred gram of dietary proteins per day (Brandtzaeg, 1998). Intestine also accommodates a large amount of microbes whose load increases along the gut, reaching $10^{12}$ bacteria per gram of gut content in the colon (Macfarlane and Macfarlane, 1997). Their overall absolute number of one hundred trillions dramatically outnumbers the host own cells (Pabst and Mowat, 2012) and hence, for the host, they represent inflammatory and infectious threats with deadly potential. If the intestinal content of the gut leaks into circulation, experimental mice survive no more than several hours (Buras et al., 2005). Thus, taking into account that mucosal barrier is relatively thin and intestinal epithelium is formed by a single layer of epithelial cells, affording intestine with powerful immune mechanisms capable of maintaining intestinal homeostasis is the essential requirement for the host well-being.

Evolutionary, in single cell organisms with immune system, such as Amoeba, both immune function and nutritive function rely on phagocytosis. These functions are indistinguishable in the initial phase and differ only by the outcome (Chen et al., 2007). That suggests tight coevolution of digestive and immune system. During the evolution of multicellular organisms, the initial extracellular digestion was replaced by an invagination forming one-way digestive system, which prevented losses of digested nutrients. Later, this evolutionary innovation developed into digestive tube with two openings. Such organ created a niche which was colonized by microbes that led to several possible scenarios of the host and colonizer interactions. Notably, microbes can be used as the source of nutrients, or host can create a beneficial association with them, or employ the innate immune system to regulate their number or to identify potentially dangerous ones. The appearance of adaptive immune system brings another layer of complexity to regulate and monitor the interactions between intestinal microbiota and the local immune system (Broderick, 2015).

Immune system in the gut must discriminate between harmful and pathogenic intruders on one side and antigens derived from ingested food and commensal microbiota, on the other. Virtually any antigenic specificity is generated by a genetic recombination of B- and T-cell antigen sensing receptors. However, because these specificities are

generated without regard to their target, i.e. foreign (non-self) versus endogenous (self) antigens, efficient tolerogenic processes occurring in the thymus and immune periphery play irreplaceable role in shaping the receptor repertoire of lymphocytes that are prone to elicit immune responses in the periphery. Indispensability of these processes can be documented by the autoimmune diseases originating from active immune responses against food antigens, microbiota, or critical cellular and molecular structures of gut epithelium (Pabst and Mowat, 2012).

In the presented thesis, first, mechanisms of immune tolerance which are controlling T-cell repertoire are reviewed, commencing with T-cells development in the thymus. Specifically, essential cellular and molecular players in positive and negative thymic selection are highlighted, followed by the description of mechanisms of peripheral tolerance with emphasis on acquired tolerance to orally administrated antigens or to microbiota. The immune function of the intestinal epithelium focusing on antimicrobial peptide (AMP)-secreting Paneth cells (PCs) and the specific role of components of hematopoietic intestinal immune system is described. The last part of the literature overview is devoted to the development of intestinal epithelium and irreplaceable role of Wnt signaling cascade in this process.

# 2. IMMUNE TOLERANCE

Immune tolerance is defined as the state of unresponsiveness to the antigen which itself display the capacity to elicit the immune response. Immune tolerance is divided according to the place where it is established to: i) central tolerance (thymus for T-cells, bone-marrow for B-cells) and ii) peripheral tolerance (immune periphery).

## 2.1. Central Tolerance

Bone-marrow derived T-cell precursors migrate into the thymus to undergo their developmental program, which is accomplished by the generation of functional T-cell receptors (TCRs). The generation of TCR diversity is directed by the process of VDJ recombination whereby the random rearrangement of defined gene segments leads to the production of a large pool of TCRs with distinct antigenic specificities (Stritesky et al., 2012). Ultimately, thymic developmental program establishes the pool of "useful and not harmful" TCR antigenic specificities directed towards non-self epitopes, including those encoded by pathogens. However, VDJ recombination also leads to the generation of "useless or potentially dangerous" T-cell clones bearing TCRs which are unable to recognize peptide-major histocompatibility complexes (pMHCs) or TCRs which are able to recognize host-encoded self-antigens and thus having the potential to be self-reactive. Thymocytes with this useless or dangerous TCR specificities are efficiently removed during T-cell thymic development by the process of central tolerance (Klein et al., 2009; von Boehmer et al., 1989).

The fate of developing T-cells in the thymus is determined by the interaction of their newly generated TCRs with pMHC complexes on the surface of thymic antigen presenting cells (APCs). Clearly, the peptide presented by MHC and its source are the key parameters. First, developing T-cells in double-positive (DP) stage (DP T-cells co-express CD8 and CD4 molecules) undergo positive selection in the thymic cortex, where they interact with cortical thymic epithelial cells (cTECs) expressing both MHC class I and II molecules. Depending on the TCR's ability to interact with MHC class I or II molecule, developing thymocytes become CD8 or CD4 positive (Klein et al., 2014). Only T-cells which are able to sense peptides presented by MHC molecules proceed to the medullary part of the thymus, where are they subjected to the process of negative selection. Negative selection is a critical event for the removal of T-cells with the ability to recognize self-antigens. The pathway describing the developing thymocyte journey through the thymus is schematically visualized in Fig. 1.

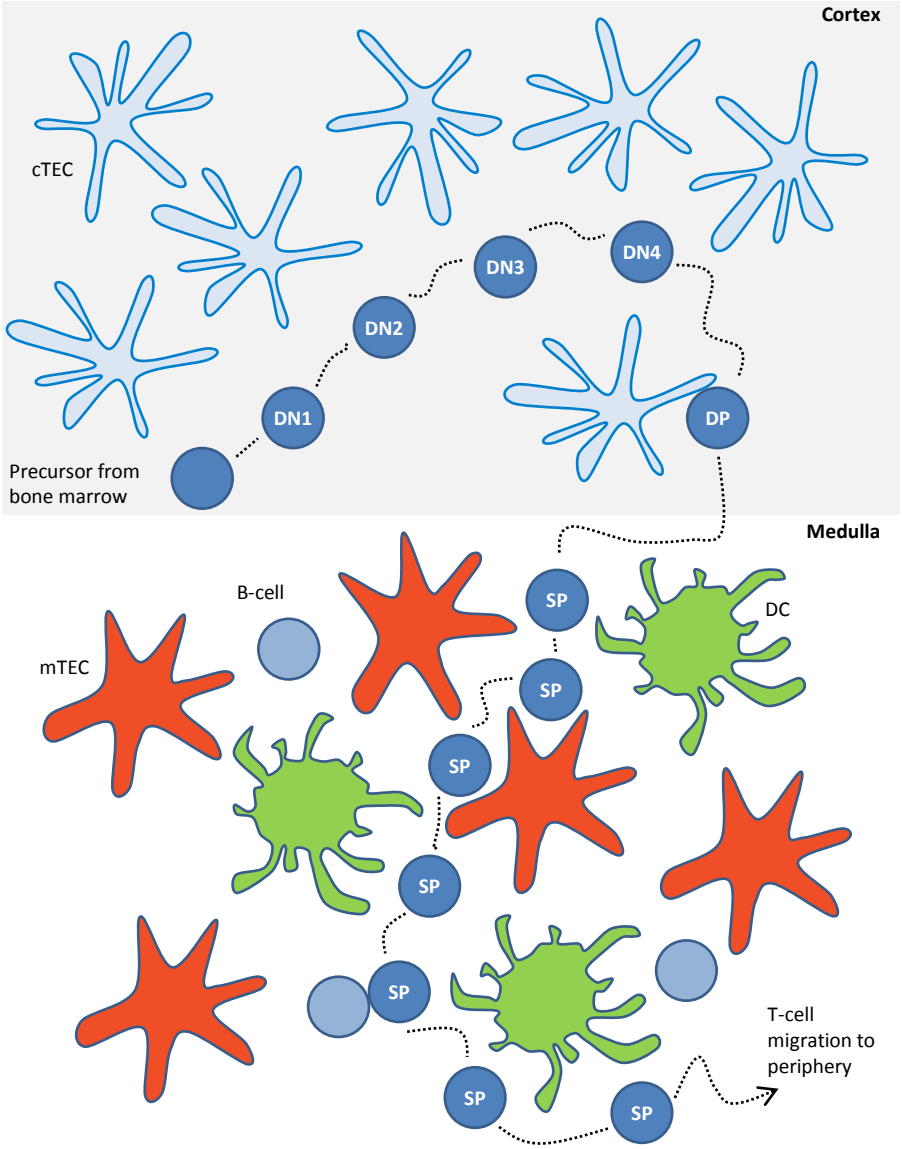


**Figure 1.** The scheme of T-cell development in the thymus and its interactions with several types of APCs. Double negative (DN) T-cell, which is not expressing CD4 nor CD8 co-receptor molecules, is undergoing TCR rearrangement (from DN1 to DN4 stage). T-cell clones with successfully rearranged TCR start to express both CD8 and CD4 molecules (DP stage) and test their ability to interact with host encoded MHC molecules by a direct contact with cTECs, resulting in the single positive (SP) stage. These T-cells translocate to the medulla, where they interact with several APCs in order to eliminate potentially self-reactive T-cells (Klein et al., 2014). It is estimated that a developing thymocyte remains in the medulla for 4-5 days during which it performs several hundred interactions with various APCs (Klein, 2009).

### 2.1.1. Positive selection

Approximately ninety percent of developing T-cells die during the process of positive selection by neglect as they fail to receive any rescuing positive signals via their TCR from the interaction with pMHC complexes and proceed to apoptosis (Klein et al., 2009). The nature and identity of peptides mediating positive selection remains still elusive. Two possible scenarios elucidating their generation were postulated: i) cTECs present generic epitopes derived from ubiquitously expressed peptides, ii) cTECs present unique epitopes from ubiquitously expressed peptides. The latter proposition was termed the "private" or "altered" peptide hypothesis and it is supported by the usage of unconventional protein-processing pathway in cTECs to generate pMHC complexes.

Concerning MHC class I presentation, instead of proteasome subunit β5 which is the integral part of conventional proteasome or β5i subunit (immunoproteasome), cTECs use a unique β5t subunit. β5t enforces so-called thymoproteasome cleavage activity with different substrate specificities in comparison to proteasome and immunoproteasome (Florea et al., 2010). Moreover, β5t subunit deficiency leads to changes in the selection parameters of $CD8^+$ T-cells (Murata et al., 2007).

MHC class II peptide presentation pathway is altered in cTECs by the expression of unique Cathepsin L (Nakagawa et al., 1998) and thymus-specific serine protease (Gommeaux et al., 2009). The deficiency in these proteases leads to inappropriate selection of $CD4^+$ T-cells (Gommeaux et al., 2009; Nakagawa et al., 1998). Interestingly, $CD4^+$ T-cells which escape from positive selection are largely deleted during negative selection in Cathepsin L deficient animals (Nakagawa et al., 1998), suggesting that epitopes generated by conventional MHC-loading pathways are not generated and presented by cTECs MHC molecules in normal, genetically unchanged conditions.

Cortical TECs also use an alternative form of peptide acquisition as they employed autophagy to process and present internally produced peptides on MHC class II molecules. Autophagy blockage leads into the alteration of the selection output in several transgenic murine strains (Nedjic et al., 2008).

In aggregate, accumulated data suggest that cTECs present a set of unique epitopes derived from ubiquitously expressed proteins in order to determine solely the ability of newly generated TCR to interact with MHC molecules encoded by the host. Nevertheless, it is of note that the nature and structural characteristics of "peptidome" presented by cTECs on their MHC molecules was not precisely determined so far.

### 2.1.2. Negative selection

The hallmark of the negative selection process is the removal of potentially self-reactive T-cells, i.e. those T-cells which, in the medulla region of thymus recognize self-antigens presented in the context of MHC molecules. Several types of cells residing or passing through the medulla affect this process: medullar thymic epithelial cells (mTECs), dendritic cells (DCs), B-cells, macrophages and granulocytes. While the role of macrophages and granulocytes in negative selection is poorly defined, the involvement of mTECs, DCs and B-cells in this process was convincingly demonstrated. A unique subpopulation with surprising capacity to produce and present virtually any protein epitope expressed in the immune periphery (so called tissue restricted antigens; TRAs) by the process of promiscuous gene expression is represented by mTECs (Derbinski et al., 2001; Kyewski et al., 2002). Promiscuous gene expression violates several rules strictly employed to regulate gene expression: i) tissue-specific genes whose expression is tightly controlled by complex and distinct biochemical pathways are expressed in rather stochastic combination in single mTEC (e.g. insulin 2, normally produced in the immune periphery by pancreatic islet β-cells and intestinal fatty acid binding protein produced by enterocytes); ii) developmentally regulated genes are expressed by mTECs without any causal connection to the developmental status of the organism (e.g. alpha-fetoprotein – physiologically produced only by the embryonic yolk sac and fetal liver produced in the mTECs of adult animals) (Derbinski et al., 2001) or iii) sex-specific genes are produced irrespectively of the organism`s gender (e.g. lactating breast`s caseins (Derbinski et al., 2008) or prostate antigens produced by mTECs in both males and females (Malchow et al., 2013). A single mTEC seems to produce from 100 up to 300 TRAs, while a single TRA is in general produced only by 1-3% of mTECs (Klein et al., 2009).

Autoimmune regulator (Aire) is the only regulator identified so far with the ability to induce the expression of substantial proportion of TRAs. Thus, at least two patterns of TRAs expression can be observed: (i) Aire-dependent TRA expression (including diabetes associated self-antigens insulin 2 or glutamic decarboxylase 2), and (ii) Aire-independent TRA expression (glutamic decarboxylase 1, C-reactive protein) (Anderson et al., 2002; Derbinski et al., 2005). Aire is promoting the expression of TRAs by binding and subsequent activation of silenced chromatin (Koh et al., 2008) coupled with unleashing the stalled RNA polymerase (Giraud et al., 2012). Aire is serving as a docking or scaffold protein for a large complex of interacting proteins including those responsible for chromatin binding, transcriptional activation and RNA splicing (Abramson et al., 2010).

Mutations in the *Aire* gene lead to severe autoimmune disease caused by the absence of Aire-regulated TRAs expression in the thymus. This results in an ineffective removal of self-reactive (TRA-specific) T-cells in the thymus and their escape to immune periphery (Anderson et al., 2002; Hubert et al., 2009; Ramsey et al., 2002). This, in turn, can lead to the destruction of host cells producing the self-antigens for which these

T-cells are self-specific (DeVoss et al., 2006; Gavanescu et al., 2007), induction of the devastating local inflammation (Anderson et al., 2002) or to providing help to self-reactive B-cells which produce autoantibodies with blocking function (Kisand et al., 2010). Human patients with AIRE-deficiency develop the autoimmune disease called autoimmune polyendocrinopathy-candidiasis-ectodermal dystrophy (APECED), which is reviewed in more details in next chapter.

The recognition of TRA-derived epitope by self-reactive TCR in the thymus leads to the deletion of self-reactive T-cell. In the study of Liston *et al.* using transgenic expression of "neo-self-antigen" (hen egg lysozyme epitope, HEL) under the insulin promotor, deletion of HEL-specific T-cells in the thymus clearly occurred. HEL neo-self-antigen is specifically expressed by Aire-positive mTECs, because these cells, due to the ability of Aire to activate insulin promoter, are also the exclusive source of insulin in the thymus. Crossing of HEL transgenic mice with Aire-deficient mice leads to the decrease of HEL expression in mTECs and to inability to delete HEL-specific T-cells which then proceed to the immune periphery (Liston et al., 2003).

In the case of $CD4^+$ T-cells, a high affinity-based recognition of TRA-epitope by self-reactive T-cell might lead to the conversion (or lineage deviation) of this cell into $Foxp3^+$ T-regulatory cell (Treg). This process of lineage conversion was revealed by the use of mice with transgenic expression of hemagglutinin or ovalbumin (OVA) under Aire promotor and the use of hemagglutinin or OVA specific T-cells (Aschenbrenner et al., 2007). Malchow *et al.* showed that prostate antigen specific MJ23 $Foxp3^+$ Tregs, which are enriched in the prostate cancer tissue, are converted to Treg lineage intrathymically in Aire-dependent manner (Malchow et al., 2013).

Despite their robust capacity to express TRAs, mTECs are not the only cells, which mediate negative selection in the thymus. DCs are the second subset integrated to this process. At least three subtypes of DCs can be distinguished in the thymus – classical (conventional) subset further divided to resident ($CD8\alpha^+$, $Sirp\alpha^-$) and migratory ($CD8\alpha^-$, $Sirp\alpha^+$) cells and plasmacytoid DCs (Li et al., 2009).

Thymic resident DCs are highly efficient in the cross-presentation of antigens (Proietto et al., 2008) and due to XCL-1 chemokine gradient co-localize in the medulla with mTECs. XCL-1 is produced exclusively by mTECs in Aire-dependent manner and XCL-1 deficient animals have lower numbers of DCs localized in medulla (Lei et al., 2011). Cross-presentation by DCs of mTEC-expressed transgenic neo-self antigens, mimicking the TRAs expression, contribute to $CD8^+$ T-cell tolerance. Moreover, the ablation of MHC class II expression on hematopoietic cells was shown to impair the negative selection of $CD4^+$ T-cell restricted epitope derived from interphotoreceptor retinoid-binding protein (expressed as TRA in mTECs in Aire-dependent manner) (Taniguchi et al., 2012). In general, it suggests that resident DCs are positioned in a close proximity to mTECs and thus gain an access to mTECs-derived TRAs which they can indirectly present and thereby increase the statistical frequency that self-reactive T-cells encounter particular cognate self-antigen.

Migratory DCs can home to the thymus loaded by antigens acquired in peripheral tissues or with blood-borne antigens (Atibalentja et al., 2009; Baba et al., 2012). Such migration is guided in CCR2-dependend manner (Baba et al., 2009) and it is prevented when migratory DCs acquire activated phenotype via Toll-like receptor ligation (Bonasio et al., 2006).

The last DC subset in the thymus are plasmacytoid DCs. These cells are well known for their antiviral, interferon type I-based responses (Reizis et al., 2011) and their poor antigen presenting capacities (Villadangos and Young, 2008), suggesting that they are not involved in negative selection. Surprisingly, and in contrast to previous notion, plasmacytoid DCs loaded with OVA translocate into the thymus in CCR9 dependent fashion, where they mediate negative selection of OVA-specific OTII $CD4^+$ T-cell (Hadeiba et al., 2012). As the CCR9 is also important for the migration into the intestine, one can speculate, if plasmacytoid DCs are able to obtain food antigens or antigens from commensal microbiota and transfer them to the thymus for induction of central tolerance.

Thymic B-cells, which are in comparison to steady-state peripheral B-cell highly positive for MHC class II molecule and costimulatory molecules CD80 and CD86 (Ferrero et al., 1999), are also able to mediate negative selection (Frommer and Waisman, 2010). Interestingly, a small proportion of thymic B-cells (approx. 3%) expresses Aire on protein level. Microarray comparison of Aire-deficient and wild-type B-cells revealed, that B-cells are also expressing several hundred TRAs. As many of them are exclusive for B-cells in comparison to mTECs, it suggests that Aire promotes TRAs expression in cell dependent manner (Yamano et al., 2015).

Interactions with several thymic APCs populations determine the fate of developing thymocytes. Although, a sophisticated thymic cellular machinery is employed to delete self-reactive T-cells, ultimately, some of them escape to immune periphery (Kim et al., 2007), where their numbers, mode of persistence and activation status are controlled by additional mechanisms of peripheral tolerance, which are reviewed in the chapter 2.2.

### 2.1.3. APECED

APECED (OMIM: 240300) is the autoimmune disease caused by mutations in *AIRE* gene (Consortium, 1997; Nagamine et al., 1997). This monogenic disease is inherited in autosomal recessive (loss-of-function mutations in both alleles) (Kisand and Peterson, 2015) or dominant manner (defective AIRE oligomerizes with intact one and oligomer losses its function) (Oftedal et al., 2015). Both types of mutations differ in their frequency across populations and in the severity of disease clinical components (see below). While the frequency of "autosomal recessive" APECED is quite low, it persists with a higher prevalence in historically isolated populations: Iranian Jews 1:9000 (Zlotogora and Shapiro, 1992), Sardinians 1:14000 (Rosatelli et al., 1998) and Finns

1:25000 (Perheentupa, 2006). The "dominant" form of APECED has a dramatically higher prevalence (1:1000) as determined by sequencing of *AIRE* gene in mixed populations (Oftedal et al., 2015). Distinct components of APECED disease are mucocutaneous candidiasis, hypoparathyroidism and Addison's disease, presented in vast majority of patients. Other components, such as type 1 diabetes, vitiligo and alopecia or gastrointestinal components are presented in lower frequency (approx. 25% of patients). Patients accumulate up to ten disease components during their life (Perheentupa, 2006). Disease components in patients bearing dominant *AIRE* mutation might be the same, but their overall number accumulated in a single patient over time seems to be lower, leading to a typically milder form of the disease (Oftedal et al., 2015).

Gastrointestinal components of APECED affects 25-30% of patients. Pernicious anemia and chronic atopic gastritis are associated with autoantibodies directed against intrinsic factor and parietal cells (Perheentupa, 2006). Diarrhea, constipation and malabsorption have several potential causes – chronic gastrointestinal candidiasis, hypocalcemia or overall nutritional deficiencies (Kluger et al., 2013; Perheentupa, 2006). Interestingly, although a low number of APECED intestinal biopsies are available, patients suffering from gastrointestinal symptoms of APECED have lymphocyte infiltrates with a major $CD8^+$ T-cell population observable in their gut (Scarpa et al., 2013), suggesting that some gastrointestinal disease components have autoimmune undertone. Indeed, enteroendocrine cells (EECs) which produce tryptophan hydroxylase (Ekwall et al., 1998; Soderbergh et al., 2004) and histidine decarboxylase enzymes, were shown to be cellular targets for intestinal autoimmune attacks (Skoldberg et al., 2003). Intestinal EECs were completely absent in some APECED intestinal biopsies (Posovszky et al., 2012) and their absence was associated with constipation. Such outcome is not surprising as EECs produce essential mediators affecting peristaltic movement of the gut and the fluidity of its content (Kluger et al., 2015). Importantly, the cross reactivity of sera obtained from APECED patients to PCs secretory granules and goblet cells (GCs) was also reported, suggesting that PCs and GCs might be also the target of autoimmune attack in the intestine (Ekwall et al., 1998; Kluger et al., 2015).

## 2.2. Peripheral tolerance

Peripheral tolerance is mediated by several processes and mechanisms responsible for keeping self-reactive T-cells which escaped from the thymus negative selection in check. Immune mechanisms and their functional relevance to the induction of gut tolerance, tolerance to microbiota or tolerance to ingested food antigens are described below.

Antigen sequestration describes the state when (i) the levels of self-antigen is too low to elicit immune response, or (ii) self-antigen is not seen by the immune system due to anatomical constrains, or (iii) the antigen is localized to immunologically privileged sites. While the first two possibilities are rather conceptual, the notion of immune privilege site is applicable in the case of brain, cornea, anterior chamber of the eye, testes and pregnant uterus. Immune responses and immune surveillance in these places are not completely abrogated, but the proinflammatory response, which can target or even damage these vitally important organs, is largely blocked. The entry of T-cells into privilege site is obstructed by the expression of several apoptosis-inducing molecules, such as Trail or Fas-ligand, and the effector function of T-cells is, in addition, suspended by the secretion of tolerogenic IL-10 and TGF-β cytokines (Forrester et al., 2008; Niederkorn, 2006). Importantly, the protection by immune privilege mechanism is breach-able as can be documented by autoimmune responses against brain-derived myelin which leads to the development of experimental multiple sclerosis (Greter et al., 2005). Although gastrointestinal tract itself is not generally considered as immune privilege site, the gut tissue is, in comparison to other tissues, highly tolerogenic, especially due to high levels of IL-10 and TGF-β produced by both hematopoietic and epithelial cells (Forrester et al., 2008).

The second peripheral tolerance mechanism is based on anergy, the state of long term hyporesponsiveness or unresponsiveness to antigen after its recognition in MHC context without proper co-stimulation (Hawiger et al., 2001; Liu et al., 2002). DCs are highly specialized in the antigen uptake and they commonly phagocyte death cells and present their antigens (Liu et al., 2002). In steady-state conditions, without the stimulation through pattern recognition receptors, DCs express only basal levels of co-stimulatory molecules CD80 and CD86 and retain tolerogenic potential (Steinman et al., 2003). Tolerogenic DCs can also mediate the conversion of $CD4^+$ T-cells into peripheral $Foxp3^+$ Tregs (Kretschmer et al., 2005).

Third, the immune suppression mediated by $Foxp3^+$ Tregs of thymic or peripheral origin is probably the most powerful mechanism employed by peripheral tolerance. Mutations in $Foxp3^+$ result in the absence of Treg lineage, leading to fatal autoimmune diseases in both human patients and experimental animal models. This suggests that certain amount of self-reactive T-cells, able to mount an autoimmune response is constantly present in the immune periphery (Kim et al., 2007; Wing and Sakaguchi, 2010). Tregs use several mechanism to control or block T-cell activation or proliferation process. For example, the constitutive upregulation of CD25 (subunit of IL-2 receptor) equips

Tregs with competitive advantage in the race with effector T-cells for IL-2, consequently, effective IL-2 deprivation then ceases the proliferation of effector T-cells (Fontenot et al., 2005). In addition, Tregs not only secrete tolerogenic cytokines (Josefowicz et al., 2012), but also express CD39 and CD73, ectoenzymes with the ability to metabolically produce cyclic adenosine monophosphate, which inhibits the proliferation of effector T-cells and also negatively impacts the activation of DCs (Deaglio et al., 2007). Other tolerogenic mechanisms imposed by Tregs include CTLA4-mediated suppression (Takahashi et al., 2000), expression of LAG3 molecule (CD4 analog, binds to MHC class II molecule and thus blocks presentation to other T-cells) (Huang et al., 2004), or TIGIT molecule with the ability to induce the production of tolerogenic cytokines in DCs (Yu et al., 2009). In aggregate, the battery of mechanisms endows Tregs with highly effective molecular machinery to suppress the proliferation of effector T-cells.

Arguably, the deletion of self-reactive T-cells occurs also in the immune periphery. Apart from forming the architecture of the lymph nodes, lymph node stromal cells (LNSCs) are also able to express at least a small fraction of TRAs (microarray analysis was not performed so far) and present them in the contest of MHC class I molecules (Fletcher et al., 2011). Several subpopulations of LNSCs were identified based on their reactivity to cellular surface makers CD31 and podoplanin. Fibroblastic reticular cells (FRCs, $CD31^-$, $podoplanin^+$) are forming the architecture of T- and B-cell zones of the lymph node. When OVA targeted to be expressed under the intestinal fatty acid binding protein promotor (specifically expressed in mature enterocytes), FRCs express and present OVA neo-self-antigen by MHC class I molecules and are able to delete OVA-specific OTI T-cells. Transcripts encoding several other TRAs were detected in these cells, suggesting that FRCs are able to produce at least a small fraction of TRAs (Fletcher et al., 2010; Lee et al., 2007; Magnusson et al., 2008). Recently, the transfer of peptide-loaded MHC class II molecules from DCs to LNSCs was shown to occur after direct contact of these cells in LNs, suggesting that $CD4^+$ T-cell tolerance might be also affected by LNSCs (Dubrot et al., 2014).

Unexpectedly, Aire presence was detected in the rare population of $CD11c^+$ $EpCAM^+$ $MHCII^+$ hematopoietic cells (Gardner et al., 2013) which were named extrathymic Aire-expressing cells, residing in the border between T- and B-cell zones of the lymph node. Aire-regulated expression of two hundreds of TRAs was observed by the microarray analysis in these cells with only slight overlap of seven genes which are also Aire-regulated in mTECs (Gardner et al., 2008). Targeting of neo-self antigen expression under the Aire promotor revealed the ability of these cells to mediate both $CD4^+$ and $CD8^+$ T-cell tolerance via the induction of anergy (Gardner et al., 2013) and cell deletion (Gardner et al., 2008), respectively.

Apart from the peripheral tolerance mechanism used generally in the lymphatic tissue, several gut-specific modifications in these mechanisms are used. First of them is the oral tolerance, presumably responsible for acquired tolerance to food antigens. Although it was anticipated, that outcomes of the process of oral tolerance depends on the load of

the ingested antigen (high antigenic loaded leads to antigen-specific T-cell anergy, while lower antigenic load prefers the conversion to Tregs) (Weiner et al., 2011), the evidence supporting anergy induction by oral tolerance is quite scarce (Pabst and Mowat, 2012). The key population responsible for the induction of oral tolerance is integrin $CD103^+$ migratory DCs (Weiner et al., 2011). They form the majority of DCs present in the intestinal lamina propria (the network of capillaries and lymph vessels underlying the epithelium) and home exclusively to mesenteric lymph nodes where they can imprint T-cells for gut-homing (Jaensson et al., 2008) or convert them into $Foxp3^+$ Tregs (Sun et al., 2007). Both of these effects are retinoic acid-dependent, and retinoic acid is acquired by DCs from their own metabolism of vitamin A. DC-metabolized retinoic acid induces gut-homing receptors CCR9 and $\alpha_4\beta_7$ on activated T-cells (Iwata et al., 2004) and, in synergic effect with TGF-β, it also supports T-cells conversion into Tregs (Sun et al., 2007). Experiments conducted before the establishment of the role of Foxp3 in Tregs biology identified the presence of suppressive Th3 and Tr1 polarized $CD4^+$ T-cell subsets as the result of oral tolerance induction. Later, it was shown, that Th3 subset is expressing Foxp3, so Th3 cells should be viewed as peripheral Tregs converted to Treg lineage in the gut and in an associated lymphoid tissue. Tr1 cells are IL-10 producing $CD4^+$ T-cells, which are not expressing Foxp3. The mechanism of IL-10 production used by these cells is not entirely clear (Maynard et al., 2007; Pabst and Mowat, 2012).

Interestingly, these properties of gut DCs are not shared by $CD103^+$ DCs derived from mucosal tissues other than gut, suggesting that these unique properties are imprinted to DCs by the gut environment (Scott et al., 2011). Physiological importance of this process in the maintenance of tolerance to food antigens is reaching its potential clinical application: this mechanism was used for the delivery of self-antigens and amelioration of autoimmune diseases such as type 1 diabetes (von Herrath et al., 1996) and experimental encephalomyelitis (Higgins and Weiner, 1988).

The second important issue in the gut homeostasis is the maintenance of tolerance to commensal microbiota. Antigens derived from them are continuously taken to draining lymph nodes by DCs sampling the gut content (Maloy and Powrie, 2011). Tregs can partly limit $CD4^+$ T-cell responses against commensal microbiota, however conflicting results determining the place of origin (i.e. thymus or periphery) of these Tregs exist (Cebula et al., 2013; Lathrop et al., 2011). Interestingly, recent data show that innate lymphoid cells (ILCs) of type 3, which are the major population of ILCs in lamina propria and mesenteric lymph node, are able to mediate deletion of activated microbiota-targeting $CD4^+$ T-cells. This subtype of ILCs is expressing MHCII molecules and presents antigens derived from microbiota (Hepworth et al., 2015). Genetic ablation of MHCII expression on ILCs leads to $CD4^+$ T-cell-dependent intestinal inflammation (Hepworth et al., 2013) and human pediatric patients suffering from inflammatory bowel disease (IBD) display decreased levels of MHCII levels on these cells. This suggests that intestine ILC3 population regulates immune responses against microbiota (Hepworth et al., 2015).

Several mechanisms are employed in order to direct and shape immune responses in the gastrointestinal tract. Central immune tolerance is setting the stage to avoid a possible autoimmune attack against the gut tissue and its principal cellular and molecular components by the deletion of self-reactive T-cells and/or by their conversion to Tregs. However, the central tolerance is owning only limited time frame to employ its tolerogenic potential during thymocytes development. Peripheral tolerance is further enforcing tolerogenic process via deletion, anergy induction or conversion of thymus-escaped self-reactive T-cell into Tregs. Moreover, peripheral tolerance is also responsible for the induction of tolerance to T-cells directed to food antigens or commensal microbiota. In the next chapter, the composition and function of intestinal epithelium is discussed concisely, with the focus on the immune role of AMP secreting-PCs.

# 3. INTESTINAL EPITHELIUM

The gut can be anatomically subdivided to the small intestine and the colon (large intestine). Three well-defined segments form the small intestine: duodenum – closest to the stomach, jejunum and the terminal part – ileum. Similarly, the colon is divided to the caecum, followed by the proximal, transverse and distal colon and terminates with the rectum and anus. Both parts of the gut differ functionally, the small intestine is largely responsible for the absorption of nutrients and minerals from digested food, the colon is taking care of water re-absorption. Both parts also vary in their cellular composition and architecture (Mowat and Agace, 2014). Differences in the gut epithelium organization in the small intestine and the colon are depicted in the Fig. 2.

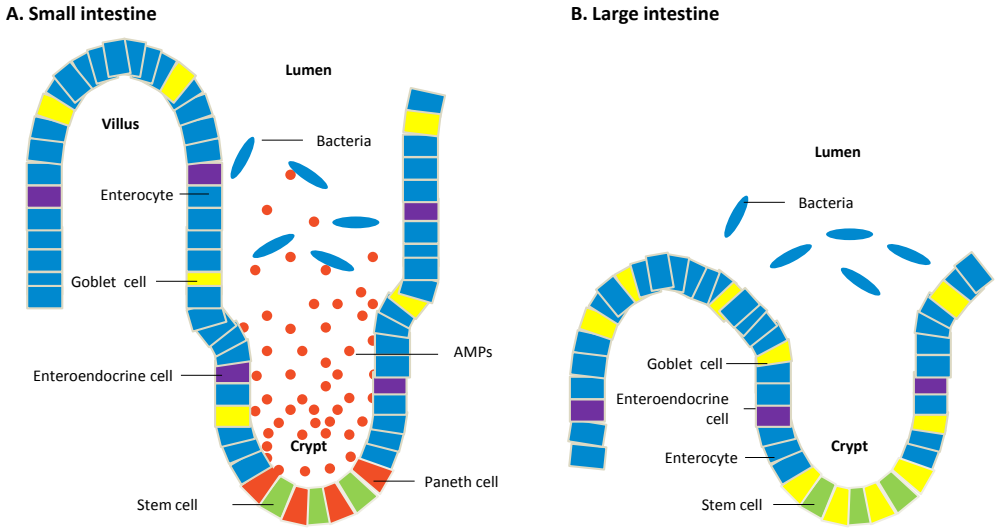


**Figure 2.** Differences in the anatomical organization of the small (**A.**) and large intestine (**B.**).

The small intestinal epithelium is organized into crypt-villus repeating units. Villi are finger-like protrusions oriented into the lumen of the gut, which maximize small intestinal absorptive surface area. They are covered by a single layer of differentiated epithelial cells with underlying network of capillaries and lymph vessels called the lamina propria. Several invagination forming crypts are attached to each villus and provide a niche for proliferating intestinal stem cells (iSCs) responsible for the self-renewal of the intestinal tissue.

At least seven terminally differentiated cell types are present in the small intestine tissue: i) Enterocytes, the largest cell population in the villi, is responsible for the acquisition of nutrients; ii) GCs, which secrete protective mucus; (iii) Microfold cells (M-cells), which form the connection between the intestinal lumen and immune cells by sampling intestinal content; iv) EECs, which produce and secrete hormones affecting peristaltic movements of the intestine and fluidity of its content; v) Tuft cells (TCs), possibly responsible for sensing of chemical substances of the intestinal content;

vi) PCs, which secrete AMPs and thus modulate the composition of intestinal microbiota; and vii) poorly defined cup cells (van der Flier and Clevers, 2009). In contrast, the colon lacks villi and therefore its surface form a flat area. Moreover, while crypts are smaller and PCs are absent in the colon, the mucine-secreting GCs population is enlarged in this part of the gut (Mowat and Agace, 2014).

## 3.1. Immunological function of intestinal epithelium

From the immunological point of view, the general function of the intestinal epithelium is the separation of its luminal content, full of the potentially harmful microorganism, from the host own body. In addition to this barrier function, intestinal epithelium uses several innate immune mechanisms to maintain the gut homeostasis. The main epithelial cell populations involved in this processes are mucus- and AMP-secreting GCs and PCs, respectively, which are described in more detail bellow.

### 3.1.1. Goblet cells

GCs are short-lived cells (lifespan 3-5 days) the proportion of which increases from the duodenum (4%) to the colon (16% of all epithelial cells) (Karam, 1999). GCs express and secrete several proteins that form the mucus. The mucus is responsible for: i) the protection against the injury mediated by chemical agents, mechanical stress and microorganisms by virtue of minimizing their contact with the epithelial cell wall or, alternatively, ii) by forming a structural matrix serving antibodies and AMP for their adhesion and action (Johansson et al., 2011). The main constituents of mucus are mucins, trefoil peptides and resistin-like molecules β (Dharmani et al., 2009).

Members of the mucin family are the most abundant in the mucus. Mucins are highly glycosylated proteins rich in amino acids serine and threonine. More than two thirds of the molecule constitutes O-linked oligosaccharide side chains. Two types of mucins have been identified: i) secretory, gel-forming mucins (*Muc2, Muc5, Muc6*) and ii) membrane-bound mucins (*Muc1, Muc3, Muc4*) which are present on the apical side of GCs and also enterocytes (Kim and Ho, 2010). *Muc2* is the most expressed member of this family. This relatively large protein forms homotrimers via disulfide bonds, which endow them with a partial resistance to cleavage by stomach produced trypsin (Godl et al., 2002). The enhancement of mucin production occurs in Myd88-dependent manner whereby, as suggested by germ-free mice or antibiotic treated animals with reduced levels of mucins, signals are provided by intestinal microbiota (Ermund et al., 2013). An essential physiological role of mucins can be documented by Muc2 deficient mice where the mucus layer is missing or it is severely reduced. In this case, the epithelial surface of the intestine is more permeable for microorganisms and a direct bacterial adherence to the epithelium is readily observable. This, in turn, leads to

the development of colitis (Van der Sluis et al., 2006), which in longitudinal studies has the tendency to develop into adenomas and further progress into adenocarcinomas (Velcich et al., 2002).

Additional, immunologically relevant function of GCs residing in the small intestine was recently recognized. During the secretion period, GCs form GC-associated antigen passages that are able to convey soluble luminal antigens to $CD103^+$ DCs. These passages represent an additional route of luminal antigen delivery to the intestinal-associated immune system (McDole et al., 2012).

### 3.1.2. Paneth cells

PCs, due to their striking morphology crowned by the presence of large secretory granules, were described almost 150 years ago by the German anatomist Gustav Schwalbe and later on by the Austrian physiologist Joseph Paneth after whom they took the name, reviewed in (Clevers and Bevins, 2013). In contrast to other epithelial cells populations, which are rather short-lived (3-5 days), PC's live span is much longer, approximately 4-5 weeks (van Es et al., 2005). Secretory granules of PCs are heavily packed with antimicrobial agents such as lysozyme (Deckx et al., 1967) and enteric α-defensins, which are the most abundant AMPs present in the intestine (Ouellette et al., 1992).

Defensins are, in general, 30-40 amino acids long peptides, containing 6 cysteine residues joined by three intramolecular disulphide bonds. The joining pattern defines three major subfamilies of defensins named α, β and θ. Apart from striking structural variations they also differ by their cellular source and the site of expression: α-defensins are further classified as myeloid (expressed primarily by neutrophils and to lesser extend by other granulocytes) (Selsted et al., 1985) or enteric (produced by PCs in the intestine) (Ouellette et al., 1989). β-defensins are produced by many epithelial cells, including enterocytes in the colon, airway epithelial cells and kidney and urinary tract epithelia (Scheetz et al., 2002). The last group, θ-defensins represents cyclic peptides which can be found only in neutrophil granules of "Old-world" primate species; in humans they persist only as pseudogenes (Tang et al., 1999).

In contrast to other antimicrobial agents produced by PCs (Hooper et al., 2003), enteric α-defensins are synthetized by PCs in a constitutive manner and their production does not require direct stimulation via pathogen-sensing receptors. This is evident from their prenatal expression by human PCs (Mallow et al., 1996) and from expression levels of enteric α-defensin by PCs of germ-free mice (Ouellette and Lualdi, 1990; Putsep et al., 2000). Enteric α-defensins expression is partly driven by PCs differentiation program – Wnt and β-catenin drive the activation of T-cell factor protein 4 (Tcf4), which in turn activates expression from defensin locus (van Es et al., 2005), reviewed in details in the last chapter.

Humans PCs are expressing two enteric α-defensin genes: *DEFA5* (Jones and Bevins, 1992) and *DEFA6* (Jones and Bevins, 1993) which slightly differ in their structure and function. Both enteric α-defensins are primarily synthetized as pro-peptides. This form of synthesis allows the storage of highly cationic defensins coupled with anionic pro-region inside the PC granules. Defensin pro-peptide (~10 kDa) is cleaved after the secretion, when its mature form (~3-4 kDa) is generated. DEFA5 is processed to active form by a trypsin, which is also synthetized by PCs (Ghosh et al., 2002).

Sequencing and assembly of the mouse genome revealed more than twenty murine enteric α-defensin genes (Shanahan et al., 2011), which are also called cryptdins (abbreviation for crypt defensins). Nevertheless, only 5 – 7 of them are abundantly expressed by a single mouse strain (Ouellette et al., 1992) and the expression profile strikingly differs between various strains (Shanahan et al., 2011). Murine enteric α-defensins are synthetized in a similar fashion as their human counterparts, i.e. as pro-peptides, but they are chopped and activated by different enzyme – matrix metalloproteinase 7 (Mmp7) (Wilson et al., 1999). Also in contrast to humans, defensin activation takes place prior to its secretion (Ayabe et al., 2002a). Mmp7 deficiency leads to the defective processing of enteric α-defensin pro-proteins and this, in turn, results in defensin deficiency and overall insufficiency in the protection against microbial infection (Wilson et al., 1999).

Secretion of granules containing defensins is govern by exocytosis into the intestinal lumen in a low rate under steady-state conditions and increases in dose dependent manner with variety of stimuli, including Toll-like receptors ligands (Ayabe et al., 2000), neurotransmitters (Satoh et al., 1995; Satoh et al., 1992), or immune mediators including IFN-γ. Notably, the presence of IFN-γ in the intestine leads to PC degranulation, followed by a cell extrusion. If IFN-γ presence is sustained for a longer time, it leads to the diminishment of PC numbers (Farin et al., 2014). In general, stimulation of the secretion-enhancing receptor leads to the intracellular increase in cytosolic $Ca^{2+}$ which activates potassium channel KCa3.1. The use of pharmacological blockers of KCa3.1 channels inhibits defensin secretion (Ayabe et al., 2002b).

The local concentration of enteric α-defensins in the base of the crypt reaches approximately 100 $mg.ml^{-1}$ (Ayabe et al., 2000; Ghosh et al., 2002), what is ten-times more than the concentration of myeloid α-defensin in the phagolysosome of the granulocyte (Ganz et al., 1985). This enormous amount of released AMPs opens the question concerning the precise role of enteric α-defensin in the intestinal antimicrobial immunity. Generally speaking, defensins are potent agents against Gram-positive and negative bacteria, fungi, protozoa and certain enveloped viruses (Selsted and Ouellette, 2005). Their mode of action is versatile, including a direct pore formation into cellular wall due to their cationic charge (White et al., 1995), binding to newly synthetized constituent of pathogen's cell wall (Sass et al., 2010), opsonisation and blocking of pathogen entry into the host cells (Selsted and Ouellette, 2005) or by

pathogen toxin binding, promoting toxins unfolding and higher susceptibility to proteolysis (Kudryashova et al., 2014).

The research conducted so far, unfortunately, lacks the demonstration of immune phenotype under the condition of genetic enteric α-defensins ablation or their complete functional deficiency. Nevertheless, indirect evidence obtained from the expression of transgenic human DEFA5 in murine PCs, or from mice carrying several mutations particularly affecting PC function, do exist.

The presence of human DEFA5 transgene in murine PCs reaches similar levels of expression as endogenous enteric α-defensins, what suggests common features in the requirement for activation of defensin loci in mouse and human. After oral infection with *Salmonella enterica typhimurium*, DEFA5 transgenic mice, in contrast to wild-type controls, are immune to infection, suggesting that the addition of a single defensin gene to murine intestinal system is sufficient to confer immunity against this pathogen bacteria and that higher defensin peptide diversity likely provides some evolutionary advantage (Salzman et al., 2003b). The same effect of "acquired" protection against various pathogens was described also in the case of DEFA6 transgenic animals (Chu et al., 2012). Moreover, tangible changes in the composition of intestinal microbiota were observed in DEFA5 transgenic animals. Notably, the authors observed the increase of *Bacterioides* phylum and decrease in *Firmincutes* phylum in the gut. In line with previous results, Mmp7 deficiency and consequent inability of PCs to degranulate processed defensin peptides (Wilson et al., 1999), leads to inverse situation: the increase of *Firmincutes* phylum and decrease of *Bacterioides* phylum. Among *Firmincutes* phylum the microbe called segmented filamentous bacteria (SFB) is specifically increased in its numbers (Salzman et al., 2010). This is important since SFBs were previously shown to induce Th17 inflammatory response in the gut, via the increase of IL-17 producing lamina propria T-cells (Ivanov et al., 2009). Consistent with this scenario, DEFA5 transgenic animals have no detectable SFBs and lower number of IL-17 producing T-cells (Salzman et al., 2010). These experimental models thus established the positive role of enteric α-defensins in anti-inflammatory modulation of intestinal microbiota and immunoprotection against pathogenic intruders under steady-state conditions.

PC compartment undergoes dramatic changes under perturbed situations which are mediated by pathogenic invasions or when genes affecting PC-dependent defensin production are mutated. These events lead to a wide spectrum of pathologies including IBD and cancer. IBD, precisely ileal form of Crohn's disease, is associated with an abnormal composition of intestinal microbiota and its higher adherence to gut mucosa (Sartor, 2008, 2010). The first gene described to be associated with Crohn's disease was *NOD2*. Some patients with Crohn's disease bear mutations in *NOD2* gene or carry its dysfunctional allelic variants (Hugot et al., 2001; Ogura et al., 2001). NOD2 is the pattern recognition receptor with the ability to sense bacteria derived muramyl dipeptide and activate NF-κB dependent cascade (Kobayashi et al., 2005). Later research determined high expression levels of NOD2 in PCs (Lala et al., 2003). Decrease in

DEFA5 and DEFA6 production was observed in patients suffering from Crohn's disease and bearing mutation in *NOD2* gene. Nevertheless, PCs themselves remain intact and their numbers remain unchanged (Wehkamp et al., 2004; Wehkamp et al., 2005). Nod2 deficient mice copy the phenotype that is observed in NOD2 deficient human patients as the genetic ablation of mouse gene leads to diminished enteric α-defensin expression (Kobayashi et al., 2005) and to changes in the composition of intestinal microbiota (Petnicki-Ocwieja et al., 2009).

Mutations in essential member of Wnt signaling pathway *TCF4* were found in some patients encoding a fully functional *NOD2* gene but still suffering from the ileal form of Crohn's disease. Such mutations in a single allele of *TCF4* are sufficient to cause the decrease in enteric α-defensin levels what diminishes their overall killing capacity in both human patients with Crohn's disease (Wehkamp et al., 2007) and the mouse model of this disease (Koslowski et al., 2009). Recently, several other Crohn's disease susceptibility genes, which are essential for PC function, were identified (Clevers and Bevins, 2013). Available data thus implicate the role of PCs and their microbicidal products in pathogenesis of Crohn's disease.

Mutations in Wnt cascade of intestine epithelial cells are also responsible for the colonic carcinoneogenesis. The constitutive activation of Wnt pathway, via Adenomatous polyposis coli (Apc) mutation for example, leads to higher proliferation and differentiation rate of intestinal crypts. The newly formed tumors consist of terminally differentiated PCs, among other cells (Andreu et al., 2005). Higher overall number of PCs leads to the higher expression of enteric α-defensins, which are in the case of adenoma and adenocarcinoma secreted also to the blood stream (Joo et al., 2009; Radeva et al., 2010). Thus enteric α-defensins might serve, in the future, as promising biomarkers for early diagnosis of colon cancer from the human sera.

Pathogens can also directly affect PC population. For example *Salmonella enterica tymphimurium* induces the expansion of PC population (Martinez Rodriguez et al., 2012), but counterintuitively, its presence leads to the downregulation of enteric α-defensins expression by these cells (Salzman et al., 2003a). Loss of PC population was observed during the infection by intracellular parasite, protozoan *Toxoplasma gondii*. As the consequence of such infection, mice generate a large amount of IFN-γ (Raetz et al., 2013), which was shown to promote PC degranulation and their extrusion (Farin et al., 2014). PC loss leads to changes in the composition of microbiota, characterized by the uncontrolled outgrowth of gram-negative *Enterobacteriaceae* (Raetz et al., 2013).

In aggregate, the homeostasis of PCs is kept in check with various mechanisms. This is essential, as PCs have a unique ability to modulate the composition of intestinal microbiota, with far reaching consequences impacting the function of the gut immune system. These instances are described in the next chapter together with the scheme of intestine-associated cellular components of immune system. In addition, PCs play

a critical role in the protection of the iSC niche in the bottom of crypts and support their homeostasis by niche signals (reviewed in the last chapter of this thesis).

## 3.2. Intestinal immune system

Priming of adaptive immune system in the gut takes place in the gut-associated lymphoid tissues (GALT) and gut-draining lymph nodes, while the effector cells are located diffusely across the epithelium or in the lamina propria. GALT includes macroscopically visible Peyer´s patches and smaller structures – isolated lymphoid follicles and cryptopatches. Each of these structures contains M-cells and DCs responsible for antigen uptake. In Payer´s patches, large B-cell and much smaller T-cell zones can be distinguished, while in smaller GALT structures, B-cells are predominant (Mowat and Agace, 2014). The lymph is drained from the gut to several anatomical locations: duodenum and transverse colon are primarily drained by duodenopancreatic lymph nodes (buried in pancreatic tissue); ileum, jeunum and parts of the colon (ceacum and proximal colon) by the mesenteric lymph node (mLN) and distal colon with rectum by caudal lymph node (Carter and Collins, 1974).

Intestinal lamina propria contains several immune effector cell populations including B-cells, T-cells, DCs, macrophages, granulocytes and mast cells, while intestinal epithelium is mostly occupied by T-cells.

### 3.2.1. B-cells

B-cells and plasma cells residing in the gut lamina propria and GALT are responsible for the secretion of IgM and IgA antibodies directed against specific luminal-derived antigens. This process requires sampling of luminal antigens by M-cells, which are then passed on and processed by DCs, which in turn, can activate T- and B-cells. Plasma cells can also undergo a class switch in order to produce IgA antibodies. Secretory IgA (sIgA; dimer of IgA joined by J-chain) or IgM (sIgM; pentamer joined by J-chain) are then transcytosed with the use of polymeric immunoglobulin receptor from the basolateral side of the enterocyte back into the lumen (Mantis et al., 2011). Microbial-epithelial cell interactions are modulated by sIgs in several ways: i) sIgs bind pathogens-derived toxins and thus prevent their activity on epithelial cells (Apter et al., 1993; Stubbe et al., 2000); ii) sIgs bind pathogen's receptors blocking their attachment to epithelial cell (Helander et al., 2004; Helander et al., 2003); iii) immune exclusion – peristaltic clearance of pathogens or toxins heavily coated by sIgs which crosslink several pathogens together and entrap them in the mucus (Stokes et al., 1975); iv) sIgAs bind to pathogens and forms immunocomplexes which can be internalized by M-cells in Dectin-1-dependent manner, these complexes are latter presented by DCs (Rochereau et al., 2013).

### 3.2.2. T-cells

T-cells are localized in the gut at two places: i) intraepithelial lymphocytes are T-cells embedded in close proximity to intestinal epithelial tissue and ii) the remaining T-cells are localized to the lamina propria. Intraepithelial lymphocytes, at least in mice, can be further subdivided by the TCR type on $\alpha\beta TCR^+$ cells with CD4 or CD8αβ coreceptors, $\alpha\beta TCR^+$ cells with CD8αα homodimer and $\gamma\delta TCR^+$. In the lamina propria $CD4^+$ and $CD8^+$ T-cells are observed in the ratio 2:1. Among $CD4^+$ T-cells Foxp3-producing Tregs cells are quite dominant. T-cells residing in the gut are responsible for the protection against potential intruders and also ensure tolerance to commensals and food antigens. TCR invariant T-cell populations are responsible mainly for non-protein pathogens derived antigens recognition (Mowat and Agace, 2014).

### 3.2.3 Myeloid cells

From the myeloid cell lineage, macrophages and DCs are the most abundant cells in a healthy lamina propria (Mowat and Agace, 2014). Macrophages are responsible for phagocytosis and the clearance of death cells and pathogens. They are also expressing high levels of tolerogenic IL-10, thus being an additional source of this cytokine in the intestine (Ueda et al., 2010). Gut-resident DCs are critical for the maintenance of oral tolerance, their role in this process was reviewed in "Peripheral tolerance" chapter.

### 3.2.4. Microbiota and intestinal immune system

Intestinal microbiota can modulate the polarization of T-cell responses and regulate the balance between the frequency and distribution of distinct immunologically relevant cellular lineages. For example, the colonization of germ-free mice with *Clostridia* species and *Bacterioides fragilis* leads to the development and enrichment of tolerogenic IL-10-producing peripheral $Foxp3^+$ Tregs (Atarashi et al., 2013; Atarashi et al., 2011; Round and Mazmanian, 2010). *Lactobacillus* was shown to cause changes in intestinal microbiota and elevated production of tolerogenic cytokines IL-10 and IL-13 (Maassen and Claassen, 2008). In contrast, SFBs or non-filamentous ATP-producing microbiota (Atarashi et al., 2008) were shown to polarize $CD4^+$ T-cells to Th17 response (Ivanov et al., 2008) by the induction of Th17-polarizing DCs (Goto et al., 2014; Ivanov et al., 2009) or by the presentation of SFB antigens by $MHCII^+$ ILC3s (Lecuyer et al., 2014). It is also of note, that gut-induced Th17 cells were associated with pathogenesis of autoimmune arthritis (Wu et al., 2010).

## 3.3. Development of the small intestinal epithelium

PCs are associated with the maintenance of iSCs niche not only via the secretion of AMPs which preserve the iSCs crypt department astonishingly clean, but they also secrete essential factors which provide support for keeping the homeostasis of iSC niche. The pluripotent activity of the iSCs was mapped into the crypt several decades ago, reviewed in (van der Flier and Clevers, 2009). Nevertheless, their precise cellular position within the crypt has remained elusive. Basically, two models are currently considered: i) +4 cell model and ii) crypt base columnar cells (CBCs) model. The former model originally proposed that cell positions from one to three (counted from the base of the crypt) are occupied by PCs while iSCs reside in the position +4. The cellular organization and numbering of crypt cells are schematically depicted in Fig. 3A. It was reported that these cells retain DNA-label, presumably due to asymmetric divisions (Potten et al., 1974) and are unusually radio-sensitive (Potten, 1977). The CBCs model suggested that putative iSCs are CBCs – small, symmetrically dividing, quickly cycling cells intermingled with PCs in the base of the crypt (Cheng and Leblond, 1974). The identification of exclusive marker of CBCs – leucine-rich repeat containing G-protein coupled receptor 5 (Lgr5) – enables the lineage tracing of differentiated cells originating from CBCs. CBCs have the potential to give rise to all intestinal epithelial lineages (Barker et al., 2007), including cells residing on +4 position, which retains Lgr5 expression (Roth et al., 2012; Wang et al., 2013). Recent studies using different lineage tracing approaches integrated these two models together, revealing that +4 cells are PC/EEC precursors with the stem cell potential. When a damage of original CBCs occurs, cells residing on +4 position replace them, forming a "reserve" pool of stem cell (Buczacki et al., 2013). The current interpretation of developmental relationships of various intestinal cells is presented in Fig. 3B.

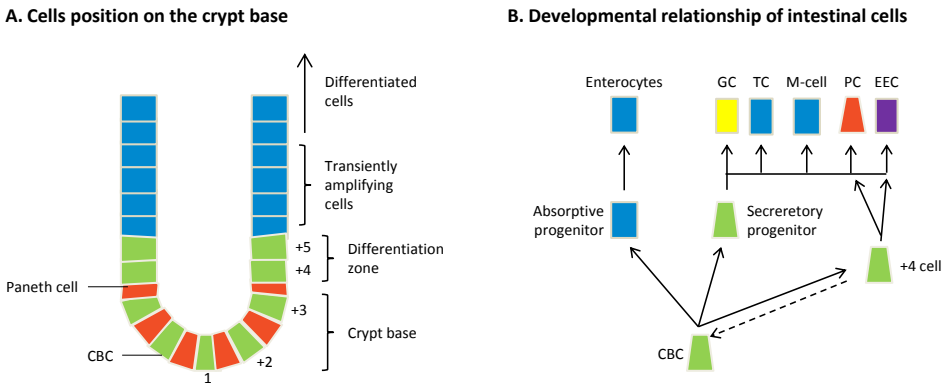


**Figure 3. A.** Position of cells in the crypt. Cells in position +4 and +5 are differentiating into absorptive or secretory lineage and cells localized in the upper position are still transiently amplifying. **B.** CBCs give rise to both absorptive and secretory lineages. Cells in the position +4 give rise to EECs and PCs. Under perturbed physiological conditions which damage CBCs and their stem cell potential, +4 cells might serve as reservoir of iSCs.

### 3.3.1 Wnt signaling pathway

Lgr5, identified as a marker of iSCs (Barker et al., 2007), is an integral regulator of Wnt signaling cascade (de Lau et al., 2011), which is essential for the development of intestinal tissue and maintenance of iSC self-renewal capacity (Korinek et al., 1998). Intracellularly, the most important player in Wnt cascade is β-catenin. Despite its involvement in catherin-based adherent junctions (Ozawa et al., 1989), it also modulates the ability of other proteins to bind DNA and thus regulate the process of gene transcription (Siegfried et al., 1994). In the absence of Wnt pathway mediated signals, the cytosolic β-catenin is destined for degradation by proteasome and this process integrates inputs from a large complex involving scaffolding proteins Axis inhibitory protein (Axin) (Ikeda et al., 1998), Apc (Rubinfeld et al., 1993) together with kinases casein kinase 1 (Ck1) and glycogen synthetase kinase 3 (Gsk3) (Siegfried et al., 1994). The cascade is shown on Fig. 4.

It should be noted, that the Wnt signaling pathway delineated in Fig. 4 is recognized as "canonical", and at least three other diversions from this main signaling pathway have been already described. The "non-canonical" Wnt pathway is largely involved in the cytoskeletal reorganization, cell polarity maintenance or calcium signaling (Nusse, 2012). Lgr5 serves as the receptor for Wnt-pathway agonists called R-spondins (de Lau et al., 2011), the recognition of which leads to the inhibition of continuous process of marking Frizzled receptors for degradation. This leads to the stabilization of Wnt-signaling (Hao et al., 2012) and consequently, to enhanced proliferation of iSCs (Kim et al., 2005).

Disruption of Wnt signaling pathway results in the disappearance of intestinal crypts, followed by the disruption of whole intestinal architecture as demonstrated by the Tcf (Korinek et al., 1998) or β-catenin (Ireland et al., 2004) genes knock-outs. Thus, Wnt signaling pathway serves as the critical molecular mechanism regulating the maintenance and homeostasis of the intestine. The importance of canonical Wnt cascade is further underlined by the occurrence of mutations in genes encoding regulatory and signaling elements of this pathway and their tight association with the process of carcinogenesis (Krausova and Korinek, 2014).

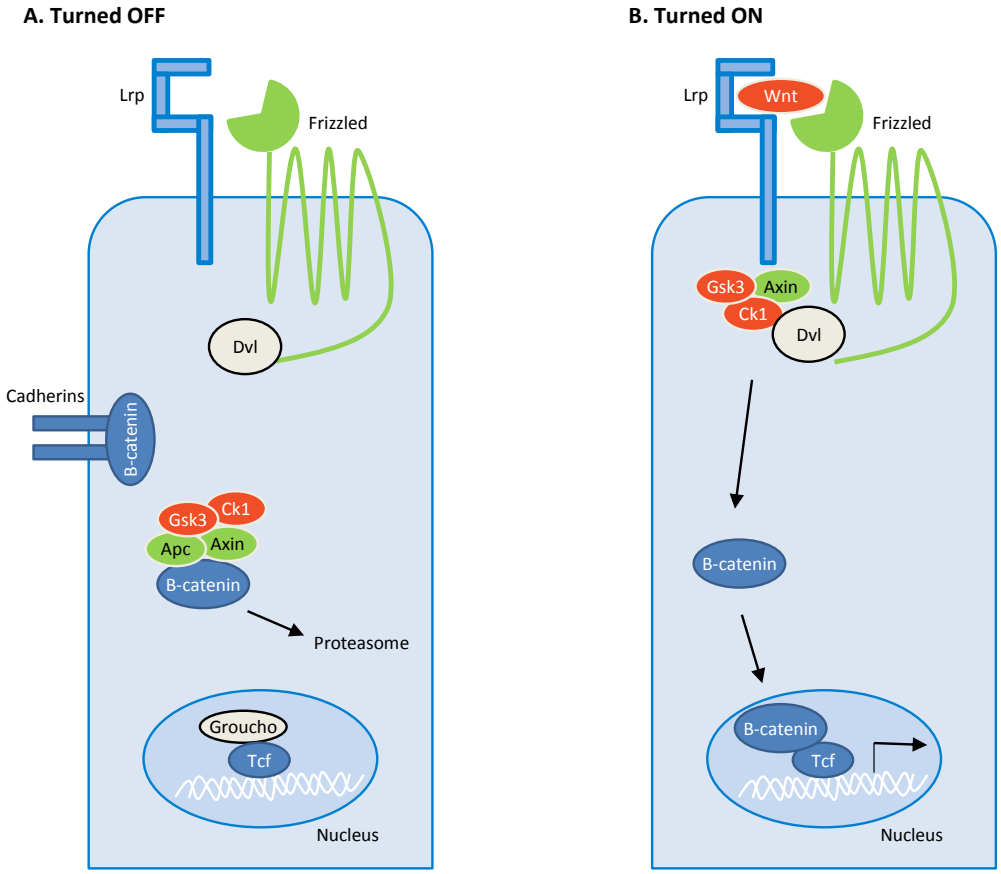


**Figure 4**. Wnt-signaling cascade. **A.** Cascade in turned-off state. **B.** Cascade in turned-on state. Wnt-signaling pathway is initiated by the binding of Wnt to its receptor complex formed by seven-transmembrane spanning domains containing protein from Frizzled family – Frizzled7 (Flanagan et al., 2015), and low-density lipoprotein receptor-related protein (Lrp) serving as co-receptor (Janda et al., 2012). The binding of Wnt ligand leads to the conformational change of its receptor Frizzled and phosphorylation of adaptor protein associated with Frizzled, named Dishevelled (Dvl) by Ck1 (Bernatik et al., 2011). Dvl and Ck1 also co-operates in the phosphorylation of Lrp cytoplasmic tail, which leads to the binding of Lrp to Axin and failure to catalyze the marking of β-catenin for degradation by Axin-Apc-Dvl-Ck1 kinase complex (Kim et al., 2013). Thus, β-catenin freely accumulates in the cytoplasm and the nucleus, where it replaces Groucho proteins in tight association with lymphoid enhancer-binding – Tcf. β-catenin and Tcf family members act together as transcriptional activators of specific target genes (He et al., 1998).

### 3.3.2 The stem cell niche and signals leading to lineages development

The iSC niche is established by cells which are in a direct contact with the base of the crypts – subepithelial myofibroblasts in basal lamina and by PCs interspersed between iSCs. Both of these populations secrete factors essential for intestinal

homeostasis and cell proliferation. Notably, myofibroblasts secrete Wnt2b and epidermal growth factor (Egf) (Farin et al., 2012) while PCs are expressing Notch ligands Delta-like 1 and 4 (Dll1 and Dll4), Egf, Wnt3 and Wnt11 (Sato et al., 2011). In the large intestine, where PCs are missing, is their role in the provision of iSC niche signals replaced by GCs (Rothenberg et al., 2012).

The dependence of iSCs on PCs and their production of niche factors have been documented in several murine models with transiently reduced numbers of PC compartment. For example, in mice lacking transcriptional repressor Gfi1, which is important for PC development (Shroyer et al., 2005) and in mice, where diphteria toxin A is expressed under the enteric α-defensin promotor (Garabedian et al., 1997), is the number of PCs reduced. This reduction leads to a lower number of iSCs, but overall, the intestinal architecture is still preserved, suggesting that even limited numbers of remaining iSCs and PCs are sufficient to maintain the intestinal homeostasis (Garabedian et al., 1997; Shroyer et al., 2005). PC-derived niche signals are responsible for the fate decision of symmetrically dividing iSCs. Newly generated iSCs compete for a cell-cell contact with PCs which provide stemness maintaining signals. If, due to spatial restriction, the loss of contact with PCs occurs, iSCs are pushed upwards from the bottom of the crypt to the line of transiently amplifying cells and starts to differentiate (Snippert et al., 2010).

Transiently amplifying cells can give rise to all differentiated intestinal lineages. The balance between Wnt and Notch signals keeps cells in undifferentiated state. When Notch signals are blocked pharmacologically (Wong et al., 2004) or genetically, only secretory GCs are being developed (Riccio et al., 2008). Conversely, the overexpression of Notch receptors on intestinal epithelium leads to the differentiation of cells exclusively towards the absorptive lineage and depletion of secretory cells (Fre et al., 2005). This strongly suggests that Notch signaling is controlling the cell-fate decision between secretory and absorptive cell lineage. Notch signaling activates genes from Hes family, which acts as repressors on Math1. Deletion of Hes1 leads to a decreased number of enterocytes and increased number of secretory cells (Suzuki et al., 2005), while the Math1 deletion leads to the presence of only one cell lineage in the gut – enterocytes (Yang et al., 2001). Math1 further activates the expression of Gft1, which is required for PC and GC, but not for EEC development, and thus the presence of the latter is increased in Gft1-deficient animals (Shroyer et al., 2005).

Essential signals for PC development are provided by continuous Wnt signaling via Frizzled 5 receptor. This signaling induces the expression of PC signature genes like enteric α-defensins in β-catenin and Tcf4-dependent manner (van Es et al., 2005).

## THESIS AIMS

Overarching aim of the thesis is to describe the mechanisms underpinning the immunological tolerance in the intestine as well as those mechanisms which contribute to the maintenance of intestinal homeostasis. Several specific questions were postulated:

I) Why are enteric α-defensins, AMPs secreted exclusively by intestinal PCs, expressed also in the thymus and how critical is the production of thymic enteric α-defensins for the maintenance of tolerance in intestinal tissue.

II) What is the role of the transcriptional regulator Hic1 in PC development and the homeostasis of intestinal tissue?

III) Is Nkd1, the regulator of Wnt cascade, expressed also by intestinal cells with active Wnt cascade?

# RESULTS

The list of applicant's publications with direct connection to presented thesis:

**Dobeš J.**, Neuwirth A., Dobešová M., Vobořil M., Balounová J., Ballek O., Lebl J., Meloni A., Krohn K., Kluger N., Ranki A., Filipp D., Gastrointestinal autoimmunity associated with loss of central tolerance to enteric α-defensins. *Gastroenterology, 2015; 149(1): 139-50.* **($IF_{2015}$ = 16.716, citing articles without self-citations: 3)**

Janečková L., Pospíchalová V., Fafílek B., Vojtěchová M., Turečková J., **Dobeš J.**, Dubuissez M, Leprince D, Baloghová N., Horázná M., Hlavatá A., Stančíková J., Šloncová E., Galušková K., Strnad H, Kořínek V., Hic1 tumor suppressor loss potentiates TLR2/NF-kappaB signaling and promotes tissue damage-associated tumorogenesis. *Molecular Cancer Research, 2015; 13(7):1139-1148.* **($IF_{2015}$ = 4.380, citing articles without self-citations: 0)**

Stančíková J., Krausová M., Kolář M., Fafílek B., Švec J., Sedláček R., Neroldová M., **Dobeš J.**, Horázná M., Janečková L., Vojtěchová M., Oliverius M., Jirsa M., Kořínek V.. NKD1 marks intestinal and liver tumors linked to abberant Wnt signaling. Cellular Signaling, 2015;27(2):245-56. **($IF_{2015}$ = 4.315, citing articles without self-citations: 2)**

The applicant also coauthored the paper reporting the link between the type 1 diabetes and high expression levels of myeloid α-defensins, as well as the article devoted to a general audience describing the phenomenon of immune tolerance:

Neuwirth A., **Dobeš J.**, Oujezdská J., Ballek O., Benešová M., Šumník Z., Včeláková J., Koloušková S., Obermannová B., Kolář M., Štechová K., Filipp D., Eosinophils from patients with type 1 diabetes mellitus express high level of myeloid alpha-defensins and myeloperoxidase. *Cellular Immunology, 2012;273(2):158-63.* **($IF_{2015}$ = 1.924, citing articles without self-citations: 3)**

Filipp D and **Dobeš J**: Immunity and Tolerance: Jin and Jang of the Immune System (Imunita a tolerancia: Jing a Jang imunitného sytému, *written in Slovak language*). *Vesmír, 2013: 92, 224-227.* **($IF_{2015}$ = without IF, popularization article).**

## 1. GASTROINTESTINAL AUTOIMMUNITY ASSOCIATED WITH LOSS OF CENTRAL TOLERANCE TO ENTERIC ALFA-DEFENSINS

Enteric α-defensins are short AMPs synthetized and secreted by crypt-based intestinal PCs (Ouellette et al., 1989; Ouellette and Lualdi, 1990). They are probably the most effective AMPs with the congruent capacity to modulate the composition of intestinal microbiota (Salzman et al., 2010) and kill pathogens (Salzman et al., 2003b). PCs, along with the synthesis of enteric α-defensins, also provide Wnt signals which are essential for the maintenance of iSCs, as both PCs and iSCs cohabitate the base of intestinal crypts (Sato et al., 2011). The loss or diminished production of enteric α-defensins by PCs are responsible for at least some aspects of the initiation and preservation of IBD (Ogura et al., 2003). PCs also produce many other important molecules supporting proper functions of intestinal immunity, such as other types of antimicrobials, cytokines and receptors involved in innate and adaptive immunity (Clevers and Bevins, 2013). All the above-described properties defines PCs as the essential cell type required for the maintenance of intestinal homeostasis.

Previous results showed reactivity of APECED patient's sera with secretory granules of PCs, suggesting a possible link between PC-synthetized self-antigen and APECED autoimmunity (Ekwall et al., 1998). In APECED patients, *AIRE* gene is inactivated by various mutations (Consortium, 1997; Nagamine et al., 1997) that can lead to the loss of AIRE-regulated TRA production (Anderson et al., 2002) and impaired negative selection of developing thymocytes (Liston et al., 2003). Gastrointestinal symptoms associated with APECED are relatively frequent and heterogenic and are often manifested as constipation, malabsorption and diarrhea, or their combinations (Perheentupa, 2006). So far, these types of gastrointestinal autoimmunity in APECED were linked to inoperative immune tolerance to self-antigens produced by EECs (Ekwall et al., 1998; Soderbergh et al., 2004). EECs are secretory intestinal cells responsible for the gut peristaltic movement and it was suspected that their loss causes autoimmune conditions with variable clinical outcome as described above (Posovszky et al., 2012).

In our presented study, we have shown that human and mouse thymic mTECs produce enteric α-defensins. Approximately 30% of APECED patients were seropositive for enteric α-defensins autoantibodies, and some of them still harbor enteric α-defensin-reactive T-cells in their peripheral blood. The presence of defensing-specific autoantibodies correlated with the diarrhea disease component. In addition, in some of these patients, the complete loss or diminishment of PCs were readily observable. In order to mechanistically test the possible role of enteric α-defensins as intestinal self-antigens, we established a new murine model of APECED disease. The model is based on the premise that due to a faulty negative selection of Aire-deficient mice, defensin-specific T-cells occur in the periphery and that their self-aggressiveness against PCs can be detected by their transfer to immunocompromised mice. Specifically, since Aire is the master regulator of enteric α-defensin expression in

murine mTECs, Aire-deficient and wild-type control mice were immunized with enteric α-defensins to amplify and visualize the presence of defensing-specific self-reactive T-cells in the immune periphery. The adoptive transfer of these T-cells derived from Aire-deficient mice to Nude mice recipients resulted in the decrease of PCs, dysbiosis of intestinal microbiota and, consequently, in the increase of pathogenic proinflammatory IL-17 and IL-23R expressing T-cells in the gut. Our data thus provide a causal link between the impaired negative selection in the thymus and intestinal autoimmunity in Aire-deficient environment (Dobeš et al., 2015). The study was recently highlighted by two commentary articles (Traverso, 2015; Yusung and Martin, 2015).

Gastroenterology 2015;149:139–150

# BASIC AND TRANSLATIONAL—ALIMENTARY TRACT

## Gastrointestinal Autoimmunity Associated With Loss of Central Tolerance to Enteric α-Defensins

Jan Dobeš,[1] Aleš Neuwirth,[1] Martina Dobešová,[1] Matouš Vobořil,[1] Jana Balounová,[1] Ondřej Ballek,[1] Jan Lebl,[2] Antonella Meloni,[3] Kai Krohn,[4,5] Nicolas Kluger,[5] Annamari Ranki,[5] and Dominik Filipp[1]

*[1]Laboratory of Immunobiology, Institute of Molecular Genetics of the AS CR, Prague, Czech Republic; [2]Department of Pediatrics, 2nd Faculty of Medicine, Charles University in Prague and University Hospital Motol, Prague, Czech Republic; [3]Pediatric Clinic II, Ospedale Microcitemico and Department of Biomedical and Biotechnological Science, University of Cagliari, Cagliari, Italy; [4]Clinical Research Institute HUCH, Helsinki, Finland; and [5]Department of Dermatology and Allergology, Department of Medicine, Helsinki University Central Hospital, Helsinki, Finland*

See editorial on page 22.

**BACKGROUND & AIMS:** Autoimmune polyendocrinopathy candidiasis ectodermal dystrophy (APECED) is an autoimmune disorder characterized by chronic mucocutaneous candidiasis, hypoparathyroidism, and adrenal insufficiency, but patients also develop intestinal disorders. APECED is an autosomal recessive disorder caused by mutations in the autoimmune regulator (AIRE, which regulates immune tolerance) that allow self-reactive T cells to enter the periphery. Enteric α-defensins are antimicrobial peptides secreted by Paneth cells. Patients with APECED frequently have gastrointestinal symptoms and seroreactivity against secretory granules of Paneth cells. We investigated whether enteric α-defensins are autoantigens in humans and mice with AIRE deficiency. **METHODS:** We analyzed clinical data, along with serum and stool samples and available duodenal biopsies from 50 patients with APECED collected from multiple centers in Europe. Samples were assessed for expression of defensins and other molecules by quantitative reverse transcription polymerase chain reaction and flow cytometry; levels of antibodies and other proteins were measured by immunohistochemical and immunoblot analyses. Histologic analyses were performed on biopsy samples. We used *Aire*$^{-/-}$ mice as a model of APECED, and studied the effects of transferring immune cells from these mice to athymic mice. **RESULTS:** Enteric defensins were detected in extraintestinal tissues of patients with APECED, especially in medullary thymic epithelial cells. Some patients with APECED lacked Paneth cells and were seropositive for defensin-specific autoantibodies; the presence of autoantibodies correlated with frequent diarrhea. *Aire*$^{-/-}$ mice developed defensin-specific T cells. Adoptive transfer of these T cells to athymic mice resulted in T-cell infiltration of the gut, loss of Paneth cells, microbial dysbiosis, and the induction of T-helper 17 cell-mediated autoimmune responses resembling those observed in patients with APECED. **CONCLUSIONS:** In patients with APECED, loss of AIRE appears to cause an autoimmune response against enteric defensins and loss of Paneth cells. *Aire*$^{-/-}$ mice developed defensin-specific T cells that cause intestinal defects similar to those observed in patients with APECED. These findings provide a mechanism by which loss of AIRE-mediated immune tolerance leads to intestinal disorders in patients with APECED.

*Keywords:* Mouse Model; Intestinal Crypt; DEFA; Microbiota.

The thymus is the site of T-cell lineage commitment and the place where T cells with a high affinity for self-antigens are removed from the developing T-cell pool through the process of negative selection. Critical cellular components of this process are medullary thymic epithelial cells (mTECs), which synthesize and present in the context of their major histocompatibility complex tissue restricted antigens (TRAs), the expression of which is otherwise restricted to peripheral organs.[1,2] The autoimmune regulator (AIRE) mediates the expression of a fraction of TRAs on the transcriptional level.[3] Presentation of TRAs by mTECs leads to the deletion of $CD4^+$ or $CD8^+$ T cells bearing a T-cell receptor that is reactive to the TRA-major histocompatibility complex[4] or conversion of such $CD4^+$ T cells into T-regulatory cells.[5]

Loss-of-function mutations in the *AIRE* gene cause a rare autosomal recessive syndrome called autoimmune polyendocrinopathy candidiasis ectodermal dystrophy (APECED; OMIM: 240300),[6,7] which is relatively frequent in Finland, Sardinia, and Iran.[1] Due to the loss of central tolerance and subsequent occurrence of self-reactive T cells and autoantibodies in the immune periphery,[8] these patients display up to a dozen clinical autoimmune components occurring in various combinations.[9] The main components of APECED are chronic mucocutaneous candidiasis, hypoparathyroidism, and adrenal insufficiency,[10] but gastrointestinal symptoms, which occur intermittently and are still difficult to explain, are also fairly common.[9,11]

***Abbreviations used in this paper:*** **AIRE, autoimmune regulator; APECED, autoimmune polyendocrinopathy candidiasis ectodermal dystrophy; cTECs, cortical thymic epithelial cells; EECs, enteroendocrine cells; FACS, fluorescence-activated cell sorting; IL, interleukin; mLN, mesenteric lymph node; mTECs, medullary thymic epithelial cells; pLN/mLN, peripheral/mesenteric lymph node; PCs, Paneth cells; SFB, segmented filamentous bacteria; TRAs, tissue restricted antigens; WT, wild-type.**


0016-5085/$36.00
http://dx.doi.org/10.1053/j.gastro.2015.05.009

Paneth cells (PCs), which reside at the bottom of small intestinal crypts, are long-lived cells that constitutively produce and secrete antimicrobial proteins and inflammatory mediators.[12] Among their bactericidal products, enteric α-defensins are the most abundant,[13] and exhibit a broad range of activities against bacteria, viruses, and fungi.[14] So far, 27 enteric α-defensins (also called cryptdins) have been identified in the mouse genome,[15] some of which are strain specific.[16] In contrast, only 2 enteric α-defensin genes, *DEFA5*[17] and *DEFA6*,[18] were recognized in humans. Enteric α-defensins protect the crypt's residential stem cells from microbial attack[19,20] and shape the composition of commensal microbiota.[21]

The gut-related autoimmune symptoms of APECED have been associated with the lack of tolerance to 2 self-antigens: tryptophan hydroxylase[22,23] and histidine decarboxylase,[24] both produced by enteroendocrine cells (EECs) of the gut epithelium. Interestingly, sera from APECED patients were shown to also cross-react with secretory granules of PCs.[23] In addition, the comparative microarray analysis between wild-type (WT) and Aire-deficient mTECs revealed that at least some members of the enteric α-defensin family are down-regulated in the latter.[3,25] Nevertheless, the potential role of PC's enteric α-defensins as self-antigens in gut-related autoimmunity of APECED patients has not been addressed so far. Here, we report that deficiencies in Aire-mediated expression of enteric α-defensins in mTECs are linked to cellular and molecular alterations in PCs-supported intestinal homeostasis and, in turn, to intestine-related autoimmunity.

## Materials and Methods

This information is provided in the Supplementary Materials.

## Results

### *Enteric α-Defensins are Present in the Human Thymus*

In the first series of experiments, we quantified the expression of the 2 enteric α-defensins *DEFA5* and *DEFA6* by quantitative reverse transcription polymerase chain reaction in the human small intestine, thymus, and spleen. As illustrated in Figure 1*A*, *DEFA5* and *DEFA6* expression in the thymus is readily detectable, although at much lower levels compared with that of the small intestine. Their expression in the spleen, used as a negative control, was barely detectable. When human thymic stromal $CD45^-$ cells were fluorescence-activated cell sorted (FACS) according to the scheme presented in Figure 1*B*, the expression of *DEFA5* and *DEFA6* was confined to the TEC population, and $CD45^+$ cells were negative (Figure 1*C*). Expression of DEFA5 protein exclusively in mTECs coexpressing AIRE was confirmed by immunofluorescence on FACS-sorted TECs (Figure 1*D*). Notably, of 150 AIRE-expressing cells, 12% (±3%, n = 3) stained positive for DEFA5. No positivity for DEFA5 was detected in AIRE-negative cells. These results demonstrated that mTECs are the exclusive cellular source of enteric α-defensins in the human thymus.

### *Autoimmune Polyendocrinopathy Candidiasis Ectodermal Dystrophy Patients Produce Enteric α-Defensin-Specific Antibodies*

We hypothesized that expression of enteric α-defensins in human mTECs is AIRE-dependent, so the presence of enteric α-defensin–specific T cells in APECED patients might impact the integrity of defensin-expressing PCs. To address this question, paraffin-embedded duodenal biopsies from APECED patients and healthy controls were stained with anti-DEFA5 antibody (Figure 1*E*). Although the crypt structure and the composition of the entire epithelium remained seemingly unaffected, DEFA5-expressing PCs were decreased in 4 samples (Table 1) and undetected in 2 of 10 APECED samples (Figure 1*E* and Table 1). This lack of DEFA5 correlated with the absence of signal revealed by histologic Masson's trichrome staining of PCs[26] (Supplementary Figure 1). This suggested a link between AIRE-deficiency and pathologic changes in the PC compartment.

We next assessed the occurrence of autoantibodies with DEFA5 specificity in the sera of APECED patients by Western blot. In the first round, 7 of 30 APECED samples (27 from Finland, 3 from Czech Republic) (approximately 23%) were positive (Figure 2*A* and Supplementary Figure 2*A*); this group of patients is separated by *dashed line* in Table 1. It is of note that all 4 duodenal biopsies from DEFA5-seropositive patients (APS1-01, -20, -24, and -31) exhibited a decreased number of, or a lack of, PCs. The analysis of an additional 20 patient samples from Sardinia revealed 14 of a total of 50 APECED patients as seropositive (approximately 28%). None of the APECED patients was seropositive for DEFA6 autoantibodies (data not shown).

Next, using healthy duodenal sections, we compared the immunoreactivity of sera collected from healthy controls with those derived from APECED patients. Although the former showed no apparent staining of both PCs and intestinal sections, sera from APECED patients displayed a complex pattern of reactivity. Specifically, the highest serum reactivity toward PCs was observed in sera from patients with undetectable PCs, followed by those seropositive for DEFA5; the lowest was observed in DEFA5-seronegative patients (Figure 2*B*). It is of note that enteric α-defensin autoantibodies were of IgG, but not IgA, isotype (Supplementary Figure 2*B*). Remarkably, this pattern of staining intensity correlated with a number as well as the seroreactivity of additional yet unidentified intestinal autoantigens (Supplementary Figure 3*A*). These autoantigens are not ubiquitously expressed (Supplementary Figure 3*B*) and do not originate from contaminating traces of bacteria (Supplementary Figure 3*C*). In support of the notion of multi-targeted autoimmunity, when 10 intestine biopsies were probed for a specific marker of EECs, chromogranin A (Supplementary Figure 4), the reduced number of these cells was observed predominantly in DEFA5-seropositive samples (Table 1). The 2 patients who lacked PCs APS1-16 and -24, also lacked and showed a decreased number of EECs,

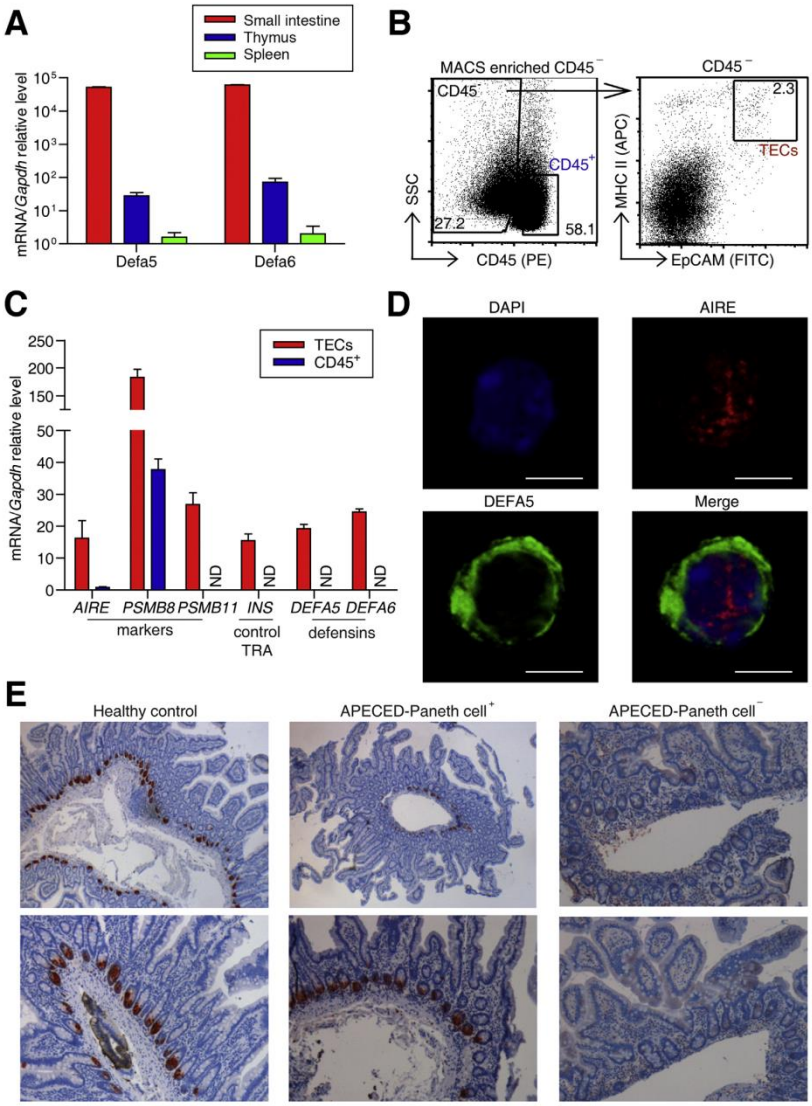


**Figure 1.** Human mTECs express enteric $\alpha$-defensins. (*A*) The relative messenger RNA levels of *DEFA5* and *DEFA6* expression in human small intestine, thymus, and spleen. (*B*) TECs were FACS-sorted as $CD45^-$ $MHCII^+$ $EpCAM^+$ cells. (*C*) The expression levels of lineage-specific markers (*AIRE*, *PSMB8*, and *PSMB11*), control TRA—insulin (*INS*) and *DEFA5* and *DEFA6* in sorted TECs. Data represent mean gene expression level ($\pm$ SD) measured in triplicate from 3 independent samples. ND, not detected. Thymic $CD45^+$ cells (*B*) were used as a control. (*D*) Microscopic detection of DEFA5 production by TECs. One representative image is shown. Scale bar = 5 $\mu$m. (*E*) The comparative antibody staining revealed the absence of DEFA5 in 2 APECED patients ($PC^-$). *Upper* and *bottom panels* represent images from 2 individuals.

respectively. These results suggest that intestine autoimmunity in patients with APECED progresses through several stages that correlate with DEFA5 seronegativity, followed by seropositivity, and culminate in the loss of PCs, the stage associated with the highest titer of multi-targeting autoantibodies.

APECED patients exhibit gastrointestinal symptoms and dysfunction.[27,28] We observed that idiopathic diarrhea was present in 9 of 14 (64.3%) DEFA5-seropositive patients (APS1-2p, -4p, -18p, -1, -3, -5, -24, -26, and -31), as well as in both patients who lacked PCs (APS1-16 and 24). Only 12 of 36 (33.3%; $P = .06$; Fisher's exact test) PC-positive DEFA5-seronegative patients suffered from this intestinal symptom. Overall, DEFA5-seropositive patients are approximately 2 times more likely to experience idiopathic diarrhea than their DEFA5-seronegative counterparts. Interestingly, when grouping Finnish and Czech patients together, the difference in the incidence of diarrhea among DEFA5-seropositive (6 of 7) compared with DEFA5-seronegative patients (6 of 23) is significant ($P = .0086$). No such association was found among Sardinian patients.

**Table 1.** Characteristics and Clinical Parameters of APECED Patients

| Patient | Nationality | Sex | Age, *y* | Diarrhea[a] | Age at the time of intestinal biopsy | CrA detection on intestinal biopsy | HD5 detection on intestinal biopsy | Anti-HD5 autantibodies in the blood |
|---|---|---|---|---|---|---|---|---|
| APS1-1p | I | M | 9 | No | — | — | — | Negative |
| APS1-5p | I | F | 20 | No | — | — | — | Negative |
| APS1-6p | I | F | 41 | No | — | — | — | Negative |
| APS1-7p | I | F | 35 | Yes | — | — | — | Negative |
| APS1-9p | I | F | 41 | Yes | — | — | — | Negative |
| APS1-11p | I | F | 37 | No | — | — | — | Negative |
| APS1-12p | I | M | 48 | Yes | — | — | — | Negative |
| APS1-13p | I | M | 17 | Yes | — | — | — | Negative |
| APS1-14p | I | F | 39 | No | — | — | — | Negative |
| APS1-15p | I | F | 7 | No | — | — | — | Negative |
| APS1-17p | I | M | 38 | Yes | — | — | — | Negative |
| APS1-19p | I | F | 24 | Yes | — | — | — | Negative |
| APS1-20p | I | M | 37 | Yes | — | — | — | Negative |
| APS1-02 | Finn | F | 42 | Yes | — | — | — | Negative |
| APS1-04 | Finn | M | 65 | Yes | — | — | — | Negative |
| APS1-06 | Finn | M | 32 | No | 24 | Normal | Normal | Negative |
| APS1-07 | Finn | F | 32 | No | — | — | — | Negative |
| APS1-08 | Finn | F | 56 | Yes | 51 | Decreased | Decreased | Negative |
| APS1-09 | Finn | F | 32 | No | — | — | — | Negative |
| APS1-10 | Finn | F | 25 | No | — | — | — | Negative |
| APS1-11 | Finn | F | 46 | No | — | — | — | Negative |
| APS1-12 | Finn | F | 50 | No | — | — | — | Negative |
| APS1-13 | Finn | M | 45 | No | 42 | Normal | NA | Negative |
| APS1-14 | Finn | M | 43 | No | — | — | — | Negative |
| APS1-15 | Finn | F | 17 | No | — | — | — | Negative |
| APS1-17 | Finn | F | 52 | No | 39 | NA | Normal | Negative |
| APS1-18 | Finn | M | 18 | No | — | — | — | Negative |
| APS1-19 | Finn | F | 53 | Yes | — | — | — | Negative |
| APS1-21 | Finn | F | 51 | No | — | — | — | Negative |
| APS1-22 | Finn | F | 8 | Yes | — | — | — | Negative |
| APS1-23 | Finn | F | 35 | No | 35 | Normal | Normal | Negative |
| APS1-25 | CZ | F | 19 | No | — | — | — | Negative |
| APS1-27 | CZ | M | 16 | No | — | — | — | Negative |
| APS1-28 | Finn | M | 44 | No | 36 | Normal | Normal | Negative |
| APS1-29 | Finn | F | 20 | No | — | — | — | Negative |
| APS1-2p | I | F | 24 | Yes | — | — | — | Positive |
| APS1-3p | I | M | 31 | No | — | — | — | Positive |
| APS1-4p | I | F | 18 | Yes | — | — | — | Positive |
| APS1-8p | I | M | 37 | No | — | — | — | Positive |
| APS1-10p | I | F | 8 | No | — | — | — | Positive |
| APS1-16p | I | M | 4 | No | — | — | — | Positive |
| APS1-18p | I | F | 39 | Yes | — | — | — | Positive |
| APS1-01 | Finn | F | 45 | Yes | 37 | Normal | Decreased | Positive |
| APS1-03 | Finn | F | 28 | Yes | — | — | — | Positive |
| APS1-05 | Finn | F | 46 | Yes | — | — | — | Positive |
| APS1-20 | Finn | F | 58 | No | 56 | Decreased | Decreased | Positive |
| APS1-26 | CZ | M | 9 | Yes | — | — | — | Positive |
| APS1-31 | Finn | F | 5 | Yes | 5 | Absent | Decreased | Positive |
| APS1-24 | Finn | M | 31 | Yes | 31 | Decreased | Absent | Positive |
| APS1-16 | Finn | M | 17 | Yes | 11 | Absent | Absent | Negative |

CZ, from Czech Republic; F, female; Finn, from Finland; I, from Italy (Sardinia); M, male; NA, not analyzed for technical reason.
[a]Diarrhea is defined as defecation >3 times a day or by unusual consistency of stools.

In general, the occurrence of autoantibodies is predicated by the presence of self-reactive T cells. We could detect defensin-specific T cells in the peripheral blood of a limited number of available DEFA5-seropositive and PC-lacking APECED patients (Supplementary Figure 5).

### *Autoimmune Regulator–Dependent Expression of Enteric α-Defensins (Cryptdins) in Mouse Medullary Thymic Epithelial Cells*

To obtain mechanistic insight into enteric α-defensin–driven gut autoimmunity, we explored Aire-deficient mice

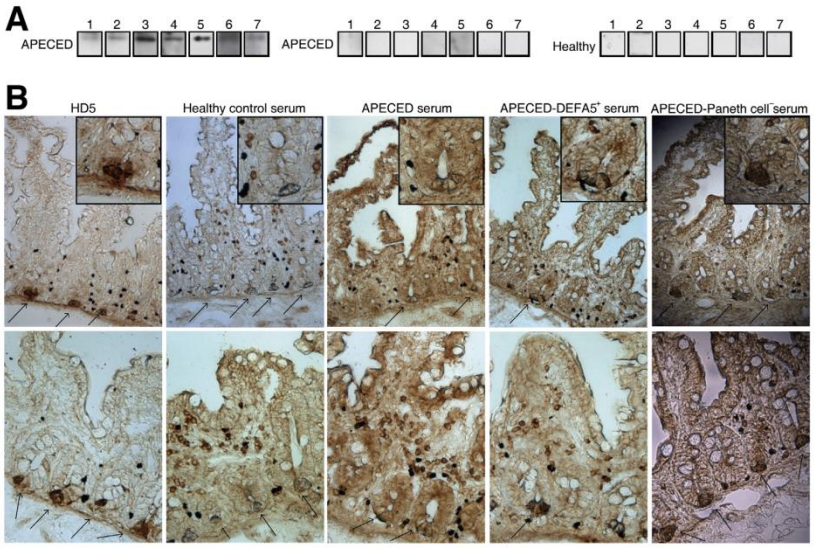


**Figure 2.** DEFA5-specific autoantibodies are present in the blood of APECED patients. (*A*) Western blot analysis revealed the reactivity of human sera to DEFA5 antigen. The seropositivity in 7 APECED samples is shown (*left panels*). For comparison, DEFA5-seronegative samples of APECED and healthy subjects are presented in the *middle* and *right panels*, respectively. (*B*). Immunohistochemistry of HD5 antibody on duodenal sections from a healthy donor, used as a positive control, revealed PCs staining on the bottom of intestinal crypts (*left panels*). Sera isolated from healthy controls show no staining (healthy control serum). Immunostaining of PCs and surrounding structures was most prominent in the serum sample derived from APECED patients lacking PCs (PCs$^-$ serum), which was slightly decreased in DEFA5-seropositive APECED patients (DEFA5Ab$^+$ serum). Sera from the remaining APECED patients also showed elevated reactivity toward PCs and surrounding structure. Representative images from 2 patients from each group are shown.

(Aire$^{-/-}$) as an experimental model of APECED. We first determined whether expression of cryptdins in the WT mouse thymus recapitulates that of enteric $\alpha$-defensins in human mTECs. We found that members of the cryptdin family that are predominantly expressed in the intestine of C57BL/6 mice (*Defcr3*, *Defcr5*, *Defcr20*, *Defcr21*, and *Defcr24*)[16] are also expressed in the mouse thymus (Figure 3*A*).

To identify the cellular source of intrathymic cryptdin production, mTECs and cortical thymic epithelial cells (cTECs) were FACS sorted according to the scheme presented in Figure 3*B*. Quantitative reverse transcription polymerase chain reaction analysis of messenger RNAs derived from mTECs, cTECs, and MACS-enriched CD45$^+$ cells confirmed the expression of cell restricted markers for each of these populations: CD45$^+$—Cathepsin S (*Ctss*), $\beta$5i proteasome subunit (*Psmb8*); cTECs—$\beta$5t proteasome subunit (*Psmb11*); mTECs—Cathepsin S, $\beta$5i proteasome subunit, *Aire*, and TRAs, such as insulin (*Ins2*), mucin 6 (*Muc6*), and glutamic acid decarboxylase 67 kDa (*Gad67*). Importantly, the exclusive expression of cryptdin messenger RNAs in mTECs (Figure 3*C*) was on the protein level restricted to Aire-expressing mTEC cells only (Figure 3*D*). Notably, of 100 Aire-positive mTECs, 36% (±9%, n = 3) co-stained for cryptdins.

The presence of cryptdins in mTECs posed questions concerning the dependency of cryptdin expression on Aire. As presented in Figure 3*E*, the expression of *Defcr3*, *5*, and *20* was completely abrogated and negligible levels of *Defcr21* and *24* (<1% of the WT) were detected in Aire$^{-/-}$ animals. *Ins2* and *Gad67*, well-characterized genes with Aire-dependent and independent expression, respectively, were used as controls. These data demonstrated that Aire controls the expression of cryptdins in mTECs.

## Cryptdin-Specific T Cells in Autoimmune Regulator–Deficient Mice

The lack of cryptdin expression in Aire$^{-/-}$ mTECs might result in impaired removal of cryptdin-specific T cells during negative selection in the thymus. To test this hypothesis, Aire$^{-/-}$ and WT littermate control mice were immunized with a mixture of cryptdin peptides and immune responses were analyzed 8 days later. As illustrated in Figure 4*A*, a sizeable fraction of CD4$^+$ and CD8$^+$ T cells derived from peripheral lymph nodes (pLNs) and mesenteric lymph nodes (mLNs) of cryptdin-immunized Aire$^{-/-}$, but not immunized WT mice or nonimmunized Aire$^{-/-}$, proliferated in response to antigen re-stimulation in vitro. In addition, the co-incubation of duodenum-derived CD8$^+$, but not CD4$^+$, T cells from cryptdin-immunized Aire$^{-/-}$ mice with FACS-sorted PCs increased the rate of cell death of the latter (Supplementary Figure 7). These results point to the presence of self-reactive cryptdin-specific T cells in the LNs of Aire$^{-/-}$ mice and their capacity to target and destroy PCs in vitro.

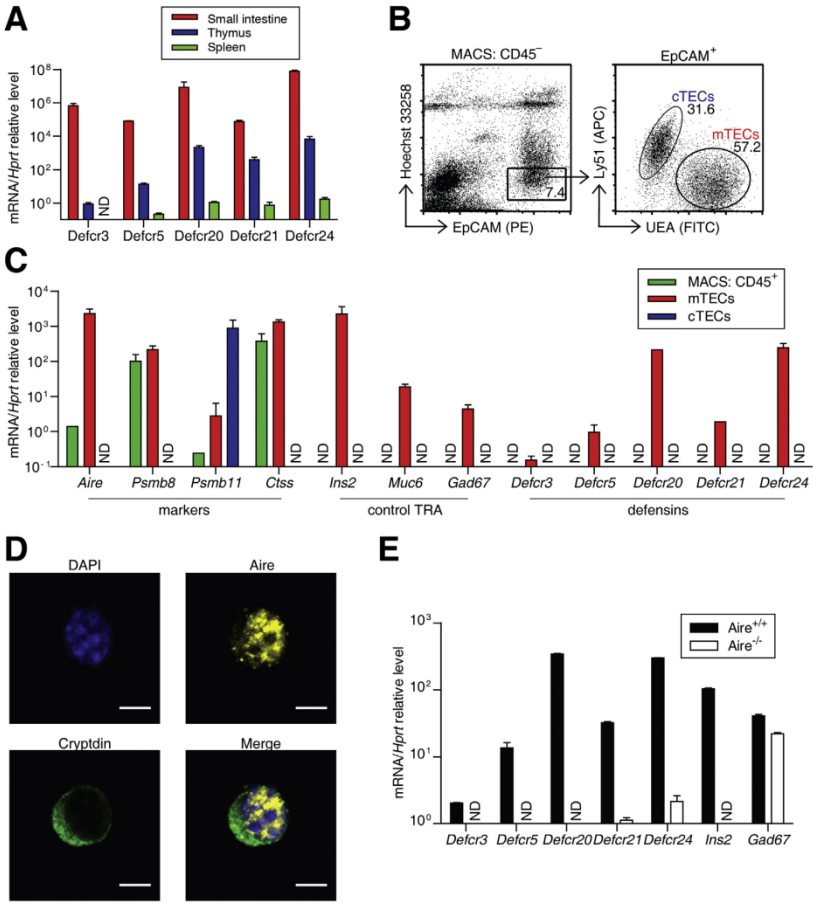


**Figure 3.** Thymic cryptdins are produced exclusively by murine mTECs. (*A*) Comparative quantitative reverse transcription polymerase chain reaction (qRT-PCR) analysis of cryptdin expression levels in the small intestine, thymus, and spleen. Data represent mean gene expression level (± SD) in organs isolated from 3 animals, each sample was assessed in triplicate. (*B*) Sorting strategy of thymic epithelial cells: CD45$^-$ EpCAM$^+$ thymic fraction (*left panel*) were separated into mTECs (UEA-1$^+$ Ly51$^{+/-}$) and cTECs (UEA-1$^{+/-}$ Ly51$^+$) (*right panel*). (*C*) The expression level of lineage-restricted markers (*Aire*, *Psmb8*, *Psmb11*, and *Ctss*), selected TRA genes (*Ins2*, *Muc6*, *Gad67*), and 5 cryptdins (*Defcr3*, *5*, *20*, *21*, and *24*) in MACS-enriched CD45$^+$ cells, mTECs, and cTECs) assessed by qRT-PCR analysis. Data shows the mean gene expression level (± SD) in denominated cells isolated and pooled from 4 animals and represents 3 independent experiments, each assessed in triplicate. ND, not detected. (*D*) Confocal immunofluorescence of mouse mTECs co-stained with antibodies specific for Aire and newly generated antibody against cryptdins marked as ED5 (Supplementary Figure 6). Nuclei are stained by 4′,6-diamidino-2-phenylindole (*blue*). Scale bar = 5 $\mu$m. One representative image is shown. (*E*) The expression of the 5 most abundant cryptdins in mTECs derived from WT and Aire$^{-/-}$ animals. Data represent the mean gene expression level (± SD) in mTECs isolated and pooled from 4 animals. Data are from 3 independent experiments, each was assessed in triplicate.

### *Cryptdin-Specific T Cells Mediate Intestinal Pathology in Nude Recipient Mice*

Next, we assessed the pathogenic relevance of cryptdin-specific T cells in vivo. T cells isolated from pLNs and mLNs of cryptdin-immunized WT or Aire$^{-/-}$ mice were re-stimulated in vitro with cryptdin-pulsed syngenic BMDCs. Subsequently, these T cells were adoptively transferred into athymic mice (Nude) that were examined 8 weeks later for signs of gut-related autoimmunity. As illustrated in Figure 4*B*, mLNs of Aire$^{-/-}$→Nude, but not Aire$^{+/+}$→Nude, were dramatically enlarged and their cellularity was increased. Concomitantly, we observed a mild increase in the frequency of CD8$^+$ T cells in both pLNs and mLNs, while the frequency of CD4$^+$ T cells remained comparable (Figure 4*C*). In addition, both mLNs and pLNs from Aire$^{-/-}$→Nude contained a significantly increased number of activated, CD69-positive

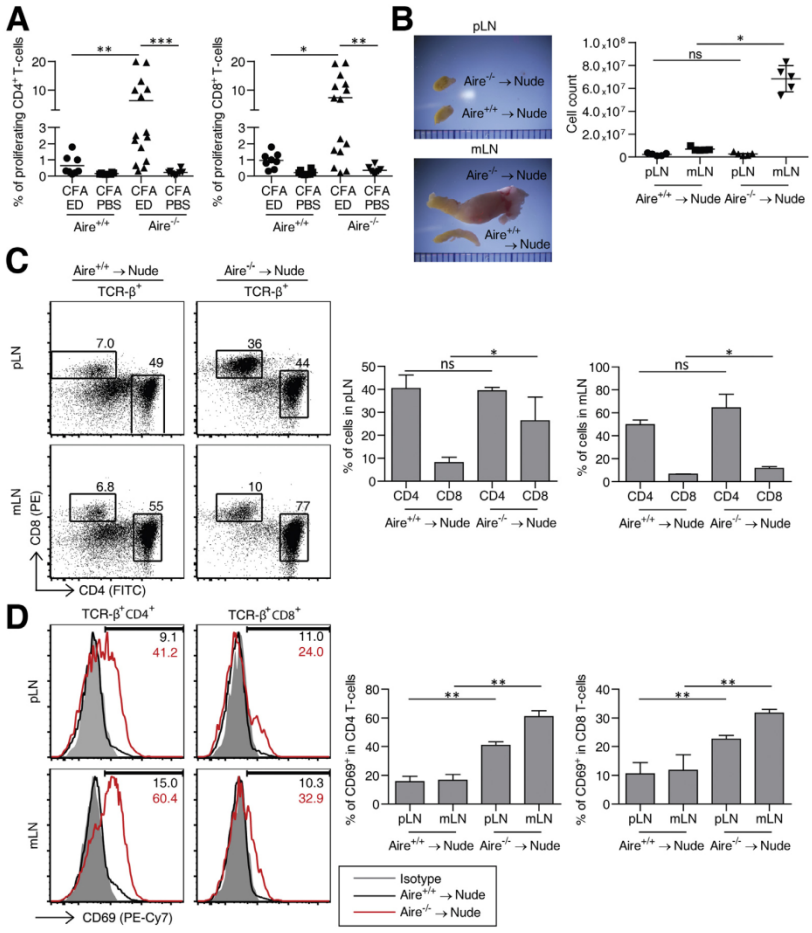


**Figure 4.** Establishment of nude mouse model of T-cell–mediated cryptdin-specific autoimmunity. (*A*) Visualization of cryptdin-specific T cells. T cells from LNs of Aire deficient ($Aire^{-/-}$) or WT ($Aire^{+/+}$) mice immunized with a mixture of Complete Freund's adjuvant with cryptdins (CFA+ED) or CFA with phosphate-buffered saline were labeled with proliferation dye and co-cultured with cryptdin-pulsed bone marrow-derived dendritic cells. The proliferation of T cells was measured by FACS. *Graphs* show the quantification of cryptdin-specific $CD4^+$ and $CD8^+$ T-cell responses. Statistical analysis was performed using 2-tailed Mann-Whitney test, $^*P < .05$; $^{**}P < .01$; $^{***}P < .001$. (*B*) The expansion of cryptdin-specific T cells in lymph nodes of nude mice. T cells from immunized $Aire^{-/-}$ or $Aire^{+/+}$ mice were transferred into nude mice recipients ($Aire^{-/-} \rightarrow$ Nude or $Aire^{+/+} \rightarrow$ Nude, respectively). *Images* illustrate the size of pLNs and mLNs. The *graph* shows the total cell count for pLN and mLN from each group of animals. Data are presented as mean ± SD, n = 5. Statistical analysis was performed using 2-tailed Mann-Whitney test, $^*P < .05$; NS, not significant. (*C*) An increased frequency of $CD8^+$ T cells in both pLNs and mLNs of $Aire^{-/-} \rightarrow$ Nude mice enumerated by FACS. Representative dot-plots are shown. The *bar graphs* show the statistical analysis of this experiment as mean ± SD, n = 5, performed using 2-tailed Student's *t* test, $^*P < .05$, ns, not significant. (*D*) LNs contained the increased number of activated $CD4^+$ and $CD8^+$ T cells. Histogram overlays represent the level of expression of the activation marker CD69 on $CD4^+$ and $CD8^+$ T cells derived from the pLN (*upper panel*) and mLN (*bottom panel*) of $Aire^{-/-} \rightarrow$ Nude (*red line*) and control $Aire^{+/+} \rightarrow$ Nude mice (*black line*), on the background of isotype control staining (*gray line*). Representative histograms are shown. The *bar graphs* show the statistical analysis of this experiment as mean ± SD, n = 5, performed using 2-tailed Student *t* test, $^{**}P < .01$.

$CD4^+$ and $CD8^+$ T cells in comparison with $Aire^{+/+} \rightarrow$ Nude (Figure 4*D*).

Microscopic data and FACS quantification performed on the duodenum of $Aire^{-/-} \rightarrow$ Nude mice showed an approximately 4-fold increase in T cells infiltrating the gut (Figure 5*A* and *B*). Consistent with the presence of self-reactive T cells capable of targeting cryptdin-expressing cells (Supplementary Figure 7), the number of PCs in these mice was markedly reduced (Figure 5*C* and *D*). Immunofluorescent examinations indicated that the destruction of PCs

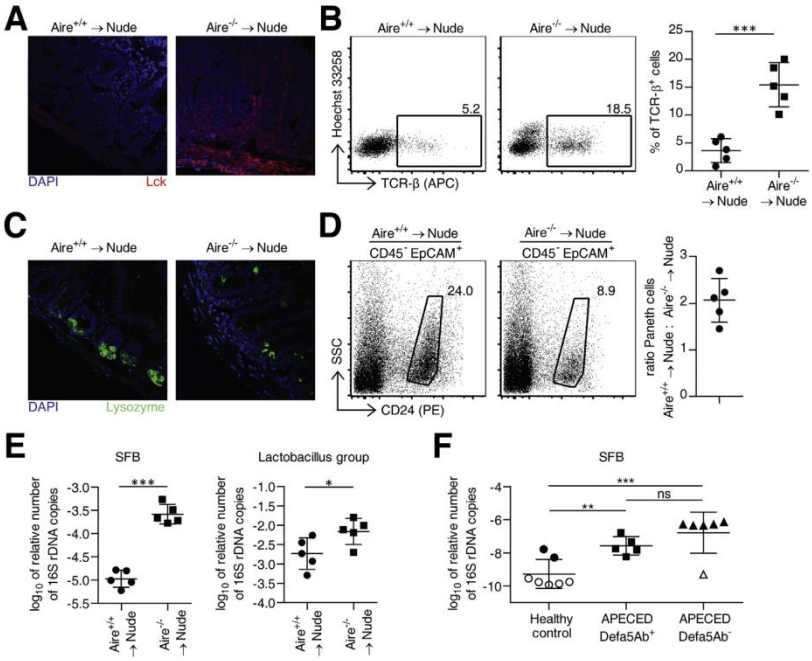


**Figure 5.** Cryptdin-specific T cells mediate intestinal autoimmunity. (*A*) Comparative anti-Lck immunostaining of small intestinal sections from Aire$^{+/+}$→Nude (*left panel*) and Aire$^{-/-}$→Nude mice (*right panel*). Representative images are shown. (*B*) The comparative analysis of frequency of gut-infiltrating T cells. T-cell receptor $\beta^+$ T cells from Aire$^{-/-}$→Nude and control Aire$^{+/+}$→Nude mice (n = 5) were quantified by FACS analysis. Data are shown as mean ± SD, ***$P < .001$, 1-tailed Student *t* test. (*C*) The loss of PCs visualized by lysozyme staining (*green*) on small intestinal sections from Aire$^{+/+}$→Nude (*left panel*) and Aire$^{-/-}$→Nude mice (*right panel*). Representative images are shown. (*D*) FACS analysis revealed the reduced number of CD24$^+$ PCs in Aire$^{-/-}$→Nude in comparison to control Aire$^{+/+}$→Nude mice (*2 left dot plot panels*). The *graph* depicts the relative fold-decrease of PCs in Aire$^{-/-}$→Nude mice. Data are presented as mean ± SD. (*E*) Changes in the microbiome composition in the gut of Aire$^{-/-}$→Nude mice in comparison to Aire$^{+/+}$→Nude controls determined by 16S quantitative reverse transcription polymerase chain reaction analysis. The relative enrichment of SFB bacteria and the Lactobacillus group are shown. Data are presented as mean ± SD, *$P < .05$; ***$P < .001$, 2-tailed Student *t* test. (*F*) The enrichment of SFB bacteria was also observed in stool samples from DEFA5-seronegative (Defa5Ab$^-$, n = 6) as well as seropositive (Defa5Ab$^+$, n = 5) APECED patients in comparison with the healthy control group (n = 7). Data are presented as mean ± SD, **$P < .01$; ***$P <$ .001, ns, not significant, 2-tailed Student *t* test. The *open circles* and *triangle* represent samples below the sensitivity threshold of quantitative polymerase chain reaction assay for SFB (see Materials and Methods).

was cell-specific, as their diminution had no apparent impact on the overall intestinal architecture (Figure 5*A* and *C*). The involvement in this destruction process of cryptdin-specific antibodies could be largely excluded as the serum from both Aire$^{+/+}$→Nude and Aire$^{-/-}$→Nude failed to show any apparent crossreactivity with PCs (Supplementary Figure 8). The very same sera showed no reactivity toward EECs (Supplementary Figure 9*A*), whose distribution, morphology, and numbers in both Aire$^{+/+}$→Nude and Aire$^{-/-}$→Nude mice remained largely comparable (Supplementary Figure 9*B*).

As PCs are the exclusive source of cryptdins, which are involved in the regulation of gut microflora, we examined the composition of microbiota in Aire$^{-/-}$→Nude and Aire$^{+/+}$→Nude mice. Of 7 prevalent bacterial groups tested, segmented filamentous bacteria (SFB) and the lactobacillus group showed significant changes in their abundance (Figure 5*E*). It is important to stress that Aire$^{-/-}$ mice, which served as a source of cryptdin-specific T cells for adoptive transfers (Figure 4*A*), also exhibited significant, albeit less dramatic enrichment in SFB 8 weeks after immunization with cryptdins (Supplementary Figure 10). The shared genetic basis of gut autoimmunity observed in Aire$^{-/-}$ mice and APECED patients led us to examine the human gut microflora as well. A comparative analysis of the intestinal microbiome of APECED patients and healthy controls also showed significant enrichment of SFB in enteric α-defensin–seropositive and seronegative patients, with a more dramatic increase in the latter group (Figure 5*F*).

Because SFB are potent inducers of intestinal Th17 cells,[29] we next examined the polarization of CD4$^+$ T cells toward inflammation-inducing Th17 phenotype. The results demonstrated an 8- to 10-fold increase in the frequency of interleukin (IL)17A producing CD4$^+$ T cells in pLN and mLN

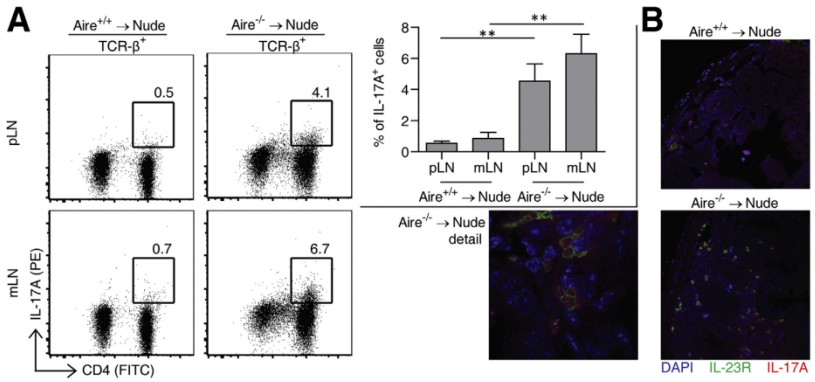


**Figure 6.** Cryptdin-specific T cells mediate inflammation-inducing Th17 phenotype. (*A*) The frequency of IL17A$^+$ CD4$^+$ T cells was determined by FACS analysis of T-cell receptor $\beta^+$ T cells from pLN (*upper panel*) and mLN (*bottom panel*) of Aire$^{-/-}$→Nude (n = 5) and control Aire$^{+/+}$→Nude mice (n = 5). The *bar graph* represents mean ± SD, $^{**}P < .01$, 2-tailed Student *t* test. (*B*) Representative images visualize the presence of pathogenic T cells co-expressing IL23 receptor (*green*) and IL17A (*red*) in the gut of Aire$^{-/-}$→Nude mice.

from Aire$^{-/-}$→Nude mice in comparison with controls (Figure 6*A*). Recently, it was reported that induction of autoimmune pathology by Th17 T cells in mice also requires the elevated co-expression of the IL23 receptor.[30] As illustrated in Figure 6*B*, immunofluorescence analysis of IL17A and IL23 receptor co-stained intestine sections showed a detectable presence of these cells in Aire$^{-/-}$→Nude but not in Aire$^{+/+}$→Nude mice. Collectively, these rodent data support the notion that self-reactive cryptdin-specific T cells are capable of infiltrating the small intestine and initiating PC-related pathologic changes in comparison with those observed in the gut of APECED patients.

## Discussion

Despite the clinical manifestation of intestinal symptoms in a relatively large proportion of APECED patients,[9,31,32] there are only a few reports related to their underlying molecular causes. So far, the absence of EECs[33] accompanied by the detection of antibodies against tryptophan hydroxylase and histidine decarboxylase produced by these cells, has been the only abnormality found in the intestines of some APECED patients.[23,24] This study identifies enteric α-defensins and their cellular source, PCs, as additional autoimmune targets in AIRE-deficient humans and mice.

We provide evidence that cryptdins are expressed by mTECs under the control of Aire. These data are consistent with previous reports that show that the *Defcr5* and *Defcr2-rs* gene expression were down-regulated in mTECs derived from mice bearing the *G228W* dominant-negative variant of Aire[25] and Aire$^{-/-}$,[3] respectively. Our results also demonstrate that several cryptdin transcripts belong to a rare class of genes whose expression in mTECs is fully dependent on Aire.[1,25]

Considering enteric α-defensins as gut-derived self-antigens, the critical step would be their presentation to, and activation of, cognate self-reactive T cells. Due to observed commonalities between Aire$^{-/-}$ mice and patients with APECED in their failure to tolerize enteric α-defensin–specific T cells, in Supplementary Figure 11, we propose a model depicting the possible steps leading to such a scenario. Specifically, bacteria-bound enteric α-defensins are picked up and presented by intestinal M cells and/or dendritic cells. After their activation, enteric α-defensin–specific CD8$^+$ T cells attack PCs and diminish their overall number. Such an outcome was observed in the entire cohort of nude mice transferred with enteric α- defensin–specific T cells and also in 6 of 10 available archival intestinal biopsies from APECED patients.

Another novel finding was the change in the composition of intestinal microbiota, especially the enrichment of SFB. These gram-positive commensal bacteria exhibit a striking ability to directly adhere to epithelial cells and induce Th17 responses.[21] Notably, while the transgenic production of human DEFA5 by mouse PCs[20] led to decreased levels of SFB,[21] diminished production of cryptdins increased both the level of SFB and the intestinal Th17 T-cell subset.[21] Similarly, de novo colonization of several mice models with SFB resulted in the robust development of the Th17 subset[29,34] and intestine autoimmunity.[35,36] These data have demonstrated a causal link among the production of cryptdins, SFB levels, and Th17-driven pro-inflammatory responses in a mouse model. Our data are also consistent with the conclusion of a previous study that the presence of SFB positively affects the abundance of Lactobacillus.[37]

Importantly, although the presence of SFB in infants and in a fraction of adult stool samples has been reported recently, their role in the regulation of human intestinal Th17 immune homeostasis is currently unknown.[37] To the best of our knowledge, this is the first report documenting the enrichment of SFB under intestinal autoimmune conditions in humans. In this context, the SFB status could be used as a clinical marker of intestinal cellular autoimmunity in APECED. However, the caveat of bluntly applying the described link among the cryptdin production, SFB levels,

and Th17 responses to humans, is that, due to the presence of neutralizing anti-IL17F antibodies, the APECED patients suffer from a significant loss of Th17 cells.[38] Although this could explain a striking difference in high and low levels of cellular infiltrates in mouse model and APECED patients, respectively, the number and contribution of intestine-residing Th17 cells to gut autoimmunity at an early stage of disease, has not yet been analyzed.

Whether the presence of DEFA5 autoantibodies in APECED is linked to any pathologic function is currently unknown. However, we could not find any evidence for their involvement in the destruction of PCs in Aire$^{-/-}$→Nude mice (Supplementary Figure 8). Similarly, no direct evidence for the adverse role of autoantibodies in Aire$^{-/-}$ mice has been found so far.[39] The association between the occurrence of DEFA5 antibodies and the incidence of diarrhea found among Finnish/Czech patients can be simply related to the presence of enteric α-defensin–reactive T cells in the periphery (Supplementary Figure 5). It is unclear why Sardinian patients failed to show a similar association. The combination of 2 distinct and prevailing AIRE mutations, R257X and R139X, in Finnish/Czech and Sardinian populations, respectively, with other genetic and environmental factors (such as HLA, diet, and climate) likely accounts for this discrepancy. The precedence for the nearly similarly different manifestation of APECED symptoms between Finnish and Sardinian patients, notably the absence of autoimmune hypothyroidism in the latter, has been recognized previously.[32] A multicenter longitudinal study of a large group of patients is needed to address this issue.

Because of the failure of central tolerance in APECED patients, the periphery contains self-reactive T-cell clones that can simultaneously target numerous intestinal components. This notion is supported by the following lines of evidence: sera from APECED patients lacking EECs cross-reacted with Paneth and Goblet cells[23] and DEFA5-seropositive patients or those lacking PCs display a deteriorated number of EECs (Table 1); DEFA5-seropositive and PC-lacking patients showed high cross-reactivity with many other, yet unidentified intestinal autoantigens (Figure 2*B* and Supplementary Figure 3*A*); intestine-related disease progresses through stages with an increasing number of self-reactivities, culminating in the probably concurrent loss or severe diminishment of PCs and EECs (Supplementary Figure 4, Table 1). Given this gradually developing nature of multi-targeted intestine autoimmunity concomitantly affecting distinct type of cells, it is seemingly difficult to establish the cellular basis for its variable manifestations, such as diarrhea, constipation, malabsorption, and abdominal pain.[11] However, our data provide an initial clue linking at least 2 of the symptoms mentioned to specific autoimmune cellular targets. First, we found a significant association between DEFA5 seropositivity and the manifestation of diarrhea among Finnish/Czech patients. Importantly, all 4 biopsies from DEFA5-seropositive patients revealed decreased or no PCs, one of them with a normal number of EECs. Second, we have recently shown that the tryptophan hydroxylase and decarboxylase seropositivity, 2 enzymes responsible for the production of the main product of EECs, serotonin, as well as the lack of serotonin-expressing EECs, significantly correlated with constipation in APECED patients.[40]

The complexities of gastrointestinal symptoms in APECED patients represents a combinatorial effect of multi-targeted autoimmune attack that includes minimal PCs and EECs, without obvious suspect of the initial autoimmune target. Although our data provide full support for such a scenario, the key point of this report is the destruction of PCs by immunologic mechanism, whereby self-reactive enteric α-defensin–recognizing T cells drive the process of initiation of PC destruction, leading to intestinal microbiome dysregulation and presumably to enhanced Th17 responses, which further amplify inflammatory autoimmunity in the intestine. Although it is impossible to evaluate this scenario in humans, our mouse data suggest that, in experimentally controlled conditions, autoimmunity toward PCs can be uncoupled from autoimmunity, which targets EECs.

Together these findings provide evidence that enteric α-defensins are clinically important self-antigens in gut-related autoimmunity in APECED patients. They also establish a mechanistic link between the disruption of central tolerance to enteric α-defensins and the onset of intestinal autoimmunity. In addition, the novel mouse model of gut-related symptoms provides a future experimental framework for clarifying the cellular and molecular basis of intestinal autoimmune processes in APECED patients. Importantly, these findings also warrant further prospective studies testing the concept that prevention strategies targeting the composition of intestinal microbiota can attenuate inflammation-propelled gastrointestinal dysbiosis and symptoms in APECED patients.

## Supplementary Material

Note: To access the supplementary material accompanying this article, visit the online version of *Gastroenterology* at www.gastrojournal.org, and at http://dx.doi.org/10.1053/j.gastro.2015.05.009.

## References

1. Mathis D, Benoist C. Aire. Annu Rev Immunol 2009; 27:287–312.
2. Klein L, Kyewski B, Allen PM, et al. Positive and negative selection of the T cell repertoire: what thymocytes see (and don't see). Nat Rev Immunol 2014;14:377–391.
3. Anderson MS, Venanzi ES, Klein L, et al. Projection of an immunological self shadow within the thymus by the aire protein. Science 2002;298:1395–1401.
4. Liston A, Lesage S, Wilson J, et al. Aire regulates negative selection of organ-specific T cells. Nat Immunol 2003;4:350–354.
5. Aschenbrenner K, D'Cruz LM, Vollmann EH, et al. Selection of Foxp3+ regulatory T cells specific for self antigen expressed and presented by Aire+ medullary thymic epithelial cells. Nat Immunol 2007;8:351–358.
6. **Nagamine K, Peterson P, Scott HS**, et al. Positional cloning of the APECED gene. Nat Genet 1997; 17:393–398.

7. Consortium F-GA. An autoimmune disease, APECED, caused by mutations in a novel gene featuring two PHD-type zinc-finger domains. Nat Genet 1997; 17:399–403.
8. Kisand K, Peterson P. Autoimmune polyendocrinopathy candidiasis ectodermal dystrophy: known and novel aspects of the syndrome. Ann N Y Acad Sci 2011; 1246:77–91.
9. Perheentupa J. Autoimmune polyendocrinopathy-candidiasis-ectodermal dystrophy. J Clin Endocrinol Metab 2006;91:2843–2850.
10. Ahonen P, Myllarniemi S, Sipila I, et al. Clinical variation of autoimmune polyendocrinopathy-candidiasis-ectodermal dystrophy (APECED) in a series of 68 patients. N Engl J Med 1990;322:1829–1836.
11. Kluger N, Jokinen M, Krohn K, et al. Gastrointestinal manifestations in APECED syndrome. J Clin Gastroenterol 2013;47:112–120.
12. Clevers HC, Bevins CL. Paneth cells: maestros of the small intestinal crypts. Annu Rev Physiol 2013; 75:289–311.
13. Bevins CL. The Paneth cell and the innate immune response. Curr Opin Gastroenterol 2004;20:572–580.
14. Selsted ME, Ouellette AJ. Mammalian defensins in the antimicrobial immune response. Nat Immunol 2005; 6:551–557.
15. **Amid C, Rehaume LM**, Brown KL, et al. Manual annotation and analysis of the defensin gene cluster in the C57BL/6J mouse reference genome. BMC Genomics 2009;10:606.
16. Shanahan MT, Tanabe H, Ouellette AJ. Strain-specific polymorphisms in Paneth cell alpha-defensins of C57BL/6 mice and evidence of vestigial myeloid alpha-defensin pseudogenes. Infect Immun 2011;79:459–473.
17. Jones DE, Bevins CL. Paneth cells of the human small intestine express an antimicrobial peptide gene. J Biol Chem 1992;267:23216–23225.
18. Jones DE, Bevins CL. Defensin-6 mRNA in human Paneth cells: implications for antimicrobial peptides in host defense of the human bowel. FEBS Lett 1993;315:187–192.
19. Wilson CL, Ouellette AJ, Satchell DP, et al. Regulation of intestinal alpha-defensin activation by the metalloproteinase matrilysin in innate host defense. Science 1999;286:113–117.
20. Salzman NH, Ghosh D, Huttner KM, et al. Protection against enteric salmonellosis in transgenic mice expressing a human intestinal defensin. Nature 2003; 422:522–526.
21. Salzman NH, Hung K, Haribhai D, et al. Enteric defensins are essential regulators of intestinal microbial ecology. Nat Immunol 2010;11:76–83.
22. Soderbergh A, Myhre AG, Ekwall O, et al. Prevalence and clinical associations of 10 defined autoantibodies in autoimmune polyendocrine syndrome type I. J Clin Endocrinol Metab 2004;89:557–562.
23. Ekwall O, Hedstrand H, Grimelius L, et al. Identification of tryptophan hydroxylase as an intestinal autoantigen. Lancet 1998;352:279–283.
24. Skoldberg F, Portela-Gomes GM, Grimelius L, et al. Histidine decarboxylase, a pyridoxal phosphate-dependent enzyme, is an autoantigen of gastric enterochromaffin-like cells. J Clin Endocrinol Metab 2003;88:1445–1452.
25. Su MA, Giang K, Zumer K, et al. Mechanisms of an autoimmunity syndrome in mice caused by a dominant mutation in Aire. J Clin Invest 2008;118:1712–1726.
26. Lewin K. The Paneth cell in disease. Gut 1969; 10:804–811.
27. Betterle C, Dal Pra C, Mantero F, et al. Autoimmune adrenal insufficiency and autoimmune polyendocrine syndromes: autoantibodies, autoantigens, and their applicability in diagnosis and disease prediction. Endocr Rev 2002;23:327–364.
28. Vogel A, Strassburg CP, Obermayer-Straub P, et al. The genetic background of autoimmune polyendocrino pathy-candidiasis-ectodermal dystrophy and its autoimmune disease components. J Mol Med (Berl) 2002; 80:201–211.
29. **Ivanov II, Atarashi K**, Manel N, et al. Induction of intestinal Th17 cells by segmented filamentous bacteria. Cell 2009;139:485–498.
30. **Lee Y, Awasthi A**, Yosef N, et al. Induction and molecular signature of pathogenic TH17 cells. Nat Immunol 2012;13:991–999.
31. Husebye ES, Perheentupa J, Rautemaa R, et al. Clinical manifestations and management of patients with autoimmune polyendocrine syndrome type I. J Intern Med 2009;265:514–529.
32. Meloni A, Willcox N, Meager A, et al. Autoimmune polyendocrine syndrome type 1: an extensive longitudinal study in Sardinian patients. J Clin Endocrinol Metab 2012;97:1114–1124.
33. Posovszky C, Lahr G, von Schnurbein J, et al. Loss of enteroendocrine cells in autoimmune-polyendocrine-candidiasis-ectodermal-dystrophy (APECED) syndrome with gastrointestinal dysfunction. J Clin Endocrinol Metab 2012;97:E292–E300.
34. Gaboriau-Routhiau V, Rakotobe S, Lecuyer E, et al. The key role of segmented filamentous bacteria in the coordinated maturation of gut helper T cell responses. Immunity 2009;31:677–689.
35. **Lee YK, Menezes JS**, Umesaki Y, et al. Proinflammatory T-cell responses to gut microbiota promote experimental autoimmune encephalomyelitis. Proc Natl Acad Sci U S A 2010;108(Suppl 1):4615–4622.
36. Wu HJ, Ivanov II, Darce J, et al. Gut-residing segmented filamentous bacteria drive autoimmune arthritis via T helper 17 cells. Immunity 2010;32:815–827.
37. Yin Y, Wang Y, Zhu L, et al. Comparative analysis of the distribution of segmented filamentous bacteria in humans, mice and chickens. ISME J 2013; 7:615–621.
38. **Kisand K, Boe Wolff AS**, Podkrajsek KT, et al. Chronic mucocutaneous candidiasis in APECED or thymoma patients correlates with autoimmunity to Th17-associated cytokines. J Exp Med 2010;207:299–308.
39. Gavanescu I, Kessler B, Ploegh H, et al. Loss of Aire-dependent thymic expression of a peripheral tissue antigen renders it a target of autoimmunity. Proc Natl Acad Sci U S A 2007;104:4583–4587.

40. Kluger N, Jokinen M, Lintulahti A, et al. Gastrointestinal immunity against tryptophan hydroxylase-1, aromatic L-amino-acid decarboxylase, AIE-75, villin and Paneth cells in APECED. Clin Immunol 2015;158:212–220.

**Author names in bold designate shared co-first authorship.**

**Reprint requests**
Address requests for reprints to: Dominik Filipp, PhD, Laboratory of Immunobiology, Institute of Molecular Genetics AS CR, Vídeňská 1083, CZ-142 20 Prague 4, Czech Republic. e-mail: dominik.filipp@img.cas.cz; fax: +420 224.310.955.

**Acknowledgments**
The authors thank Zdeněk Cimburek from the Flow Cytometry Core Facility at the Institute of Molecular Genetics for expert technical assistance and Jasper Manning for assistance in preparation of the manuscript. The authors are greatly indebted to Ludger Klein (Institute for Immunology, LMU, Munich, Germany) and Philippe Poussier (Sunnybrook Research Institute, Toronto, Canada) for helpful comments on the manuscript.

Writing assistance received from Jasper Manning.

**Conflicts of interest**
The authors disclose no conflicts.

**Funding**
This work was supported by grant P302/12/G101 from the Grant Agency of Czech Republic (GA ČR). Annamari Ranki and Nicolas Kluger were supported by Helsinki University Hospital Research Grant TYH2013235 and Nicolas Kluger also by Finska Läkaresällskapet.

## 2. HIC1 TUMOR SUPPRESOR LOSS POTENTIATES TLR2/NF-κB SIGNALLING AND PROMOTES TISSUE DAMAGE-ASSOCIATED TUMORIGENESIS

Hypermethylated in cancer 1 (Hic1) is a transcriptional repressor which controls the expression of several genes implicated in the control of cell cycle and stress responses in sequence-specific manner (Rood and Leprince, 2013), or via the interaction with other transcription factors, as it was shown for its binding to Tcf4, leading to the inhibition of Tcf4-dependent genes expression (Valenta et al., 2006). Tcf4 is the essential factor for Wnt signaling pathway which also controls the intestinal tissue development and function (Korinek et al., 1998; Wehkamp et al., 2007). Hic1 was also shown to repress the expression of *Math1* and *Sox9* genes (Briggs et al., 2008) which are responsible for the development of intestinal secretory cells including PCs (Durand et al., 2012), suggesting potential role of Hic1 in intestine development and homeostasis maintenance.

*HIC1* gene is frequently inactivated by DNA methylation in solid tumors of human patients (Wales et al., 1995) and mice deficient in a single *Hic1* allele develop spontaneously malignant tumors due to the inactivating methylation of the remaining *Hic1* healthy allele (Chen et al., 2003).

The tissue-specific ablation of Hic1 in the intestinal epithelium leads to increased frequency of PCs. Their transcriptional analysis revealed higher expression levels of *Math1* and *Sox9*. This suggests that the absence of Hic1 leads to the loss of the negative regulatory loop shifting the overall intestinal development towards the secretory lineages. The transcriptional profiling of wild-type and Hic1-deficient mouse embryonal fibroblasts revealed *Toll-like receptor 2 (Tlr2)* as the candidate gene heavily repressed by Hic1 presence. Chromatin immunoprecipitation with Hic1 specific antibodies showed direct association of Hic1 with *Tlr2* regulatory elements. Moreover, Hic1 deficiency leads to the overall increase in Tlr2 expression in a large fraction of intestinal epithelial cells and higher susceptibility of experimental animals to colitis-associated tumorigenesis (Janeckova et al., 2015).

Applicant's contribution: FACS analysis of intestinal populations and PCs, FACS analysis of Tlr2 expression by intestinal cells, isolation of PCs by FACS-sort.

Oncogenes and Tumor Suppressors

Molecular Cancer Research

# HIC1 Tumor Suppressor Loss Potentiates TLR2/NF-κB Signaling and Promotes Tissue Damage–Associated Tumorigenesis

Lucie Janeckova[1], Vendula Pospichalova[1], Bohumil Fafilek[1], Martina Vojtechova[1], Jolana Tureckova[1], Jan Dobes[1], Marion Dubuissez[2], Dominique Leprince[2], Nikol Baloghova[1], Monika Horazna[1], Adela Hlavata[1], Jitka Stancikova[1], Eva Sloncova[1], Katerina Galuskova[1], Hynek Strnad[1], and Vladimir Korinek[1]

## Abstract

*Hypermethylated in cancer 1* (*HIC1*) represents a prototypic tumor suppressor gene frequently inactivated by DNA methylation in many types of solid tumors. The gene encodes a sequence-specific transcriptional repressor controlling expression of several genes involved in cell cycle or stress control. In this study, a *Hic1* allele was conditionally deleted, using a Cre/loxP system, to identify genes influenced by the loss of Hic1. One of the transcripts upregulated upon Hic1 ablation is the *toll-like receptor 2* (*TLR2*). *Tlr2* expression levels increased in Hic1-deficient mouse embryonic fibroblasts (MEF) and cultured intestinal organoids or in human cells upon *HIC1* knockdown. In addition, HIC1 associated with the *TLR2* gene regulatory elements, as detected by chromatin immunoprecipitation, indicating that *Tlr2* indeed represents a direct Hic1 target. The Tlr2 receptor senses "danger" signals of microbial or endogenous origin to trigger multiple signaling pathways, including NF-κB signaling. Interestingly, Hic1 deficiency promoted NF-κB pathway activity not only in cells stimulated with Tlr2 ligand, but also in cells treated with NF-κB activators that stimulate different surface receptors. In the intestine, Hic1 is mainly expressed in differentiated epithelial cells and its ablation leads to increased Tlr2 production. Finally, in a chemical-induced mouse model of carcinogenesis, Hic1 absence resulted in larger Tlr2-positive colonic tumors that showed increased proportion of proliferating cells.

**Implications:** The tumor-suppressive function of Hic1 in colon is related to its inhibitory action on proproliferative signaling mediated by the Tlr2 receptor present on tumor cells. *Mol Cancer Res; 13(7); 1139–48. ©2015 AACR.*

## Introduction

The *HIC1* gene was isolated as a candidate tumor suppressor gene during tumor DNA hypermethylation screen of the chromosome 17 short arm, a chromosomal region which is frequently reduced to homozygosity in human cancers (1). *Hic1*$^{-/-}$ mice die prenatally due to severe developmental defects of craniofacial structures and limbs (2). *Hic1*$^{+/-}$ mice are viable; however, they develop spontaneous malignant tumors that are Hic1 deficient due to the intact *Hic1* allele methylation (3). Hic1 protein functions as an evolutionarily conserved transcription repressor, which cooperates with several partners to regulate expression of multiple target genes (4). The protein is composed of three structural domains. The Broad complex, Tramtrack, Bric à brac/POx viruses, and Zinc finger (BTB/POZ) domain responsible for Hic1 multimerization is situated N-terminally, followed by the central region binding co-repressors such as C-terminal binding protein (CtBP). The C-terminal domain consists of five zinc fingers providing affinity to the specific Hic1-responsive (HiRE) sequence motif in DNA (5). The known Hic1 target genes participate in diverse cellular processes, including cell-cycle regulation, cell differentiation, DNA damage response, and metastatic invasion (reviewed in ref. 4). *Hic1* transcription is positively regulated by p53 protein, a key molecule inducing either cell-cycle arrest or apoptosis upon various cellular stress-inducing insults (6). Conversely, the p53 activity is restrained by a protein deacetylase encoded by the *sirtuin 1* (*Sirt1*) gene, whose expression is blocked by Hic1. *Hic1* inactivation thus leads to functional suppression of p53, allowing damaged cells to escape the p53-mediated response (7). Besides the direct regulation of gene expression, Hic1 attenuates transcription via interaction with other transcription factors. For example, association with Wnt pathway effector T-cell factor 4 (TCF4) sequesters TCF4 (and its transcriptional activator β-catenin) to nuclear speckles called Hic1 bodies. Subsequently, expression of the TCF4/β-catenin-responsive genes is inhibited (8).

The tissue maintenance of the single-layer intestinal epithelium is sustained by intestinal stem cells (ISC) that reside at the bottom

[1]Institute of Molecular Genetics, Academy of Sciences of the Czech Republic, Prague, Czech Republic. [2]CNRS UMR 8161, Institut de Biologie de Lille, Université Lille Nord de France, Institut Pasteur de Lille, Lille Cedex, France.

**Note:** Supplementary data for this article are available at Molecular Cancer Research Online (http://mcr.aacrjournals.org/).

Current address for V. Pospichalova: Faculty of Science, Masaryk University, Kotlarska 2, 611 37 Brno, Czech Republic.

**Corresponding Author:** Vladimir Korinek, Institute of Molecular Genetics AS CR, Videnska 1083, 142 20 Prague 4, Czech Republic. Phone: 420-241063146; Fax: 420-244472282; E-mail: korinek@img.cas.cz

**doi:** 10.1158/1541-7786.MCR-15-0033

of invaginations called intestinal crypts, where ISCs divide regularly and give rise to transit amplifying cells (TA). Rapidly dividing TA cells migrate upward and while exiting the crypt, they differentiate to absorptive enterocytes, mucus-producing goblet cells, and hormone-secreting enteroendocrine cells. In the small intestine, differentiated cells cover finger-like protrusions called villi; the surface of the colon is flat. The intestinal epithelium self-renewing in 3 to 5 days represents one of the most rapidly self-renewing tissues in the mammalian body. One exception from the outlined scheme are Paneth cells that secrete bactericidal cryptidins, defensins, or lysozyme. These relatively long-lived cells are present in the small intestine only. Moreover, during maturation, the Paneth cell does not migrate from the crypt but stays at the crypt bottom, where it persists for 6 to 8 weeks (reviewed in ref. 9). Owing to the dynamic turnover, the intestinal epithelium is at high risk of carcinogenesis. Although aberrant activation of the Wnt pathway initiates the majority of colorectal carcinomas (reviewed in ref. 10), CRC development is a multistep process that entails accumulation not only of genetic, but also of epigenetic changes in epithelial cells (11). The physiologic role of HIC1 in the intestine has not yet been elucidated in detail. However, in the mouse, Hic1 represses *atonal homolog 1* (*Atoh1*) and *SRY-box containing gene 9* (*Sox9*) genes, which are involved in the cell fate determination of secretory cell lineages in the small intestine (12–14).

In the present study, we used a conditional knock-out of the *Hic1* gene (15) to identify genes repressed by Hic1. Expression profiling of mouse embryonic fibroblasts (MEF) revealed six novel Hic1 target genes, including *Tlr2*. Tlr2 functions as a microbial sensor to initiate inflammation and immune responses. In addition, the receptor recognizes endogenous inflammatory mediators released from dead cells (review in ref. 16). Upon ligand binding, Tlr2 triggers several signal transduction pathways, including NF-κB signaling that activates expression of proinflammatory cytokines and enzymes, such as tumor necrosis factor-alpha (TNFα), interleukin 6 (IL6), and cyclooxygenase-2 (Cox2) (17). Solid tumors contain inflammatory infiltrates, and many recent studies have shown association between inflammation and increased risk of cancer development and progression. Furthermore, there is growing evidence that Tlr2 activators released from cancer cells might initiate persistent inflammation found in many tumors (reviewed in ref. 18). However, two recent studies documented an inflammation-independent Tlr2 role in promoting gastric and intestinal cancer (17, 19). Here, we show that *Hic1* depletion in the intestinal epithelium resulted in increased Tlr2 expression that promoted proliferation of colonic tumors induced by chemical carcinogenesis.

## Materials and Methods

### Experimental mice

Housing of mice and *in vivo* experiments were performed in compliance with the European Communities Council Directive of 24 November 1986 (86/609/EEC) and national and institutional guidelines. Animal care and experimental procedures were approved by the Animal Care Committee of the Institute of Molecular Genetics (Ref. 82/2011). Generation and genotyping of $Hic1^{flox/flox}$ and Hic1 citrine reporter ($Hic1^{cit/+}$) mice was described previously (15). The *Rosa26-CreERT2* [B6.129-Gt (ROSA)26Sor$^{tm1(cre/ERT2)Tyj}$/J] mouse strain was purchased from The Jackson Laboratory and was genotyped as recommended by the provider. *Villin-CreERT2* and *Villin-Cre* transgenic mice (20) were kindly provided by Sylvie Robine (Institut Curie, Centre de Recherche, Paris, France). Animals were housed in specific pathogen-free conditions. Tumors of the colon and rectum were collected from adult $Hic1^{flox/flox}$ *Villin-Cre*$^{+}$ mice 5 weeks after a single subcutaneous injection of azoxymethane [(AOM); 10 mg/kg; purchased from Sigma] that was followed by a 5-day dextran sodium sulfate (DSS) treatment in drinking water [2% (w/v) DSS; MW 36–50 kDa; MP Biomedicals]. The mice were euthanized and the intestines were dissected, washed in PBS, and fixed in 4% formaldehyde (v/v) in PBS for 3 days. Fixed intestines were embedded in paraffin, sectioned and stained. The number and size of the neoplastic lesions were quantified using Ellipse software (ViDiTo). Colitis was induced by DSS (2% in the drinking water for 5 days) without AOM treatment. Colons were collected 2, 6, and 9 days upon DSS withdrawal.

### Cell and organoid culture, 4-hydroxytamoxifen (4-OHT) treatment

MEFs were isolated from embryos obtained at embryonic day (E) 11 to E14, details of the procedure are given in Supplement. For Cre-mediated recombination, cells were cultured in the presence of 4-OHT at a final concentration of 2 μmol/L (prepared from 1 mmol/L solution in ethanol; Sigma). Control cells were treated with the corresponding amount of ethanol. Small intestinal crypts were isolated and cultured according to the previously published protocol (21). Colonic crypts were isolated using the same procedure, but the culture medium was additionally supplemented with conditioned medium obtained from mouse Wnt3a-producing L cells (L-Wnt3a; ref. 22). L-Wnt3a, HEK293, and BJ-Tert cells were purchased from the ATCC (Cat. No.: CRL-2647, CRL-1573, and CRL-4001, respectively). All cell lines were obtained in 2006 and maintained in DMEM (Sigma) supplemented with 10% FBS (Gibco), penicillin, streptomycin, and gentamicin (Invitrogen). Upon receipt, cells were expanded and aliquots of cells at passage number <10 were stored frozen in liquid nitrogen. Cells from one aliquot were kept in culture for less than 2 months after resuscitation. The cell identity was not authenticated by the authors.

### Microarray analysis

Total RNA was isolated from MEFs harvested 24, 48, 72, and 120 hours upon 4-OHT addition using RNeasy Plus Mini Kit (Qiagen). Control cells were grown with the same volume of vehicle (ethanol). The quality of isolated mRNA was checked using Agilent Bioanalyzer 2100; RNAs with RNA integrity number (RIN) above 8 were further processed. Two biologic replicates were used for each time point and treatment. The RNA samples were analyzed using MouseRef-8 v2.0 Expression BeadChip (Illumina). Raw data were processed using the beadarray package of Bioconductor and analyzed as described previously (23). Gene set enrichment analysis (GSEA) was performed using the Enricher gene analysis tool (http://amp.pharm.mssm.edu/Enrichr; ref. 24). Microarray data were deposited in ArrayExpress (http://www.ebi.ac.uk/arrayexpress) under accession number E-MTAB-3486.

### Luciferase reporter assay, biochemistry, RNAi

MEFs were electroporated (details are given in Supplement); transfection of HEK293 cells was performed using Lipofectamine 2000 reagent (Invitrogen). Luciferase reporter constructs NF-κB-Luc and pRL-TK were purchased from Promega. To generate Tlr2-Luc reporter plasmid, genomic DNA containing the mouse Tlr2 promoter region encompassing nucleotides −796 to +52 (the

transcription start site corresponds to position +1) was amplified by PCR and cloned into the pGL4.26 luciferase reporter vector (Promega). The HIC1 construct was described previously (8). Details of the luciferase assay and NF-κB pathway stimulation are given in Supplement. For RNAi, BJ-Tert fibroblasts were reverse-transfected with Lipofectamine RNAiMax (Invitrogen) according to manufacturer's instructions using 10 nmol/L small interfering RNA (siRNA) targeting *HIC1* (HIC1 siGENOME SMART Pool M-006532-01, Dharmacon) or a scrambled control siRNA (siCtrl; siGENOME RISC free control siRNA, Dharmacon) and harvested 2 days upon transfection.

### ChIP and droplet digital PCR

Chromatin immunoprecipitation (ChIP) using chromatin obtained from immortalized BJ-Tert fibroblasts was performed as described previously (25). Occupancy of gene regulatory regions by HIC1 was assayed by ddPCR (QX200, Bio-Rad) using EvaGreen master mix (Bio-Rad). PCR primers are listed in Supplement.

### FACS

Paneth cell sorting was performed according to the previously published protocol (26). Antibodies used for flow cytometry: phycoerythrin (PE)-conjugated anti-CD24 (12-0242-81, eBioscience), allophycocyanin (APC)-conjugated anti-EpCam (17-5791-80, eBioscience), FITC-conjugated anti-CD45 (ED7018, ExBio).

### IHC

The technique was performed as described previously (27, 28). Hematoxylin and eosin (Sigma) were used for counterstaining. Antibodies are given in Supplement. For visualization of citrine fluorescence, intestines dissected from $Hic1^{cit/+}$ and wild-type (wt) mice were snap frozen in liquid nitrogen and immediately sectioned. Specimens were stained with 4′,6-diamidino-2-phenylindole, dihydrochloride (DAPI; Life Technologies) and the citrine fluorescence signal was evaluated using a laser scanning confocal microscope (Leica TCS SP5).

### Western blotting and antibodies

Hic1-specific polyclonal antisera were generated in rabbit or chicken immunized with the recombinant His-tagged fragment of human HIC1 protein (amino acids 154-396). Commercially available antibodies are given in Supplement.

### RNA purification and reverse-transcription quantitative PCR

Total RNAs were isolated from cells and tissues using RNeasy Mini Kit (Qiagen) and reversely transcribed and analyzed by qRT-PCR as described previously (29). The primers are listed in Supplementary Table S1.

### Statistical analysis of data

Results of the gene reporter assay, Ellipse, and qRT-PCR analysis were evaluated by the Student *t* test. Datasets obtained using DNA microarrays were analyzed in the R environment using the package LIMMA (Linear Models for Microarray Data LIMMA; ref. 30).

## Results

### Identification of *Tlr2* as a novel target gene repressed by Hic1 in mouse and human cells

To investigate the biologic function of transcription repressor Hic1, we have recently developed the $Hic1^{flox/flox}$ mouse strain that enables conditional inactivation of the *Hic1* gene (15). These mice were crossed to *Rosa26-CreERT2* animals expressing Cre recombinase estrogen receptor T2 fusion protein (CreERT2) from the *Rosa26* locus (31). The fusion protein resides in the cytoplasm until an antagonist of the estrogen receptor, tamoxifen (or its active metabolite 4-OHT), is administered. Subsequently, Cre enzyme is translocated into the nucleus, where it allows excision of DNA sequences flanked, that is, "floxed", by loxP sites (32). MEFs were isolated from embryos, cultured with 4-OHT or vehicle (ethanol) and genotyped by PCR to confirm locus recombination and generation of the $Hic1^{delEx2}$ allele. Simultaneously, the presence of Hic1 protein was detected by immunoblotting (Fig. 1A). Subsequently, total RNA was isolated at four time points after the addition of 4-OHT (or vehicle) into the culture media, and microarray analysis of the expression profile was performed. The analysis revealed genes whose expression was changed significantly ($q < 0.05$) after the *Hic1* locus recombination. Furthermore, six genes were upregulated in at least two time points and more than twice [the binary logarithm of fold change (log FC) > 1; Fig. 1B and Supplementary Fig. S1 and Supplementary Table S2]. These genes were *angiopoietin-like 7* (*Angptl7*), *carbonyl reductase 2* (*Cbr2*), *death-associated protein kinase 2* (*Dapk2*), *HSP, α-crystallin-related, B6* (*Hspb6*), *Tlr2*, and *WAP four-disulfide core domain 2* (*Wfdc2*). In addition, increased expression of previously identified HIC1 target genes *cyclin-dependent kinase inhibitor 1a* (*CDKN1A*; ref. 33), *Sox9* (13), and *Sirt1* (7) was observed, but these genes did not satisfy the significance criteria (not shown). Rather unexpectedly, the GSEA analysis using the Enricher gene library online tool (24) revealed that the inactivation of the *Hic1* gene in MEFs mainly altered expression of genes involved in lipid metabolism (Supplementary Table S3).

As recent evidence supports the role of TLR signaling in inflammation-associated tumorigenesis in the gastrointestinal tract (reviewed in ref. 34), we further investigated the relationship between Hic1 and *Tlr2* expression. First, we generated a Tlr2-Luc reporter by subcloning genomic DNA harboring the *Tlr2* promoter region before the luciferase sequence. Then, we cotransfected the Tlr2-Luc reporter together with the expression construct encoding HIC1 into HEK293 cells and performed the luciferase reporter assay. As expected, increasing amounts of HIC1 resulted in reduced activity of the reporter, whereas cotransfection with a control "empty" plasmid had no significant effect (Fig. 1C). Moreover, we used a HIC1-specific antibody to perform ChIP using chromatin isolated from BJ fibroblasts that express detectable amounts of endogenous HIC1 (25). Droplet digital PCR confirmed the enrichment of genomic DNA encompassing the promoter regions of *TLR2* and *SIRT1* (used as positive control) genes in the precipitate. Importantly, none of these regions was precipitated using a control "irrelevant" antibody and, furthermore, the anti-HIC1 antibody did not pull down the *β-ACTIN* promoter used as negative control. In addition, upregulation of *TLR2* and *SIRT1* was detected upon *HIC1* mRNA knockdown (Fig. 1D and data not shown). The *Tlr2* gene is activated by NF-κB signaling (35); therefore, the luciferase assay was performed in MEFs stimulated with NF-κB pathway activators TNFα, LTα, and with synthetic bacterial lipopeptide Pam3csk4, which functions as the Tlr2 ligand (36). Interestingly, Pam3csk4 appeared to be the most potent enhancer of the Tlr2-Luc activity, especially upon Hic1 deletion; however, the Tlr2-Luc activity was also significantly increased upon stimulation with unrelated LTα. In addition, the luciferase reporter assay clearly showed increased Tlr2-Luc activity

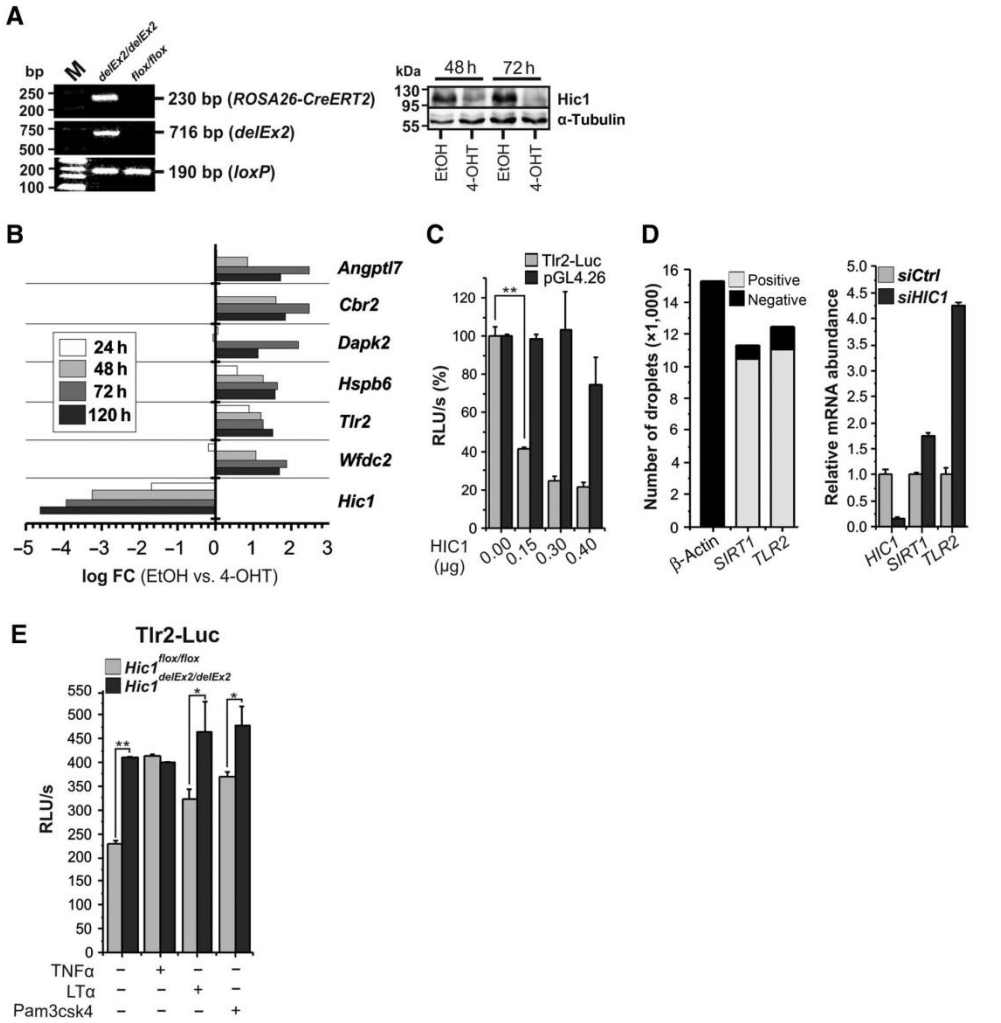


**Figure 1.**

*Tlr2* represents a novel direct target gene of transcriptional repressor Hic1. A, left, PCR genotyping of MEFs isolated from *Hic1*$^{flox/flox}$ *Rosa26*$^{CreERT2/+}$ embryos. Cells were cultured with 4-OHT for 4 days. PCR on the homozygous *flox/flox* and hemizygous *CreERT2* allele produced 190 bp or 230 bp DNA fragments, respectively. Cre-mediated recombination generated the *delEx2* allele lacking the second *Hic1* exon encoding the major part of the protein. The recombination is documented by the presence of the 716-bp PCR product. Right, immunoblotting of *Hic1*$^{flox/flox}$ *Rosa26*$^{CreERT2/+}$ cell lysates obtained from MEFs 48 and 72 hours after adding 4-OHT or solvent [ethanol (EtOH)]. Western blotting with an anti–α-tubulin antibody was used as a loading control. B, expression profile of *Hic1*$^{delEx2/delEx2}$ MEFs compared to *Hic1*$^{flox/flox}$ cells at the indicated time points after adding 4-OHT. The decrease in *Hic1* mRNA levels was accompanied by significant upregulation ($q < 0.05$) of six genes; log FC, binary logarithm of fluorescent intensity of the indicated gene-specific probe upon hybridization with labeled RNA isolated from MEFs treated with 4-OHT versus fluorescent intensity obtained using RNA isolated from cells treated with vehicle only. C, luciferase reporter assays in HEK293 cells cotransfected with the Tlr2-Luc reporter or control vector pGL4, respectively, together with increasing amounts of HIC1-producing plasmid. D, left, ddPCR using genomic DNA obtained from human BJ cells by ChIP with an anti-HIC1 antibody. Although PCR using primers designed from the promoter regions of *SIRT1* and *TLR2* genes, that is, genes directly repressed by HIC1, produced mainly droplets containing a PCR product, PCR with primers designed from the *β-ACTIN* promoter gave droplets without any product. Right, qRT-PCR analysis of BJ cells upon HIC1 knockdown. Expression level of the respective gene in cells treated with non-silencing siRNA (siCtrl) was set to 1. E, luciferase reporter assays in MEFs electroporated with Tlr2-Luc reporter plasmid. Cells were stimulated overnight with TNFα, LTα, or Pam3csk4. The histograms represent average luciferase light units per second (RLU/s) obtained in three independent experiments performed in triplicates. The values were corrected for efficiency of electroporation using *Renilla* luciferase as the internal control. Error bars represent SDs; *, $P < 0.05$; **, $P < 0.01$.

in Hic1-deficient MEFs when compared with cells with the intact *Hic1* locus (Fig. 1E). Several studies indicate the NF-κB pathway activation via Tlr2 signaling (37, 38). Thus, we next examined the consequence of *Hic1* deficiency for the NF-κB pathway. Luciferase reporter assay using the NF-κB-Luc reporter showed increased NF-κB signaling even in unstimulated $Hic1^{delEx2/delEx2}$ cells (compared with MEFs before Cre-mediated *Hic1* inactivation). Treatment of cells with Pam3csk4 further potentiated the reporter activity. However, increased NF-κB signaling was also observed upon stimulation with LTα and TNFα, indicating that the NF-κB pathway output was not completely dependent on Tlr2 (over) expression (Fig. 2A). The augmentation of the NF-κB pathway activity in Hic1-deficient MEFs was confirmed by qRT-PCR analysis that showed increased expression of the putative NF-κB target genes *Cox2* and *TNFα* (Fig. 2B). In agreement with these results, immunoblotting revealed increased levels of the phosphorylated transcriptionally active form of the nuclear mediator of NF-κB signaling p65 (Fig. 2C). In summary, all the data supported direct transcriptional repression of *Tlr2* by Hic1 and, moreover, potentiation of the NF-κB pathway activity upon loss of the *Hic1* gene.

### Hic1 depletion in the intestinal epithelium results in *Tlr2* upregulation

In the intestinal epithelium, the *Hic1* expression was examined using previously generated Hic1-citrine "reporter" mice. In this mouse strain, the sequence encoding the central and C-terminal portions of Hic1 protein was replaced by cDNA encoding citrine (yellow) fluorescent protein (15). In both the small and large intestine, native citrine fluorescence was observed in epithelial cells (Fig. 3A). Subsequently, production of Hic1 protein in the gut epithelia was confirmed by immunoblotting using cell lysates prepared from crypts and differentiated cells lining the villi in the small intestine or intercrypt regions (ICR) in the colon. The analysis revealed higher amounts of Hic1 in the villus and ICR fractions when compared with the crypts. This result was confirmed by qRT-PCR using total RNA isolated from the same epithelial fractions (Fig. 3B). In order to evaluate the expressional changes of the putative Hic1 target genes in epithelial cells, we established three-dimensional "organoid" cultures (21) from the small intestinal crypts of $Hic1^{flox/flox}$ *Villin-CreERT2*$^{+}$ mice producing tamofixen-regulated Cre enzyme in all intestinal cell lineages (20). Interestingly, Cre-mediated inactivation of the *Hic1* gene increased mRNA levels of all genes identified by the microarray analysis. Furthermore, like in MEFs, Hic1 deficiency resulted in upregulation of the NF-κB-responsive genes *Cox2* and *TNFα* (Fig. 3C). In addition, Tlr2 was analyzed in $Hic1^{flox/flox}$ *Villin-Cre*$^{+}$ mice expressing the constitutively active form of Cre enzyme in the embryonic and adult gut epithelia (20). Although efficient recombination and generation of the $Hic1^{delEx2}$ allele along the rostrocaudal axis of the gastrointestinal tract was confirmed by PCR genotyping (data not shown), these mice—lacking *Hic1* in the intestinal epithelium—were viable, showing no signs of any health problems. However, IHC staining showed increased Tlr2 positivity in the small intestine and colon (Fig. 3D).

### Hic1-deficient intestinal epithelium contains increased numbers of secretory cell lineages

As morphology and proliferation of the $Hic1^{loxP/loxP}$*Villin-Cre*$^{+}$ intestinal epithelium appeared to be normal, we performed detailed analysis of all major cellular lineages present in the small intestine. Maturation of Paneth cells is driven by transcription factors *Atoh1* and *Sox9* (14). Interestingly, Hic1 is a transcriptional repressor of *Atoh1* and *SOX9* in the mouse developing cerebellum and in U2OS osteosarcoma cells, respectively (12, 13). Using

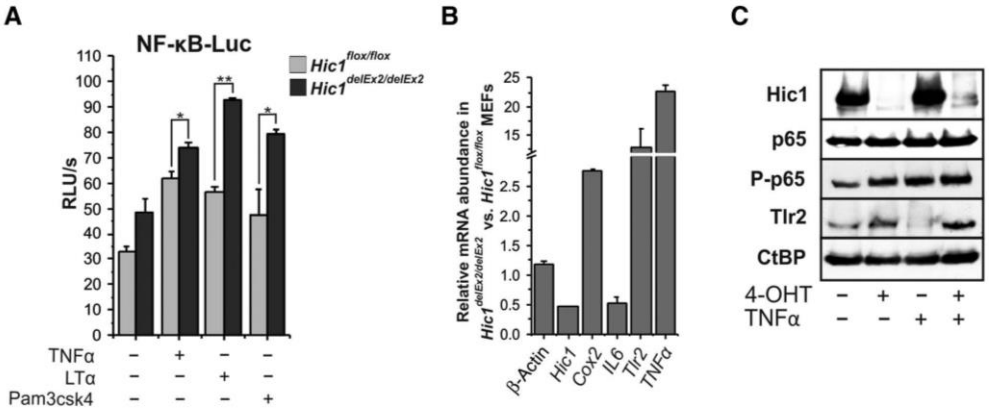


**Figure 2.**
Hic1-deficient MEFs display upregulated NF-κB signaling. A, luciferase reporter assays in MEFs cultured with 4-OHT or vehicle (ethanol) for 3 days and then electroporated with the NF-κB-Luc reporter. Six hours upon electroporation, TNFα, LTα, or Pam3csk4 was added to the culture medium and the cells were harvested 12 hours later. The assay was performed in triplicates, representative results are shown. *, $P<0.05$; **, $P < 0.01$. B, qRT-PCR analysis of putative target genes of NF-κB signaling *Cox2*, *IL6*, and *TNFα* in *Hic1*-deficient or control vehicle-treated MEFs. Total RNA was isolated from cells cultured with 4-OHT or vehicle for 3 days and then stimulated with the indicated ligand overnight. The results were normalized to the *Ubiquitin B* (*Ubb*) housekeeping gene; the relative expression of another housekeeping gene, *β-actin*, is also shown. The expression level of the respective gene in control vehicle-treated cells was arbitrarily set to 1. The analysis was performed in triplicates; error bars: SDs. C, immunoblotting of lysates prepared from MEFs cultured with 4-OHT or vehicle for 3 days and then stimulated with TNFα for 30 minutes. The experiment was repeated twice, representative blot is presented. CtBP, loading control; P-p65, immunoblotting with an antibody recognizing p65 phosphorylated at S536.

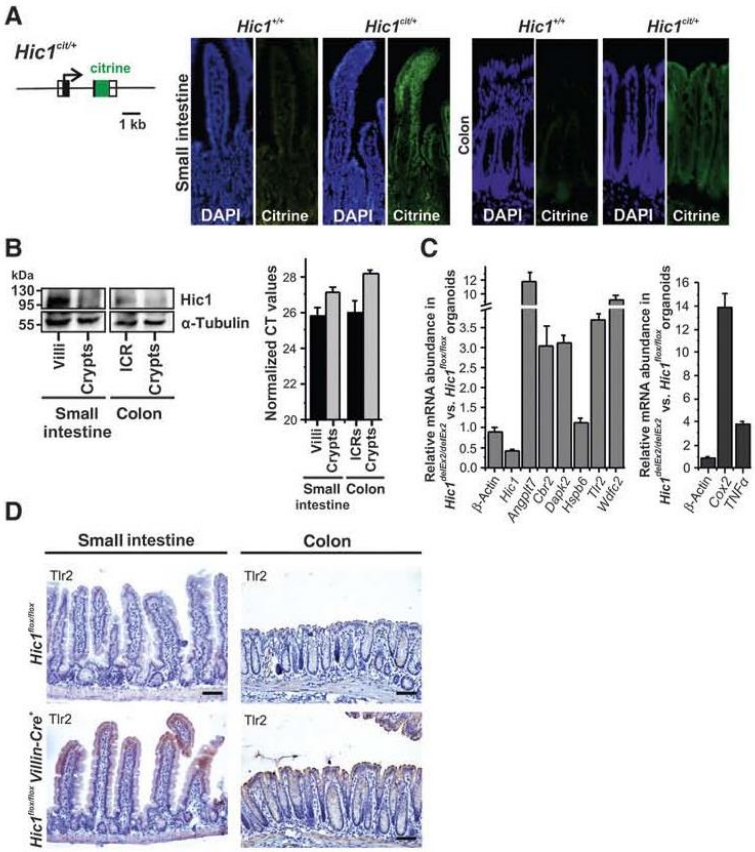


**Figure 3.**

Increased expression of *Tlr2* in *Hic1*-deficient small intestinal organoids and intestinal epithelia. A, production of Hic1-citrine fusion protein in $Hic1^{cit/+}$ mouse is restricted to the epithelium of the small intestine and colon. Left, a scheme of the *Hic1-citrine* reporter allele producing citrine fluorescent protein from the *Hic1* locus. Exons are depicted by boxes; coding sequences are filled, arrow indicates the transcription start site. Right, fluorescent microphotographs of cryosections of the small intestine and colon of $Hic1^{+/+}$ and $Hic1^{cit/+}$ mouse counterstained with DAPI nuclear stain (blue fluorescence). The right image from each pair was gained in "citrine" (green fluorescence) channel to monitor expression from the *Hic1* locus. No citrine fluorescence was observed in the intestine of control $Hic1^{+/+}$ animals. B, left, Western blotting from separated epithelial lining of the wt small intestinal villi and crypts and from the wt intercrypt regions (ICRs) and crypts of the colon; α-tubulin, loading control. Right, qRT-PCR analysis of total RNA isolated from the indicated regions of the intestinal epithelium. Cycle threshold ($C_t$) values normalized to *Ubb* are shown. C, qRT-PCR analysis of RNA isolated from organoids established from the small intestinal crypts of $Hic1^{flox/flox}$ *Villin-CreERT2*$^{+}$ mice. Vehicle (EtOH) or 4-OHT was added to the culture medium third day after the crypt isolation and the organoids were harvested after another 3 days. The expression level of the respective gene in vehicle-treated organoids was arbitrarily set to 1. The scheme represents results obtained in two independent experiments (each) performed in triplicates. Errors bars: SDs. D, IHC staining of Tlr2 [brown 3,3′-Diaminobenzidine (DAB) stain] in $Hic1^{flox/flox}$ and $Hic1^{flox/flox}$ *Villin-Cre+* intestines. The specimens were counterstained with hematoxylin (blue nuclear stain). Scale bar: 0.15 mm.

expression profiling of sorted Paneth cells isolated from the $Hic1^{flox/flox}$ *Villin-Cre*$^{+}$ and control ($Hic1^{flox/flox}$) small intestinal crypts, we observed a significant increase in *Atoh1*, *Sox9*, and *Tlr2* mRNA levels upon loss of Hic1. Moreover, FACS analysis showed a slight increase in Paneth cell counts in $Hic1^{flox/flox}$ *Villin-Cre*$^{+}$ animals (Fig. 4A). Increased Paneth cell numbers along the rostro-caudal axis of the small intestine were also recorded using paraffin sections stained with an antibody recognizing Paneth cell-specific marker lysozyme (Fig. 4B). In addition, the numbers of mucin-producing goblet cells and chromogranin A-positive enteroendocrine cells were also elevated. In contrast, the differentiation and number of absorptive enterocytes seemed unchanged in the Hic1-deficient intestine (Supplementary Fig. S2).

### Loss of Hic1 promotes colitis-associated tumorigenesis

Recently, Mohammad and colleagues described accelerated formation of tumors upon loss of *Hic1* in the $Apc^{Min/+}$ mouse model of intestinal cancer (39). Because inflammation is an important tumor promoter in colorectal neoplasia, the role of Hic1 was examined utilizing colitis-associated tumorigenesis. In

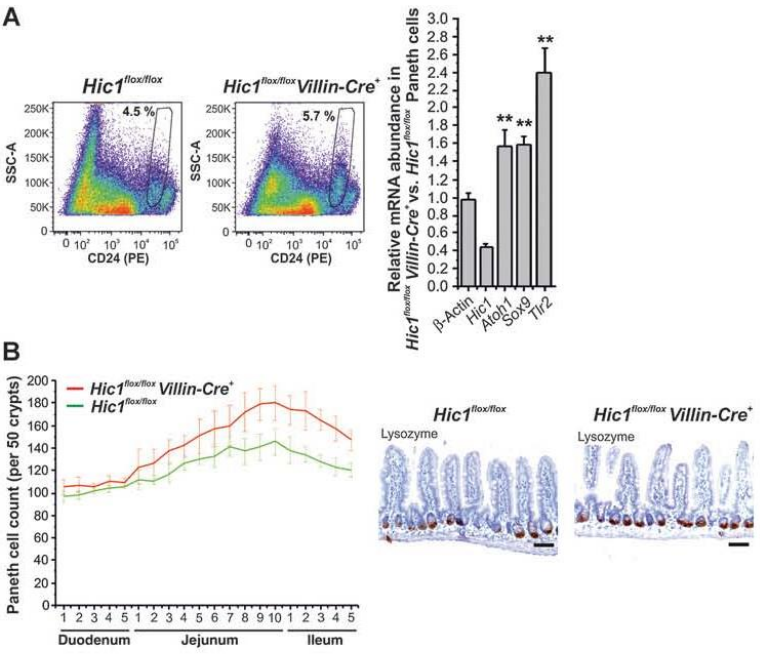


**Figure 4.**
Loss of the Hic1 function results in increased counts of Paneth cells. A, left, FACS analysis of Paneth cells obtained from the indicated mouse strains. Representative histograms show higher numbers of Paneth cells in the Hic1-deficient small intestine. Four animals per strain were used for the experiment. Right, qRT-PCR of sorted Paneth cells. Decreased *Hic1* expression results in upregulation of Hic1 target genes *Atoh1*, *Sox9*, and *Tlr2*. The expression level of the respective gene in *Hic1* wt cells was arbitrarily set to 1. **, $P < 0.01$. B, Paneth cell distribution in the indicated segments of the small intestine. Specimens obtained from four $Hic1^{flox/flox}$ and four $Hic1^{flox/flox}$*Villin-Cre*$^{+}$ mice were stained using an anti-lysozyme antibody to visualize Paneth cells (right images). Lysozyme-positive cells were counted in 50 neighboring crypts in several different fields indicated by numbers on the *x*-axis. Scale bar: 0.15 mm; error bars: SDs.

the acute colitis phase – induced by DSS treatment – no differences in the extent of tissue damage were observed in histologic specimens obtained from $Hic1^{flox/flox}$ *Villin-Cre*$^{+}$ and $Hic1^{flox/flox}$ mice. However, $Hic1^{flox/flox}$ *Villin-Cre*$^{+}$ individuals displayed more robust DSS treatment-associated transcriptional response of the *Cox2*, *Tlr2*, and *TNFα* genes, that is, genes upregulated upon *Hic1* loss. Analysis of the colon during the regenerative phase, that is, 6 and 9 days upon DSS withdrawal, showed a more robust hyperproliferative response of the colonic epithelium of $Hic1^{flox/flox}$ *Villin-Cre*$^{+}$ individuals when compared with their $Hic1^{flox/flox}$ littermates (Fig. 5A). Moreover, a continuous increase of *Cox2*, *Tlr2*, and *TNFα* expression was observed at these time points (Supplementary Fig. S3). Strikingly, upon combined AOM/DSS treatment, Hic1 deficiency significantly increased the size of colonic and rectal tumors (Fig. 5B; average tumor size in $Hic1^{flox/flox}$ mouse – 3.1 $mm^2$ vs. 8.7 $mm^2$ in $Hic1^{flox/flox}$ *Villin-Cre*$^{+}$; $P = 0.00862$). IHC examination revealed decreased numbers of p53-positive cells within the tumor mass of *Hic1*-negative mice. Nevertheless, even in $Hic1^{flox/flox}$ mice, cells displaying nuclear p53 staining were rare and scattered throughout the neoplastic tissue. However, expression of the p21 cell-cycle inhibitor, the most prominent in wt cells at the surface area of the tumors, was reduced in *Hic1* knock-outs. Strikingly, proliferating cell nuclear antigen (PCNA) expressing cells were localized in wt mice in areas clearly distinguished from the regions containing p21-positive cells. In contrast, in Hic1-deficient mice, proliferating cells were more abundant and dispersed throughout the neoplastic tissue. Finally, no differences were noted in the numbers of apoptotic cells (Fig. 5C and not shown).

## Discussion

In the present study, we used a gene inactivation-based screen to identify genes regulated by the Hic1 tumor suppressor. Interestingly, none of the identified presumptive Hic1 target genes was described previously. As the expression of all tested genes reacted to the Hic1 presence not only in MEFs, but also in intestinal organoids, we can exclude the possibility that the genes represent a small (sub)set of tissue-specific Hic1 targets. More likely, because the majority of previous studies utilized cells (over)producing ectopic HIC1 or cells treated with HIC1-specific siRNA (33), we suggest that (our) genes represent Hic1 target genes whose expression is relieved when the Hic1 steady-state levels are diminishing. On the other hand, the previously identified targets might represent genes efficiently repressed (or activated) immediately upon perturbation of the Hic1 protein levels. We used Hic1-reporter mice, Western blotting, and FACS analysis to demonstrate that in the adult intestine, Hic1 is mainly expressed in the differentiated epithelial cells. The expression of its target gene, *Tlr2*, was documented in ISCs (19). However, in the Hic1-deficient gut, Tlr2 was upregulated in differentiated cells, confirming the inverse Hic1-Tlr2 relationship. Moreover, intestinal ablation of *Hic1* resulted in a moderate increase in Paneth, goblet, and enteroendocrine cell numbers. Such phenotype might be attributed to upregulation of *Atoh1*, the Hic1 target gene functioning as the master regulator of secretory cell lineages in the small intestine (14). Upon ligand binding, Tlr2 triggers several signal transduction pathways, including NF-κB signaling (17). Interestingly, qRT-PCR analysis and luciferase reporter assays revealed that not only

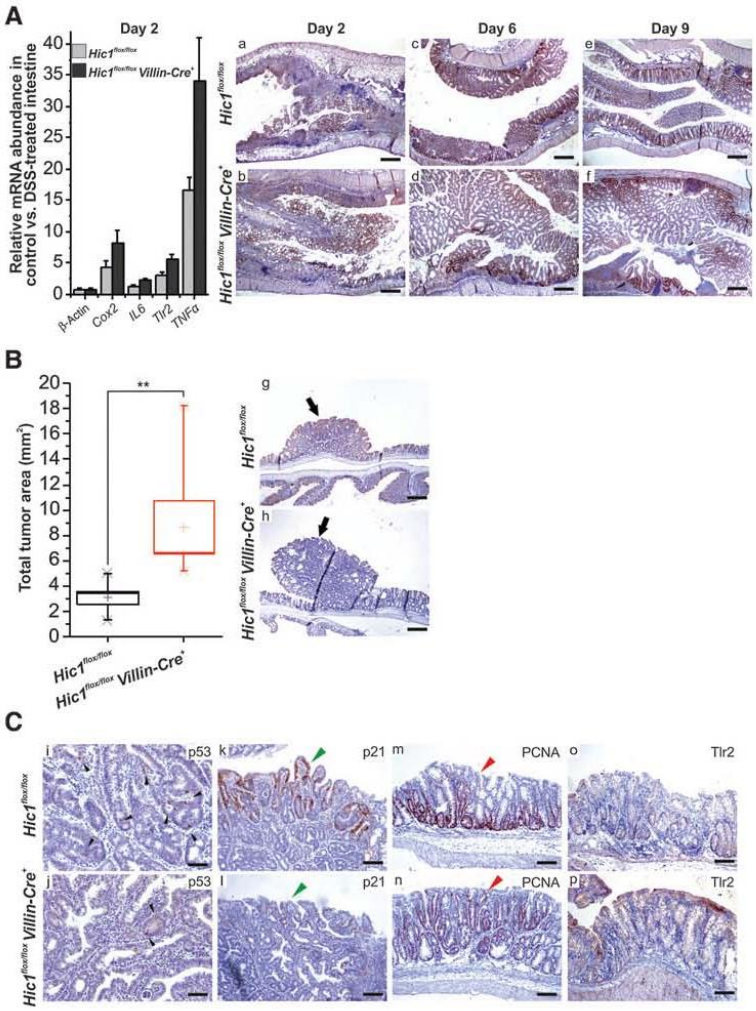


**Figure 5.**
*Hic1* deficiency increased the size of colonic tumors generated upon AOM/DSS treatment. A, acute colitis and regeneration after DSS treatment. Left, DSS-induced transcriptional response in the colon of $Hic1^{flox/flox}$ and $Hic1^{flox/flox}$ *Villin-Cre*$^{+}$ mice 2 days upon DSS withdrawal. The expression level of the corresponding genes in mice without DSS treatment was arbitrarily set to 1. Four animals for each genotype were analyzed. Right, representative microscopic images of the colon two (a, b), six (c, d) and nine (e, f) days upon DSS withdrawal. The specimens were stained using an anti-PCNA antibody to detect proliferative cells (brown nuclear precipitate) and counterstained with hematoxylin (blue nuclear staining). B, tumor size in the colon generated in the indicated mouse strains upon combined AOM/DSS treatment. Intestines dissected from seven animals in each group were analyzed 5 weeks after the AOM/DSS application. Left, quantification of the total tumor area indicating significantly increased tumor burden in the *Hic1*-deficient colon. The total tumor area determined in each individual is indicated in the boxplots. The boxed areas correspond to the second and third quartiles; the spread of the values is given by "whiskers" above and below each box. Median (transverse line) and mean (cross) is marked inside each box. **, $P < 0.01$; error bars: SDs. Right, representative microscopic images of the colon; neoplastic outgrows are indicated by black arrows. The specimens were counterstained with hematoxylin and an anti-β-catenin antibody. C, IHC detection of tumor suppressor p53 [black arrowheads in panel (i) and (j)], cell-cycle inhibitor p21 [green arrowheads in (k) and (l)], PCNA-positive [(m, n); red arrowheads indicate differentially stained tumor surface] and Tlr2-producing (o, p) cells in colonic tumors. Scale bar: 0.75 mm (a–h); 0.15 mm (i, j); 0.3 mm (k–p).

ligand-induced, but also basal levels of the NF-κB signaling are elevated in Hic1-deficient cells (Fig. 2A and B). As the NF-κB pathway activity was more pronounced even in cells stimulated with other NF-κB inducers, the observed NF-κB (hyper)activity cannot be solely attributed to the increase in Tlr2 expression or function. Indeed, Western blotting confirmed that $Hic1^{delEx2/delEx2}$ cells displayed higher amounts of phosphorylated nuclear NF-κB mediator p65 (Fig. 2C). The exact reason(s) why Hic1 deficiency potentiates NF-κB signaling remains to be determined. Nevertheless, since several studies reported interaction between the STAT3 and NF-κB pathways (reviewed in ref. 40), we suggest that the autocrine IL6-STAT3 signaling might also be linked to the observed "boosts" in cellular reactivity to the stimuli activating the NF-κB pathway and to the increase in p65 stability and phosphorylation.

Several studies have demonstrated that *Tlr2* expression is increased during intestinal inflammation (41) or in human patients with ulcerative colitis (42). In addition, Maeda and colleagues showed that conditioned medium obtained from cultured colon cancer cells might activate NF-κB signaling via Tlr2 (43). These data are in accordance with our observation that in damaged tissue, transcription of *Tlr2* and genes linked to active NF-κB signaling is elevated. Importantly, in the *Hic1*-deficient colon, the damage-induced transcriptional response was more robust than in wt mice, supporting the Hic1 repressive role in *Tlr2* expression and NF-κB activation (Fig. 5A and Supplementary Fig. S3). Interestingly, several recent studies reported decreased tumor burden in $Apc^{+/Min}$ mice deficient in Tlr2 or its intracellular adaptor myeloid differentiation primary response protein-88 (Myd88; refs. 19, 44). Furthermore, deletion of *Tlr2* (or *Myd88*) reduced development of

colonic tumors in DSS-treated animals. Moreover, functional blocking of TLR2 inhibited *in vitro* growth of cancer cells (19). In another study, epithelial expression of Tlr2 and Tlr2/NF-κB signaling promoted growth and survival of gastric cancer cells (17). In summary, all these results support the cell-autonomous and inflammation-independent role of Tlr2 in cancer.

HIC1 participates in the cellular network regulating the DNA damage response (7). HIC1-mediated repression of deacetylase *SIRT1* gene promotes p53 stability and potentiates transcription of p53-dependent genes such as *p21* (45) and, in a positive regulatory feedback loop, also *HIC1* itself (1, 46). Unexpectedly, only a small fraction of cells in tumors generated by AOM/DSS treatment displayed stabilized p53 (Fig. 5C). Although the portion of p53-positive cells was decreased in *Hic1*$^{-/-}$ neoplastic tissues, it is unlikely that the increased tumor size observed upon Hic1 deletion is linked to the attenuated p53-mediated response. In human cells, HIC1 directly represses transcription of the *CDKN1A* gene encoding p21 (33). Strikingly, in Hic1-deficient tumors, we observed the opposite effect of Hic1 absence, that is, reduced p21 staining (Fig. 5C). Nevertheless, the observed discrepancy of the results might be explained by the fact that next to p53 and HIC1, p21 levels might be controlled by many other stimuli and also by post-transcriptional mechanisms (reviewed in ref. 47). As we noted increased cell proliferation upon DSS-induced epithelial damage and in Hic1-negative AOM/DSS tumors, we suggest that besides compromising the p53-mediated tumor-suppressive mechanisms the loss of Hic1 might potentiates tumor-promoting proproliferative Tlr2/NF-κB signaling.

## Disclosure of Potential Conflicts of Interest

No potential conflicts of interest were disclosed.

## Authors' Contributions

**Conception and design:** L. Janeckova, V. Pospichalova, V. Korinek
**Development of methodology:** V. Pospichalova, M. Dubuissez, D. Leprince, A. Hlavata, V. Korinek
**Acquisition of data (provided animals, acquired and managed patients, provided facilities, etc.):** L. Janeckova, V. Pospichalova, M. Vojtechova, J. Tureckova, J. Dobes, M. Dubuissez, D. Leprince, N. Baloghova, M. Horazna, A. Hlavata, J. Stancikova, E. Sloncova
**Analysis and interpretation of data (e.g., statistical analysis, biostatistics, computational analysis):** L. Janeckova, V. Pospichalova, A. Hlavata, H. Strnad, V. Korinek
**Writing, review, and/or revision of the manuscript:** L. Janeckova, V. Pospichalova, D. Leprince, V. Korinek
**Administrative, technical, or material support (i.e., reporting or organizing data, constructing databases):** K. Galuskova
**Study supervision:** V. Korinek

## Acknowledgments

The authors thank S. Robine for Villin-Cre and Villin-CreERT2 mice, and S. Takacova for critically reading the manuscript.

## Grant Support

This work was supported by Grant Agency of the Czech Republic Grant No. P305/12/2347, institutional Grant No. RVO 68378050, and project BIOCEV – Biotechnology and Biomedicine Centre of the Academy of Sciences and Charles University (CZ.1.05/1.1.00/02.0109) from the European Regional Development Fund.

The costs of publication of this article were defrayed in part by the payment of page charges. This article must therefore be hereby marked *advertisement* in accordance with 18 U.S.C. Section 1734 solely to indicate this fact.

Received January 19, 2015; revised March 20, 2015; accepted April 1, 2015; published OnlineFirst May 1, 2015.

## References

1. Wales MM, Biel MA, el Deiry W, Nelkin BD, Issa JP, Cavenee WK, et al. p53 activates expression of HIC-1, a new candidate tumour suppressor gene on 17p13.3. Nat Med 1995;1:570–7.
2. Carter MG, Johns MA, Zeng X, Zhou L, Zink MC, Mankowski JL, et al. Mice deficient in the candidate tumor suppressor gene Hic1 exhibit developmental defects of structures affected in the Miller-Dieker syndrome. Hum Mol Genet 2000;9:413–9.
3. Chen WY, Zeng X, Carter MG, Morrell CN, Chiu Yen RW, Esteller M, et al. Heterozygous disruption of Hic1 predisposes mice to a gender-dependent spectrum of malignant tumors. Nat Genet 2003;33:197–202.
4. Rood BR, Leprince D. Deciphering HIC1 control pathways to reveal new avenues in cancer therapeutics. Expert Opin Ther Targets 2013; 17:811–27.
5. Pinte S, Stankovic-Valentin N, Deltour S, Rood BR, Guerardel C, Leprince D. The tumor suppressor gene HIC1 (hypermethylated in cancer 1) is a sequence-specific transcriptional repressor: definition of its consensus binding sequence and analysis of its DNA binding and repressive properties. J Biol Chem 2004;279:38313–24.
6. Guerardel C, Deltour S, Pinte S, Monte D, Begue A, Godwin AK, et al. Identification in the human candidate tumor suppressor gene HIC-1 of a new major alternative TATA-less promoter positively regulated by p53. J Biol Chem 2001;276:3078–89.
7. Chen WY, Wang DH, Yen RC, Luo J, Gu W, Baylin SB. Tumor suppressor HIC1 directly regulates SIRT1 to modulate p53-dependent DNA-damage responses. Cell 2005;123:437–48.
8. Valenta T, Lukas J, Doubravska L, Fafilek B, Korinek V. HIC1 attenuates Wnt signaling by recruitment of TCF-4 and beta-catenin to the nuclear bodies. EMBO J 2006;25:2326–37.
9. Clevers HC, Bevins CL. Paneth cells: maestros of the small intestinal crypts. Annu Rev Physiol 2013;75:289–311.
10. Krausova M, Korinek V. Wnt signaling in adult intestinal stem cells and cancer. Cell Signal 2014;26:570–9.
11. De Sousa EMF, Wang X, Jansen M, Fessler E, Trinh A, de Rooij LP, et al. Poor-prognosis colon cancer is defined by a molecularly distinct subtype and develops from serrated precursor lesions. Nat Med 2013;19:614–8.
12. Briggs KJ, Eberhart CG, Watkins DN. Just say no to ATOH: how HIC1 methylation might predispose medulloblastoma to lineage addiction. Cancer Res 2008;68:8654–6.
13. Van Rechem C, Rood BR, Touka M, Pinte S, Jenal M, Guerardel C, et al. Scavenger chemokine (CXC motif) receptor 7 (CXCR7) is a direct target gene of HIC1 (hypermethylated in cancer 1). J Biol Chem 2009;284: 20927–35.
14. Gerbe F, van Es JH, Makrini L, Brulin B, Mellitzer G, Robine S, et al. Distinct ATOH1 and Neurog3 requirements define tuft cells as a new secretory cell type in the intestinal epithelium. J Cell Biol 2011;192: 767–80.
15. Pospichalova V, Tureckova J, Fafilek B, Vojtechova M, Krausova M, Lukas J, et al. Generation of two modified mouse alleles of the Hic1 tumor suppressor gene. Genesis 2011;49:142–51.
16. Kim S, Karin M. Role of TLR2-dependent inflammation in metastatic progression. Ann N Y Acad Sci 2011;1217:191–206.
17. Tye H, Kennedy CL, Najdovska M, McLeod L, McCormack W, Hughes N, et al. STAT3-driven upregulation of TLR2 promotes gastric tumorigenesis independent of tumor inflammation. Cancer Cell 2012;22:466–78.
18. Campana L, Bosurgi L, Rovere-Querini P. HMGB1: a two-headed signal regulating tumor progression and immunity. Curr Opin Immunol 2008; 20:518–23.
19. Scheeren FA, Kuo AH, van Weele LJ, Cai S, Glykofridis I, Sikandar SS, et al. A cell-intrinsic role for TLR2-MYD88 in intestinal and breast epithelia and oncogenesis. Nat Cell Biol 2014;16:1238–48.

20. el Marjou F, Janssen KP, Chang BH, Li M, Hindie V, Chan L, et al. Tissue-specific and inducible Cre-mediated recombination in the gut epithelium. Genesis 2004;39:186–93.
21. Sato T, Vries RG, Snippert HJ, van de Wetering M, Barker N, Stange DE, et al. Single Lgr5 stem cells build crypt-villus structures *in vitro* without a mesenchymal niche. Nature 2009;459:262–5.
22. Willert K, Brown JD, Danenberg E, Duncan AW, Weissman IL, Reya T, et al. Wnt proteins are lipid-modified and can act as stem cell growth factors. Nature 2003;423:448–52.
23. Melenovsky V, Benes J, Skaroupkova P, Sedmera D, Strnad H, Kolar M, et al. Metabolic characterization of volume overload heart failure due to aorto-caval fistula in rats. Mol Cell Biochem 2011; 354:83–96.
24. Chen EY, Tan CM, Kou Y, Duan Q, Wang Z, Meirelles GV, et al. Enrichr: interactive and collaborative HTML5 gene list enrichment analysis tool. BMC Bioinformatics 2013;14:128.
25. Dubuissez M, Faiderbe P, Pinte S, Dehennaut V, Rood BR, Leprince D. The Reelin receptors ApoER2 and VLDLR are direct target genes of HIC1 (Hypermethylated In Cancer 1). Biochem Biophys Res Commun 2013; 440:424–30.
26. Fafilek B, Krausova M, Vojtechova M, Pospichalova V, Tumova L, Sloncova E, et al. Troy, a tumor necrosis factor receptor family member, interacts with lgr5 to inhibit wnt signaling in intestinal stem cells. Gastroenterology 2013;144:381–91.
27. Waaler J, Machon O, Tumova L, Dinh H, Korinek V, Wilson SR, et al. A novel tankyrase inhibitor decreases canonical Wnt signaling in colon carcinoma cells and reduces tumor growth in conditional APC mutant mice. Cancer Res 2012;72:2822–32.
28. Doubravska L, Krausova M, Gradl D, Vojtechova M, Tumova L, Lukas J, et al. Fatty acid modification of Wnt1 and Wnt3a at serine is prerequisite for lipidation at cysteine and is essential for Wnt signalling. Cell Signal 2011;23:837–48.
29. Lukas J, Mazna P, Valenta T, Doubravska L, Pospichalova V, Vojtechova M, et al. Dazap2 modulates transcription driven by the Wnt effector TCF-4. Nucleic Acids Res 2009;37:3007–20.
30. Kerr MK. Linear models for microarray data analysis: hidden similarities and differences. J Comput Biol 2003;10:891–901.
31. Ventura A, Kirsch DG, McLaughlin ME, Tuveson DA, Grimm J, Lintault L, et al. Restoration of p53 function leads to tumour regression *in vivo*. Nature 2007;445:661–5.
32. Indra AK, Warot X, Brocard J, Bornert JM, Xiao JH, Chambon P, et al. Temporally-controlled site-specific mutagenesis in the basal layer of the epidermis: comparison of the recombinase activity of the tamoxifen-inducible Cre-ER(T) and Cre-ER(T2) recombinases. Nucleic Acids Res 1999;27:4324–7.
33. Dehennaut V, Loison I, Boulay G, Van Rechem C, Leprince D. Identification of p21 (CIP1/WAF1) as a direct target gene of HIC1 (Hypermethylated In Cancer 1). Biochem Biophys Res Commun 2013;430: 49–53.
34. Slattery ML, Herrick JS, Bondurant KL, Wolff RK. Toll-like receptor genes and their association with colon and rectal cancer development and prognosis. Int J Cancer 2012;130:2974–80.
35. Matsuda A, Suzuki Y, Honda G, Muramatsu S, Matsuzaki O, Nagano Y, et al. Large-scale identification and characterization of human genes that activate NF-kappaB and MAPK signaling pathways. Oncogene 2003; 22:3307–18.
36. Aliprantis AO, Yang RB, Mark MR, Suggett S, Devaux B, Radolf JD, et al. Cell activation and apoptosis by bacterial lipoproteins through toll-like receptor-2. Science 1999;285:736–9.
37. Takeuchi O, Kaufmann A, Grote K, Kawai T, Hoshino K, Morr M, et al. Cutting edge: preferentially the R-stereoisomer of the mycoplasmal lipopeptide macrophage-activating lipopeptide-2 activates immune cells through a toll-like receptor 2- and MyD88-dependent signaling pathway. J Immunol 2000;164:554–7.
38. Faure E, Thomas L, Xu H, Medvedev A, Equils O, Arditi M. Bacterial lipopolysaccharide and IFN-gamma induce Toll-like receptor 2 and Toll-like receptor 4 expression in human endothelial cells: role of NF-kappa B activation. J Immunol 2001;166:2018–24.
39. Mohammad HP, Zhang W, Prevas HS, Leadem BR, Zhang M, Herman JG, et al. Loss of a single Hic1 allele accelerates polyp formation in Apc (Delta716) mice. Oncogene 2011;30:2659–69.
40. Grivennikov SI, Karin M. Dangerous liaisons: STAT3 and NF-kappaB collaboration and crosstalk in cancer. Cytokine Growth Factor Rev 2010; 21:11–9.
41. Hausmann M, Kiessling S, Mestermann S, Webb G, Spottl T, Andus T, et al. Toll-like receptors 2 and 4 are up-regulated during intestinal inflammation. Gastroenterology 2002;122:1987–2000.
42. Frolova L, Drastich P, Rossmann P, Klimesova K, Tlaskalova-Hogenova H. Expression of Toll-like receptor 2 (TLR2), TLR4, and CD14 in biopsy samples of patients with inflammatory bowel diseases: upregulated expression of TLR2 in terminal ileum of patients with ulcerative colitis. J Histochem Cytochem 2008;56:267–74.
43. Maeda S, Hikiba Y, Sakamoto K, Nakagawa H, Hirata Y, Hayakawa Y, et al. Colon cancer-derived factors activate NF-kappaB in myeloid cells via TLR2 to link inflammation and tumorigenesis. Mol Med Rep 2011; 4:1083–8.
44. Rakoff-Nahoum S, Medzhitov R. Regulation of spontaneous intestinal tumorigenesis through the adaptor protein MyD88. Science 2007;317: 124–7.
45. el-Deiry WS, Tokino T, Velculescu VE, Levy DB, Parsons R, Trent JM, et al. WAF1, a potential mediator of p53 tumor suppression. Cell 1993;75:817–25.
46. Britschgi C, Rizzi M, Grob TJ, Tschan MP, Hugli B, Reddy VA, et al. Identification of the p53 family-responsive element in the promoter region of the tumor suppressor gene hypermethylated in cancer 1. Oncogene 2006;25:2030–9.
47. Abbas T, Dutta A. p21 in cancer: intricate networks and multiple activities. Nat Rev Cancer 2009;9:400–14.

## 3. NKD1 MARKS INTESTINAL AND LIVER TUMORS LINKED TO ABERRANT WNT SIGNALING

Wnt signaling is the essential pathway for intestinal tissue development and homeostasis maintenance (Clevers and Bevins, 2013). The proper regulation of this pathway is vitally needed to prevent the onset of several diseases, including the malignant growth (Cadigan and Peifer, 2009). Naked cuticle homolog 1 (Nkd1) is the negative regulator of Wnt signaling pathway. It interacts with the signal transducer Dvl and mediates its degradation (Rousset et al., 2001). Recent studies also suggested that Nkd1 might act as a passive regulator by virtue of inhibiting Wnt signaling above certain threshold (Angonin and Van Raay, 2013). However, the precise expression pattern of Nkd1 and its role in intestinal Wnt signaling pathway have not been determined so far.

Presented study analyzes Nkd1 expression pattern. Multiple approaches were used to map its presence in the intestine, including the genetic lineage tracing approach in model animals. These experiments confirmed its expression in the crypt compartment of the gut and in virtually all cells with active Wnt signaling. Interestingly, the analysis of multiple murine models of intestinal carcinogenesis reveled higher expression of Nkd1 in neoplastic tissues. The collection of patient's carcinoma neoplastic tissue expression profiling datasets supported this notion, and similar results were obtained from the "*in silico*" bioinformatics analysis of publically available data derived from human colon cancer tissues. This suggests that Nkd1 can be used as a marker of active Wnt signaling cascade in intestinal tissues as well as in cancer cells derived from this organ (Stancikova et al., 2015).

Applicant's contribution: Determination of the FACS-based strategy applicable for the isolation of intestinal epithelial subpopulations and isolation of intestinal epithelial cells populations by FACS-sort.

Contents lists available at ScienceDirect

Cellular Signalling

journal homepage: www.elsevier.com/locate/cellsig

# NKD1 marks intestinal and liver tumors linked to aberrant Wnt signaling

Jitka Stancikova [a,d,1,2], Michaela Krausova [a,2], Michal Kolar [a], Bohumil Fafilek [a], Jiri Svec [a,b], Radislav Sedlacek [a], Magdalena Neroldova [c], Jan Dobes [a], Monika Horazna [a], Lucie Janeckova [a], Martina Vojtechova [a], Martin Oliverius [c], Milan Jirsa [c], Vladimir Korinek [a,*]

[a] Institute of Molecular Genetics, Academy of Sciences of the Czech Republic, Videnska 1083142 20 Prague 4, Czech Republic
[b] Second Department of Internal Medicine, Third Faculty of Medicine, Charles University, Prague, Srobarova 50, 100 34 Prague 10, Czech Republic
[c] Institute for Clinical and Experimental Medicine, Videnska 1958/9, 140 21 Prague 4, Czech Republic
[d] Faculty of Science, Charles University in Prague, Albertov 6, 128 43 Praha 2, Czech Republic

ARTICLE INFO

*Article history:*
Received 17 August 2014
Received in revised form 24 October 2014
Accepted 8 November 2014
Available online 14 November 2014

*Keywords:*
Wnt signaling
NKD1
Intestine
Liver
Colorectal cancer
Hepatocellular carcinoma

ABSTRACT

The activity of the Wnt pathway undergoes complex regulation to ensure proper functioning of this principal signaling mechanism during development of adult tissues. The regulation may occur at several levels and includes both positive and negative feedback loops. In the present study we employed one of such negative feedback regulators, naked cuticle homolog 1 (Nkd1), to follow the Wnt pathway activity in the intestine and liver and in neoplasia originated in these organs. Using lineage tracing in transgenic mice we localized *Nkd1* mRNA to the bottom parts of the small intestinal crypts and hepatocytes surrounding the central vein of the hepatic lobule. Furthermore, in two mouse models of intestinal tumorigenesis, *Nkd1* expression levels were elevated in tumors when compared to healthy tissue. We utilized a collection of human intestinal polyps and carcinomas to confirm that *NKD1* represents a robust marker of neoplastic growth. In addition, expression analysis of *NKD1* in liver cancer showed that high expression levels of the gene distinguish a subclass of hepatocellular carcinomas related to aberrant Wnt signaling. Finally, our results were confirmed by bioinformatic analysis of large publicly available datasets that included gene expression profiling and high-throughput sequencing data of human colon and liver cancer specimens.



## 1. Introduction

The Wnt pathway represents one of the principal signaling mechanisms regulating development and tissue homeostasis in metazoan species. In the adult organism, aberrant Wnt signaling is involved in various diseases including cancer (reviewed in [1]). The central mediator of the best studied so-called canonical Wnt pathway is β-catenin, a protein playing a dual role in cell adhesion and signaling (reviewed in [2]). In the absence of an extracellular Wnt stimulus the β-catenin destruction complex, which is composed of casein kinase 1 alpha (CK1α) and glycogen synthase kinase 3 (GSK3), and scaffolding proteins adenomatous polyposis coli (Apc) and axin/conductin, phosphorylates β-catenin on the N-terminal serine/threonine residues. The phosphorylated protein is ubiquitinylated and subsequently degraded by the proteasome. Consequently, in unstimulated cell, the cytoplasmic levels of β-catenin remain low. Interaction of Wnt ligand with the receptor complex comprised of the Frizzled receptor and low-density lipoprotein receptor-related protein 5/6 (LRP5/6) co-receptor disrupts the function of the destruction complex. Subsequently, β-catenin accumulates in the cytoplasm and in the nucleus, where it associates with transcription factors of the lymphoid enhancer-binding factor/T-cell factor (LEF/TCF) family (further referred to as TCFs). Since β-catenin contains a transactivation domain, the TCF-β-catenin complexes act as bipartite transcriptional activators of the Wnt-responsive genes, such as *Axin2*, *c-Myc*, *CD44* or *cyclin D1* (for more comprehensive survey about the Wnt signaling target genes refer to the Wnt signaling home page: http://web.stanford.edu/group/nusselab/cgi-bin/wnt/target_genes).

*Abbreviations:* APC, adenomatous polyposis coli; BAC, bacterial artificial chromosome; CBC, crypt base columnar; Cp, crossing point; CRC, colorectal carcinoma; CTNNB1, the *β-CATENIN* gene; Dvl, dishevelled; EGFP, enhanced green fluorescent protein; EphB2, ephrin type-B receptor 2; GI, gastrointestinal; GS, glutamine synthetase; HBV, hepatitis B virus; HCC, hepatocellular carcinoma; HCV, hepatitis C virus; ISC, intestinal stem cell; ISH, *in situ* hybridization; LacZ, β-galactosidase; Lgr5, leucine-rich repeat containing G protein-coupled receptor 5; Min, multiple intestinal neoplasia; Nkd, naked cuticle homolog; Olfm4, olfactomedin 4; PCA, principal component analysis; qRT-PCR, reverse-transcription quantitative polymerase chain reaction; SD, standard deviation; TA, transit amplifying; TCF, T-cell factor; TCGA, The Cancer Genome Atlas.

* Corresponding author at: Institute of Molecular Genetics AS CR, Videnska 1083, 142 20 Prague 4, Czech Republic. Tel.: +420 241063146; fax: +420 244472282.
*E-mail address:* korinek@img.cas.cz (V. Korinek).

[1] Affiliation to the Faculty of Science is related to the support of the first author from the Grant Agency of Charles University in Prague; none of the results presented in this article were generated, obtained, or analyzed in relation to this affiliation.

[2] These authors contributed equally to this work.

http://dx.doi.org/10.1016/j.cellsig.2014.11.008
0898-6568/

The intestinal epithelium represents one of the most dynamic tissue in mammalian body (reviewed in [3]). The single-layer epithelium of the small intestine is formed by microscopic projections into the intestinal lumen called villi, and invaginations into underlying mesenchyme, so-called crypts of Lieberkühn. Tissue homeostasis is maintained by intestinal stem cells (ISCs) residing in the bottom part of the crypts. ISCs divide asymmetrically, giving rise to fast-cycling transit amplifying (TA) cells located above the stem cell zone. Descendants of TA cells move up along the crypt/villus axis. At the crypt orifice these cells differentiate to generate specialized cell lineages of the gut that mainly include absorptive enterocytes, mucus-secreting goblet cells, and enteroendocrine cells producing hormones. Differentiated cells continue their movement up to the top of the villus, where they are extruded to the intestinal lumen. The process of epithelial self-renewal is completed in 3–5 days. One exception from this scheme are Paneth cells. The life span of these cells is 6–8 weeks. Furthermore, mature Paneth cells do not migrate from the crypt but stay at the crypt bottom, where they produce antibacterial cryptidins, defensins, and lysozyme (reviewed in [4]). The tissue architecture of the colon reminds the small intestine; however, it does not contain Paneth cells and its surface is flat without the extruding villi. ISCs, alternatively named according to their slender appearance and localization in the lower portion of the crypt as crypt base columnar (CBC) cells, can be recognized by expression of leucine-rich repeat containing G protein-coupled receptor 5 (Lgr5) [5]. Recently, several other markers of ISCs were discovered. These include the tumor necrosis factor receptor family member Troy [6], transcription regulator achaete-scute complex homolog 2 (Ascl2), and an extracellular matrix glycoprotein, olfactomedin 4 (Olfm4) [7]. In addition, CBCs produce high levels of transmembrane ephrin type-B receptor 2 (EphB2), whose expression declines in TA cells, and Paneth cells are EphB2 negative [8].

A number of studies established the Wnt pathway as the main constituent of the signaling network regulating ISCs pluripotency and proliferation (reviewed in [9]). For example, the expression of stem cell markers *Ascl2*, *Lgr5* and *Troy* is governed by the canonical Wnt pathway. Moreover, genetic disruption of genes encoding the Wnt pathway effectors *Tcf4* [10,11] or *β-catenin* [12,13] is associated with demise of intestinal crypts. Interestingly, Wnt/β-catenin signaling plays a key role in the metabolic zonation of the liver (reviewed in [14]). To fulfill its metabolic function, the liver tissue is organized into hepatic lobules, hexagonal-shaped functional units of hepatic parenchyma composed of 15–25 cells. The hepatocytes in the center of the lobule are called perivenous, since they surround a hepatic centrilobular vein. The outer row of lobular hepatocytes line the portal space. These periportal cells are in close contact with the so-called portal triad consisting of the hepatic artery, portal vein and bile duct. Consequently, the periportal hepatocytes receive a mixture of blood originating from both vessels. The portocentrovenular axis of the lobule is the basis for the zonation of the metabolic functions in the adult organ. Cells in different areas of the hepatic lobule are not equal, but they express different genes involved in the metabolism of carbohydrates, xenobiotics, bile production, and detoxification of ammonia. The perivenous hepatocytes contain nuclear β-catenin and they display active Wnt signaling. The Wnt pathway regulates genes encoding enzymes of ammonia detoxication and transport. The genes include *glutamine synthetase* (*GS/Glul*), *ornithine aminotransferase* (*Oat*), and *leukocyte cell-derived chemotaxin-2* (*Lect2*). In contrast, high Apc protein levels in the periportal hepatocytes suppress the Wnt pathway activity. This leads to production of a different set of enzymes mainly participating in ammonia, urea, and carbohydrate metabolism such as *glutaminase 2* (*Gls2*), *arginase 1*, and *phosphoenolpyruvate carboxykinase 1* (*Pck1*) [15].

Aberrant Wnt signaling is found in a multitude of solid tumors, particularly in carcinoma of the colon and rectum [colorectal carcinoma (CRC) [reviewed in [16]]. It is assumed that in the majority of sporadic CRCs the "driver" mutation providing selective advantage to the prospective cancer cell occurs in the *APC* tumor supressor [17,18]. The mutational changes in *APC* lead to production of truncated APC polypeptide that compromises proper functioning of the β-catenin destruction complex (reviewed in [19]). The Wnt pathway might also be activated by inactivating mutations in *AXIN1* [20] or *AXIN2* [21]. In addition, approximately 5% of CRCs contain oncogenic mutations in the *CTNNB1* gene (this gene encodes β-catenin) that alter regulatory amino acid residues at the β-catenin N-terminus and stabilize the protein [22]. The most common type of liver cancer is hepatocellular carcinoma (HCC). The etiology of the disease is heterogeneous and is frequently linked to hepatitis B virus (HBV) or hepatitis C virus (HCV) chronic infection or to alcoholism-related cirrhosis (reviewed in [23]). Recently, several studies performed gene expression profiling and/or high-throughput DNA sequencing to identify the molecular subclasses of HCC or to detect the driver mutations related to liver carcinogenesis [24,25]. Importantly, approximately one-half of HCCs display elevated expression levels of genes activated by Wnt signaling, and oncogenic mutations in the *CTNNB1* gene are found in 20-30% of all HCCs. Analogically to CRC, high levels of stabilized β-catenin and inappropriate transcriptional activation of the TCF-β-catenin target genes is a hallmark of a significant portion of HCCs (reviewed in [26]).

In our previous study we employed chromatin immunoprecipitation in combination with DNA microarray analysis (so-called ChIP-on-chip) to identify genes activated by aberrant Wnt/β-catenin signaling in human CRC cells. One of the genes bound by the TCF4-β-catenin complexes was *naked cuticle homolog 1* (*NKD1*) [6]. Nkd1 is an evolutionarily conserved feedback inhibitor of the Wnt pathway [27]. It interacts with dishevelled (Dvl1) and mediates degradation of this cytoplasmic Wnt signal transducer [28]. Nkd1 reduces aberrant Wnt signaling; nevertheless, in the absence the excessive Wnt signal, its function is less apparent [29,30]. Simultaneous inactivation of both vertebrate paralogs *Nkd1* and *Nkd2* in the mouse leads to only subtle alterations in the morphology of cranial bones and slightly reduced litter size, but the mice are otherwise normal [31]. Based on these and other results mainly obtained in zebrafish [30], Angonin and Van Raay proposed that Nkd1 functions as a "passive antagonist" that acts only when the Wnt signaling levels exceed some threshold [32].

In the present study, we analyzed the *Nkd1* expression pattern in adult mouse gut and liver tissue. Using lineage tracing approaches in transgenic animals we show that *Nkd1* expression is confined to the areas with active Wnt signaling. Furthermore, *Nkd1* transcription was robustly increased in tumors developed in multiple intestinal neoplasia (Min) of mice or in hyperplastic crypts generated by conditional deletion of the *Apc* gene. Using a panel of sporadic tumors of the colon we confirmed that elevated expression of *NKD1* marks neoplastic tissue. In hepatic neoplasia, high *NKD1* mRNA levels, together with upregulation of *AXIN2*, *EPHB2*, and *GS*, distinguish a class of HCCs with deregulated Wnt signaling.

## 2. Materials and methods

### 2.1. Experimental animals

$Apc^{+/Min}$ [33,34], Lgr5-EGFP- IRES-CreERT2 [5], Rosa26R [35], and Rosa26R-EYFP [36] mice were purchased from the Jackson Laboratory (Bar Harbor, ME). $Apc^{cKO/cKO}$ [37] mice were obtained from the Mouse Repository (National Cancer Institute, Frederick, MD). Villin-CreERT2 mice [38] were kindly provided by Sylvia Robine (Institut Curie, Paris, France). Animals were housed and handled according to the guidelines approved by the institutional committee. Tamoxifen (Sigma-Aldrich, St. Louis, MO) administration was done by intraperitoneal injection of 1 mg of the compound dissolved in 0.1 ml of corn oil. DNA from tail clippings was used for genotyping. Tissue samples were digested in Proteinase K solution (Thermo Fisher Scientific, Waltham, MA) and precipitated using ethanol; pellets were dissolved in 20 μl of TE buffer (10 mM Tris-HCl, 1 EDTA, pH 8) and 1 μl was used for PCR performed with DreamTaq PCR Master Mix (Thermo Fisher Scientific, Waltham, MA).

*2.2. Generation of Nkd1-CreERT2 transgenic mice*

The Nkd1-CreERT2 bacterial artificial chromosome (BAC) transgenic construct was generated using homologous recombination in bacteria according to the previously published protocol [39]. The BAC clone RP23-301 N2 was purchased from imaGenes (Berlin, Germany); a construct containing CreERT2 cDNA was kindly provided by M. Cepko via Addgene. The adapters "a" (5′-TCCTTTCTTTCCGGCTCCCGCCGCCGCCGC CGCGCGCGATGTGCCCGCAGCCatgtccaatttactgaccgtac- 3′; the *Nkd1*-specific sequence is capitalized, the part complementary to the CreERT2 expression cassette is given in lowercase) and "b" (5′-AGAGACCAAGTT CTCCGGAGTAGGGGCTGGCGACTAGAGGAAGGCGCAAGTGGCGGCCGC TCTAGAACTAGTG- 3′) were derived from the sequence of the *Nkd1* second exon. The adapters were employed for PCR amplification, the product was purified from agarose gel and electroporated into the *E. coli* strain EL250 harboring the BAC clone. Bacterial clones containing correctly recombined BACs were verified by PCR. Isolated recombinant BAC DNA was linearized and used for pronuclear injection of fertilized eggs (C57Bl/6 J background). Two Nkd1-CreERT2 transgenic founder lines were produced using the service of the Transgenic Unit of the Institute of Molecular Genetics (IMG). Two lines exhibited a virtually identical pattern of the Cre recombinase activity.

*2.3. X-gal staining, immunohistochemistry, antibodies, and periodic acid-Schiff (PAS) staining*

Mouse tissues were stained with X-gal (Amresco, Solon, OH) prior to paraffin embedding. Tissue processing and staining was performed as described previously [5]. Slides were immersed in a steam bath (20 min, 10 mM citrate buffer, pH 6) for antigen retrieval. The following rabbit polyclonal antibodies were used for immunohistochemistry: anti-chromogranin A (cat. No. ab15160, Abcam, Cambridge, UK), anti-lysozyme (cat. No. A0099, Dako, Glostrup, DK), anti-glutamine synthetase (cat. No. ab73593, Abcam). PAS (Diapath, Martinengo, IT) staining was performed according to the standard protocol provided by the supplier. Slides were counterstained using either hematoxylin (Penta, Prague, CZ) or nuclear fast red (Diapath, Martinengo, IT).

*2.4. RNA probes and in situ hybridization (ISH)*

Both sense and antisense RNA probes were derived from the following regions of the analyzed genes: *Axin2* (accession: NM_015732.4), nucleotides (nt) 2069-2938; *Nkd1* (NM_001163660.1), nt 509-944. DNA fragments encompassing the indicated regions were subcloned into pBluescript SK II (Stratagene, La Jolla, CA). The constructs were linearized, and digoxigenin-labeled antisense RNA and control sense probes were generated from the template using the DIG RNA Labeling Kit (Roche Applied Science, Basel, Switzerland). Dissected small intestinal and liver tissue was embedded in O.C.T. medium (Tissue-Tek, Sakura Finetek Europe B.V., The Netherlands). Ten μm sections were cut and mounted on Super Frost Plus slides (Electron Microscopy Sciences, Hatfield, PA). Sections were post-fixed in 4% (w/v) paraformaldehyde in phosphate-buffered saline (PBS; 4 °C, 10 min), acetylated for 10 min (acetic anhydride, 0.25%; Sigma-Aldrich) and hybridized with digoxigenin-labeled probes overnight at 62 °C. ISH was carried out as described previously [40]. Whole-mount ISH was performed according to the protocol of Cepko and Tabin (http://genepath.med.harvard.edu/~cepko/protocol/ctlab/ish.ct.htm).

*2.5. Isolation of intestinal crypt cells and hepatocytes, fluorescence-activated cell sorting (FACS)*

Crypts from the proximal part of the small intestine of Lgr5-EGFP-IRES-CreERT2 mice were isolated according to the protocol published previously [41]. Single-cell suspension was obtained upon incubation of fresh crypts with dispase I (0.8 mg/ml, 10 min at 37 °C; Sigma-Aldrich) and passing the resulting suspension through 70-μm strainer (Fisher Scientific, Waltham, MA). Cell suspension was stained by biotinylated *Ulex europaeus* agglutinin I (UEA I) (Vector Laboratories, Burlingame, CA) and streptavidin-PE-Cy7 (BD Biosciences, Mississauga, ON). Hepatocytes were isolated from perfused liver of Nkd1-CreERT2$^{+}$/Rosa26R-EYFP mice as described previously [42]. The animals were injected twice (with 24-hour interval between injections) with tamoxifen (1 mg in 100 μl of corn oil per dose) and utilized the next day upon the second injection.

*2.6. RNA isolation and reverse-transcription quantitative polymerase chain reaction (qRT-PCR)*

Total RNA was extracted from tissues or sorted cells using RNAeasy MiniKit with DNase treatment (Qiagen, Hilden, Germany) following the manufacturer's instructions and reverse transcribed using MAXIMA reverse transcriptase (Thermo Fisher Scientific, Waltham, MA). The LightCycler 480 apparatus and SYBR Green I Master Mix (Roche Applied Science) were employed for qRT-PCR. Primers are listed in Supplementary Table S1.

*2.7. Collection and analysis of human colorectal lesions*

The study was approved by the Clinical and Experimental Medicine and the Thomayer University Hospital Research Ethics Committee and the Ethics Committee of the Third Faculty of Medicine, Charles University in Prague. Processing and histopathological evaluation of samples of 35 precancerous and 20 malignant lesions of colorectal tissue were described in full detail previously [6]. Briefly, genomic DNA and total RNA was isolated from tumor segments and matched healthy mucosa. RNA was reverse transcribed and used for qRT-PCR analysis; PCR reactions were run in triplicates with two negative controls (RT reactions in which reverse transcriptase was omitted). Mutational analysis of the *APC* gene was performed with genomic DNA extracted from CRC specimens only. To obtain relative expression levels (-ΔCp) (Cp indicates the crossing point value), individual Cp values were normalized by geometric average of internal housekeeping genes *β-ACTIN* (*ACTB*), *UBIQUITIN B* (*UBB*) and *AXIN1* (premalignant lesions of the colon), or using *ACTB* as a sole reference gene (CRC-derived samples). Differential expression was examined by non-parametric Wilcoxon's rank-sum test. In addition, the individual background of the patients was encompassed in a REML-fitted linear model, described by the formula ΔCp ~ patient + tissue/(stage * *APC* mutation) for CRC specimen and ΔCp ~ patient + tissue_stage in cases of precancerous lesions, respectively. Biopsies of surrounding non-tumor tissue constitute a single group (ΔΔCp) in both collections. In corresponding figures and tables, the number of asterisks represents statistically significant changes with the following P values: *$P < 0.05$, **$P < 0.01$, and ***$P < 0.001$. All analyses were performed in R language. Primer sequences are listed in Supplementary Table S1.

*2.8. Collection and analysis of human hepatic lesions*

Neoplastic liver tissues were obtained from 28 consecutive patients at the time of surgical resection performed at the Transplant Surgery Department of the Institute for Clinical and Experimental Medicine. Collection of clinical samples was accomplished in concordance with the standards and approved by the Institute for Clinical and Experimental Medicine and Thomayer University Hospital Research Ethics Committee; all study subjects signed the informed consent. The paired, non-tumor tissue specimens were used as controls. Histopathology was scored in hematoxylin and eosin stained sections by two independent pathologists; clinical characteristics are given in Supplementary Table S2. Diagnoses of HCC were predominant within the cohort. Total RNA was purified using the RNeasy Mini kit in automated QIAcube extractor (Qiagen). Reverse transcription was performed with 250 ng of

input RNA using RevertAid H Minus First Strand cDNA Synthesis kit supplied with 25 ng/μl oligo(dT)$_{18}$ primers (Thermo Scientific). PCR reactions were run in triplicates using Light Cycler 480. Relative expression levels (-ΔCp) were obtained upon normalization by geometric average of internal housekeeping genes *ACTB* and *UBB*. To detect differences in expression, we employed Wilcoxon's rank-sum test and, in addition, the linear model (REML) described by the formula ΔCp ~ patient + tissue_fibrosis score. Statistical significance levels were set identically to CRC samples.

### 2.9. CTNNB1 mutation analysis in HCC

Genomic DNA was purified from snap-frozen samples of tumor and matched surrounding tissue using DNeasy Blood & Tissue Kit (Qiagen). Exon 3 of *CTNNB1*, including intron-exon boundaries, was amplified using gene-specific primers: forward: 5′taatac gactcactatag TGCTTTTCTTGGCT GTCTTTCAG 3′; reverse: 5′tgaaa cagctatgaccatgTCCACAGTTCAGCATTTACCTAAG 3′; overhang sequences corresponding to universal sequencing primers T7 and RP, respectively, are given in lowercase letters. Each fragment was directly sequenced from both sides using the BigDye® Terminator v3.1 cycle sequencing kit and ABI 3130 Genetic Analyzer (Applied Biosystems, Life Technologies, Prague, Czech Republic).

### 2.10. CRC and HCC datasets obtained from The Cancer Genome Atlas (TCGA)

CRC [TCGA_COADREAD; 154 cases of colon cancer (dataset COAD-TP); 73 cases of rectal cancers, (dataset READ-TP)] [18] and HCC (TCGA_LIHC; 197 cases) datasets were downloaded from the Broad Institute using the utility firehose_get (http://gdac.broadinstitute.org, Broad Institute/Massachusetts Institute of Technology, USA) on July 18, 2014. RNA-seq data were extracted from the archive "gdac.broadinstitute.org_COADREAD.Merge_rnaseqv2__illuminaga_rnaseqv2__unc_edu__Level_3__RSEM_genes_normalized__data.Level_3.2014061400.0.0" (CRC) and "gdac.broadinstitute.org_LIHC.Merge_rnaseqv2__illuminahiseq_rnaseqv2__unc_edu__Level_3__RSEM_genes_normalized__data.Level_3.2014061400.0.0" (HCC). Mutation data were obtained from the archive: "gdac.broadinstitute.org_COADREAD.Mutation_Packager_Calls.Level_3.2014061400.0.0" (CRC) and "gdac.broadinstitute.org_LIHC.Mutation_Packager_Calls.Level_3.2014061400.0.0" (HCC). Clinical data were retrieved from the files: "gdac.broadinstitute.org_COADREAD.Merge_Clinical.Level_1.2014061400.0.0/COADREAD.clin.merged.txt" (CRC) and "gdac.broadinstitute.org_LIHC.Merge_Clinical.Level_1.2014061400.0.0/LIHC.clin.merged.txt" (HCC). No further processing was applied to the data. In CRC datasets only samples classified as colon cancer (COAD) and with a determined mutation status of the *APC* gene (104 cases) are presented. DNA methylation data were retrieved from the file: "gdac.broadinstitute.org_COADREAD.Merge_methylation__humanmethylation450__jhu_usc_edu__Level_3__within_bioassay_data_set_function__data.Level_3.2014061400.0.0". Only those data subsets were analyzed that had both expression and methylation data available (366 cases). Positions of the CpG-islands predicted by the algorithm of Wu and colleagues [43] were obtained from the file: "http://rafalab.jhsph.edu/CGI/model-based-cpg-islands-hg19.txt" (accessed on September 8, 2014). North and south shores (N/S-shores) were defined as chromosomal regions flanking the corresponding CpG island 2 kb upstream or downstream, respectively. North/south shelves (N/S-shelves) were defined as chromosomal regions flanking the shores further 2 kb upstream/downstream [44]. Base 2 logarithm of fold change (logFC) of *NKD1* expression intensity between tumor samples and the median of available normal tissue samples was determined. The CRC samples were clustered according to methylation β-values (methylated/overall intensity) for the probes assigned to the *NKD1* gene (**Infinium Human Methylation** 450 array, Illumina). All analyses were performed in the R environment.

## 3. Results

### 3.1. Nkd1 expression marks Apc-deficient intestinal tumors in the mouse

To analyze *Nkd1* expression in mouse tumors we performed ISH using specimens obtained from Min mice. These mice (designated Apc$^{+/Min}$) harbor a nonsense mutation in the coding region of the *Apc* gene and all adult animals develop numerous Apc-deficient polyps that progress to malignancy [34]. *Nkd1* mRNA was clearly detected in the small intestinal tumors; nevertheless, we did not observe any

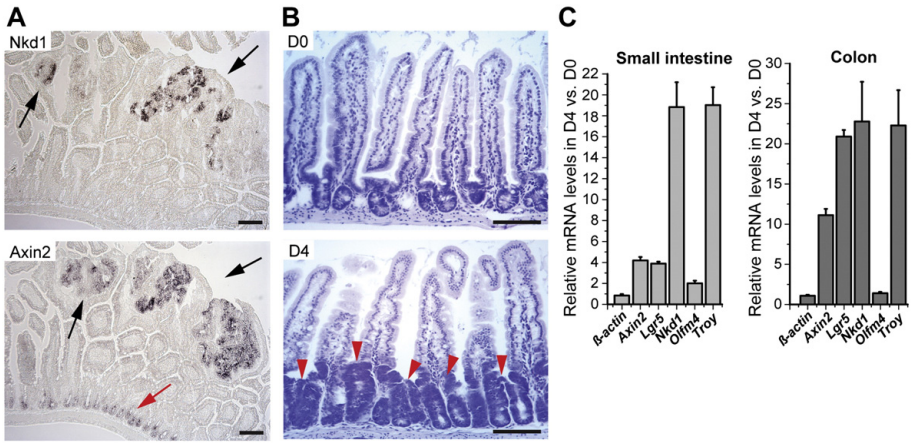


**Fig. 1.** *Nkd1* mRNA is enriched in mouse intestinal tumors. (A) ISH of *Axin2* and *Nkd1* mRNAs in small intestinal tumors (black arrows) of Apc$^{+/Min}$ mice. In the healthy part of the tissue *Axin2* was also detected in lower parts of the crypts (red arrow). (B) Conditional deletion of the *Apc* allele results in crypt hyperplasia. Hematoxylin-stained sections of the jejunum of Villin-CreERT2$^{+}$/Apc$^{cKO/cKO}$ mice obtained at day 0 (D0) and day 4 (D4) after tamoxifen administration. Hyperproliferative crypts are indicated by red arrowheads. Scale bar: 0.1 mm. (C) Quantitative RT-PCR analysis of total RNA isolated from crypts at D0 and D4. The results were normalized to *Ubiquitin B* (*Ubb*) mRNA levels; another housekeeping gene, *β-actin*, was also included in the test. The expression level of a given gene in the crypt cells at D0 was arbitrarily set to 1. Error bar: standard deviation (SD).

(specific) *Nkd1* signal in non-neoplastic tissue. This was in contrast to *Axin2*, which was clearly enriched not only in tumors, but also at the bottom of the intestinal crypts (Fig. 1A). To confirm that *Nkd1* expression is directly connected to the loss of *Apc* we employed animals harboring conditional alleles (cKO) of this tumor suppressor. Cre-mediated excision of the floxed exon 14 in $Apc^{cKO/cKO}$ mice results in production of a truncated polypeptide related to nonfunctional Apc protein produced in $Apc^{+/Min}$ mice [37]. The *Apc* gene inactivation was performed in Villin-CreERT2$^{+}$/$Apc^{cKO/cKO}$ mice expressing tamoxifen-regulated Cre enzyme throughout the epithelia of the gastrointestinal tract [38]. As expected, robust hyperplasia of the small intestinal and colonic crypts was observed several days upon tamoxifen administration (Fig. 1B and data not shown). Quantitative RT-PCR analysis of crypt cells isolated from animals prior and four days after tamoxifen treatment showed more than 18- and 20-fold increase in the *Nkd1* mRNA levels in the Apc-deficient small intestine and colon, respectively. Wnt signaling target genes *Axin2*, *Lgr5*, and *Troy* were also upregulated. In contrast, transcription of *Olfm4*, a marker of small intestinal stem cells which is not driven by active Wnt signaling [7], was slightly elevated in the hyperproliferative crypts isolated from the small intestine and not from the colon (Fig. 1C).

### 3.2. Nkd1 is produced in the Wnt-responsive areas of the small intestine and liver

Next we analyzed the distribution of Nkd1 in the healthy gut tissue. Since the localization of *Nkd1* mRNA and protein using ISH or immunohistochemical staining was inconclusive, we used transgenesis to follow the expression pattern of the gene. BAC carrying the mouse *Nkd1* locus was employed to generate Nkd1-CreERT2 transgenic mice. In the BAC-based construct, cDNA encoding tamoxifen-inducible Cre enzyme was inserted into the second exon of the *Nkd1* gene. The insertion is in frame with the translation start codon located in the preceding exon (Fig. 2A). The activity of CreERT2 recombinase produced from the Nkd1-CreERT2 BAC transgene was visualized in embryos derived from crossing Nkd1-CreERT2 and Rosa26R mice. Rosa26R animals express bacterial *β-galactosidase* (*LacZ*) mRNA from the ubiquitously active *Rosa26* allele. The mRNA is not translated unless a transcriptional blocker flanked by two loxP sites is excised by Cre [35]. Developing embryos removed from pregnant females one day after tamoxifen injection were used to stain the LacZ-expressing tissue. Importantly, the expression pattern of Nkd1-CreERT2 visualized by the chromogenic X-gal substrate phenocopied the sites of expression of endogenous *Nkd1* mRNA obtained by whole-mount ISH (Fig. 2B). Furthermore, the sites of the CreERT2 activity were in agreement with the previously described *Nkd1* expression pattern [31].

Subsequently, adult Nkd1-CreERT2$^{+}$/Rosa26R mice were injected with a single dose of tamoxifen and sacrificed at several time points later. In the gastrointestinal (GI) tract, Cre-mediated recombination was the most efficient in the duodenum and jejunum, much less effective in the ileum, and virtually no staining was observed in the colon (Fig. 2C). Since we [6] and others [45] observed that Cre-mediated recombination is less efficient in the distal parts of the GI tract, we supposed that the observed variability in LacZ staining was caused by the inefficient recombination of the floxed blocker rather than heterogeneous expression of *Nkd1*. Therefore, the histological analysis was performed using specimens obtained from the proximal part of the small intestine. One day after the Cre induction, cells producing LacZ were located in the lower parts of the crypts (Fig. 2D). Two distinct staining patterns were observed seven days after the recombination. Some of "blue" cell clones started to extend along the whole crypt axis. However, other clones separated from the crypts and moved as a stripe of cells on the villus, indicating that the recombined cell was possibly a TA cell. Finally, three weeks after recombination, continuous "ribbons" of labelled cells emanating from the crypts and reaching the top of the villi were observed. In addition, blue cells were also found at the bottom of the crypts, i.e. in the positions where mature Paneth cells are localized (green arrow in Fig. 2D). Importantly, Nkd1-CreERT2-expressing cells differentiated into all major cell lineages present in the small intestine (Fig. 2E). The recombined clones persisted in the small intestine for more than two months, confirming that besides Paneth and TA cells some CreERT2-positive cells are indeed ISCs (not shown). To verify that the Nkd1-CreERT2 activity mimics expression of endogenous *Nkd1*, crypt cells obtained from Lgr5-EGFP-IRES-CreERT2 mice were sorted and analyzed using qRT-PCR. Lgr5-IRES-EGFP-CreERT2 animals express enhanced green fluorescent protein (EGFP) from the *Lgr5* locus, and therefore the EGFP protein can be used as a surrogate marker of ISCs [5]. Besides EGFP florescence, cell labeling with UEA I lectin was applied. The lectin binds proteoglycan residues on the surface of secretory cell lineages including Paneth cells and their precursors. Crypts isolated from the jejunum were used for the sorting procedure since this part of the small intestine contains only a minimal count of UEA I-positive goblet cells [46]. The highest *Nkd1* expression (when compared to TA cells negative for UEA and GFP) was detected in mature Paneth cells (phenotype: UEA$^{+}$GFP$^{-}$cryptidines$^{+}$) and Lgr5$^{+}$ ISCs (UEA$^{-}$GFP$^{++}$-EphB2$^{+}$), although expression of cryptidines in the latter population indicated that we did not obtain a homogenous cell population. Interestingly, high levels of *Nkd1* mRNA were also detected in putative progenitors of the Paneth cell lineage that are positive for UEA and GFP, and produce Lgr5 and cryptidins as well [46]. The result was consistent with the frequency of blue cells detected by immunohistochemical staining of crypts in Nkd1-CreERT2$^{+}$/Rosa26R mice one day after tamoxifen administration (Fig. 2G).

Since previous reports indicated *Nkd1* expression in pericentral hepatocytes [31], we followed the Nkd1-CreERT2 activity in adult liver tissue. One day after tamoxifen administration, X-gal staining was detected in hepatocytes surrounding the putative central vein (Fig. 3A). The identity of LacZ-positive cells was subsequently confirmed by co-staining with an antibody recognizing GS, a robust marker of pericentral hepatocytes (Fig. 3B). Additionally, we intercrossed Nkd1-CreERT2 animals with Rosa26R-EYFP reporter mice that express enhanced yellow fluorescent protein (EYFP) instead of LacZ from the *Rosa26* locus [36]. We performed gene expression profiling of total RNA isolated from EYFP-positive and EYFP-negative hepatocytes sorted from these mice. The analysis confirmed that endogenous *Nkd1* mRNA is robustly enriched in EYFP$^{+}$ cells along with the perivenous hepatocyte-specific genes *GS*, *Lect2*, and *Oat*. In accordance with the literature, these cells also produce increased levels of *Axin2* mRNA [15]. *Apc* and the "housekeeping" gene *glyceraldehyde-3-phosphate dehydrogenase* (*GAPHD*) did not show any differential distribution among the sorted cell populations; however, the periportal *Pck1* gene displayed an inverse expression pattern to the perivenous genes, confirming the quality of the sorting procedure (Fig. 3C).

### 3.3. Elevated levels of NKD1 mRNA in sporadic premalignant lesions of the colon and in CRC

As a next step, we examined the expression pattern of human *NKD1* in tumors arising in the gut. In dysplastic premalignant stages of CRC, we observed robust upregulation of *NKD1* expression. The increase in *NKD1* mRNA abundance showed an ascending tendency as the lesions progressed towards more advanced phenotypes. In contrast, in hyperplastic polyps *NKD1* transcription was significantly decreased when compared to the matched healthy mucosa (Fig. 4A). In CRC the elevated *NKD1* expression occurred irrespective of the *APC* mutational status and hence resembled deregulation of *LGR5* (Fig. 4B) [6].

To explore the alterations in *NKD1* transcription in a larger panel of CRCs, we interrogated relevant datasets from TCGA (227 specimens in total) [18]. The analysis was less straightforward, since the expression data obtained from healthy matched tissue were not accessible from these datasets. Intestinal cancers were stratified according to disease progression, and subsequently, the tumors were further subdivided using the classification system associated with the cellular phenotype

[47] or according to genetic stability [18]. In early-stage tumors *NKD1* mRNA was enriched (similarly to *AXIN2*) in microsatellite stable (MSS) lesions [when compared to lesions displaying low (MSI-L) or high (MSI-H) microsatellite instability (MSI)]. Moreover, in both early and advanced CRCs the *NKD1* transcript was abundant in the progenitor ("TA") type of tumors (Supplementary Fig. S1).

### 3.4. NKD1 transcription indicates HCC displaying aberrant Wnt signaling

The *NKD1* expression was analyzed in 28 neoplastic liver tissues obtained at the time of surgery. Paired, non-tumor tissue specimens were used as controls. Recently, Lachenmayer and colleagues employed expression data of 642 HCCs to define two classes of HCC displaying dysregulation of the Wnt pathway. The "Wnt class" is characterized by nuclear accumulation of β-catenin and upregulation of liver-specific Wnt signaling target genes. The "Wnt-TGFβ" class is defined by expression of a different set of genes (see further) regulated by Wnt signaling [25]. In the initial analysis we observed a clear separation of a fraction of the HCC samples into the Wnt class that was established by simultaneous upregulation of *AXIN2*, *EPHB2* and *GS*. However, we did not observe any clustering of HCCs to the Wnt-TGFβ class as examined by transcription levels of the *PLAU*, *MMP7*, *SALL1* and *RUNX2* genes (not shown). Thus, we stratified the HCC samples into subgroups defined by the Wnt-signature only. We employed the MCLUST algorithm [48] to group the samples according to their *AXIN2*, *EPBH2*, and *GS* Cp values. The algorithm identified four clusters, three of which showed low and

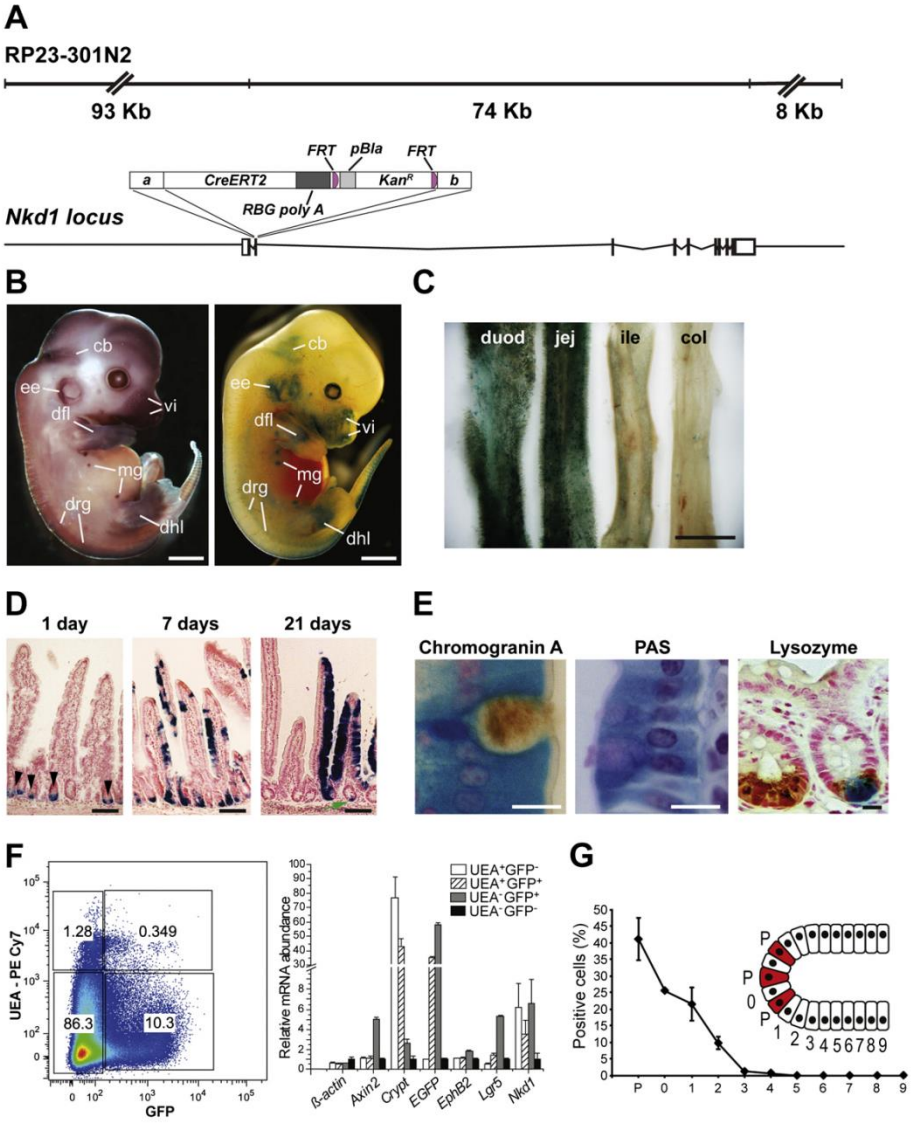

one (11 samples) exhibited high Wnt-signature "intensity". Due to small cluster sizes, we merged the Wnt signature-negative clusters into a single class and subsequently obtained two classes of HCC designated "HCC" and "HCC_Wnt" (Supplementary Fig. S2). An alternative clustering method, partitioning around medoids (with k = 2), resulted in virtually identical grouping (not shown). To further validate the result, we used the algorithm to predict the class of all other samples, i.e. healthy liver parenchyma, precancerous tissues, cholangiocellular carcinoma, and other than HCC liver neoplasia, which we expected to be negative for the Wnt-signature. Indeed, all these samples were correctly classified outside of the HCC_Wnt class (not shown). Finally, we analyzed the *CTNNB1* gene mutation status in genomic DNA obtained from all liver samples. The exon 3 sequence encoding amino acid residues regulating β-catenin protein stability was used for the analysis. Missense mutations in codons for regulatory serines/threonines (or in codons closely adjacent to these residues) were found in 11 HCCs; nine of these tumors were assigned to the HCC_Wnt class (Supplementary Table S3). Consistently, transcription levels of *NKD1* were positively correlated with expression of the genes defining the HCC_Wnt class (*AXIN2, EPHB2*, and *GS*), as well as with additional target genes of canonical Wnt/β-catenin signaling *LGR5* and *TROY*. In contrast, transcription of the paralogous *NKD2* gene, which is not regulated by the Wnt pathway, was not elevated in specimens assigned to the HCC_Wnt class (Fig. 5).

Next, we analyzed relevant HCC datasets from TCGA (197 specimens). The expression levels of the Wnt-signature genes *AXIN2*, *EPBH2*, and *GS* and the MCLUST algorithm were employed to group the HCC specimens. The algorithm identified three clusters of HCCs designated HCC_1 (12 samples), HCC_2 (148 samples), and HCC_Wnt (37 samples) (Supplementary Fig. S3). Additionally, we employed genomic DNA sequencing data to determine the *APC*, *AXIN1/2*, and *CTNNB1* mutational status (mutations were classified according to references [49, 50]). In the examined tumors *APC* was compromised in 3%, *AXIN1* in 5%, and *AXIN2* in 2% cases. In contrast, mutations activating *CTNNB1* occurred in 26% of specimens. Consistent with other studies [51], nonsynonymous gene alterations in either the *AXIN1* or *APC* tumor suppressors and *CTNNB1* were mutually exclusive, with only one specimen displaying concurrent oncogenic mutations in the *CTNNB1* exon 3 together with disruption of *AXIN2* (not shown). Since the HCC TCGA dataset contains exome sequencing data, we utilized the mutational status of the *APC*, *CTNNB1*, and *AXIN1/2* genes to divide all specimens to three mutation groups (designated "Wnt_WT", "Wnt_MUT", and "Other"). As expected, HCC_Wnt class-specific genes *AXIN2*, *EPHB2* and *GS* were robustly overexpressed in the Wnt_MUT group (sample count 38) defined by *CTNNB1* (activating) and *APC* (inactivating) mutations (Supplementary Fig. S4). Importantly, in the TCGA HCC1 samples *NKD1* transcription was also positively correlated with *AXIN2*, *EPBH2*, and *GS*, and, furthermore, *NKD1* mRNA was significantly enriched in the Wnt_MUT group (Fig. 6A). Interestingly, in five HCC specimens that were assigned to the HCC_Wnt expression class, no oncogenic mutations in *APC*, *CTNNB1*, and *AXIN1/2* were detected (one sample was assigned to the mutational subgroup "Other" and four other HCCs to the subgroup Wnt_WT) (Supplementary Table S4). Careful scrutiny of genomic DNA from the tumor in the "Other" group revealed that this lesion harbors a missense mutation (c.G417T/p.L139F) in exon 4 of the *CTNNB1* gene that possibly compromises the structural integrity of the first armadillo repeat of β-catenin. Consequently, the alteration might lead – by inhibiting phosphorylations by CK1 – to β-catenin stabilization and inappropriate signaling [52]. We investigated the molecular background of four other samples from the Wnt_WT mutation group. Interestingly, we detected increased levels of *LGR5* in these specimens. In addition, in two tumors, copy-number identified amplification of the *R-spondin 2* (*RSPO2*) gene that encodes the LGR5 ligand and functions as an extracellular Wnt agonist (Fig. 6B; HCCs with *RSPO2* amplification are indicated as orange and violet triangles) [53].

We used data deposited by the TCGA consortium to analyze mutations or genomic rearrangement of the *NKD1* locus in cancer tissue. Previous reports identified the *NKD1* mutations within CRCs displaying MSI [54]. However, the coding region of *NKD1* in the corresponding TCGA dataset showed that the gene was modified only marginally, with one nonsense (p.R294X), one missense (p.P230L), and one silent mutation (p.L142L) detected within CRC samples and one silent mutation (p.C248C) found in rectal cancers, respectively. In addition, TCGA CRC samples were explored using the COSMIC interface (http://cancer.sanger.ac.uk/cancergenome/projects/cosmic/). The open reading frame of *NKD1* was found to be altered by one silent (p.G312G), one missense mutation (p.A374T) and one in-frame deletion (p.K104delK). Of note, neither of the missense mutations affect the NKD1 EFX domain presumably required for the interaction with DVL proteins [27]. Moreover, unlike reported [54], the integrity of the *NKD1* exon 10 poly$(C)_7$ stretch was impaired in a single case. Moreover, the *NKD1* genomic region was never subjected to significant amplification or deletion (data not shown). In line with CRC, mutational inactivation of *NKD1* is rare in HCC, with one p.P349L substitution detected within the HCC TCGA dataset and similarly, two *NKD1* missense mutations (p.R31P and p.K116R) recorded within COSMIC data survey (827 samples).

Finally, the methylation status of the *NKD1* locus in 366 CRC samples from the TCGA dataset

was analyzed and correlated to the *NKD1* transcription level. Whereas the CpG island (and adjacent loci) proximal to the *NKD1* promoter

**Fig. 2.** Tracking *Nkd1* expression using Nkd1-CreERT2 BAC transgenic mice.(A) Schemes depicting the BAC clone RP23-301N2 harboring the Nkd1 locus and generation of Nkd1-CreERT2 transgenic mice. CreERT2 was inserted into the second coding exon of the *Nkd1* gene of bacteria using homologous recombination. The insertion is in frame with the translation start located in the *Nkd1* first exon. The non-coding or translated regions are indicated by empty and black boxes, respectively. a,b, *Nkd1* sequences employed for homologous recombination; RGB poly A, a poly A signal derived from the rabbit β-globulin gene; KanR, the kanamycin resistance gene; pBla, β-lactamase promoter. Prior to pronuclear injection, the bacterial resistance cassette was excised from recombinant BAC using Flp recombinase and FRT sites (violet semicircles) flanking the cassette. (B) Comparison of the whole-mount hybridization of wild-type mouse embryo at embryonic day (E) 14.5 using an antisense probe against *Nkd1* (left image) with the activity of CreERT2 recombinase produced from the Nkd1-CreERT2 BAC transgene in Nkd1-CreERT2$^+$/Rosa26R embryos obtained at the same developmental stage (right). Tamoxifen was injected intraperitoneally into pregnant females and the animals were sacrificed one day later. cb, cerebral plate; dfl, distal forelimb; dhl, distal hindlimb drg, dorsal root ganglion; ee, ear; ma, maxilla; mg, mammary gland primordium; vi, vibrissae. (C) Stereoscopic images of whole-mount staining of LacZ in different anatomical parts of the intestine of Nkd1-CreERT2$^+$/Rosa26R mice six days after tamoxifen administration. duod, duodenum; jej, jejunum; ile, ileum; col, colon. (D) Lineage tracing in the duodenum of Nkd1-CreERT2$^+$/Rosa26R mice. The LacZ activity was detected in histological specimens at indicated days after tamoxifen administration. The slides were counterstained with nuclear red. One day upon tamoxifen administration the bottom parts of the crypts were labelled (black arrowheads in the left image), whereas three weeks later cellular clones formed blue ribbons extending from the crypts to the villi (right image). In addition, the tissue contains labelled Paneth cells residing at the crypt bottom (green arrow in the left image). (E) Double labeling shows that blue cells express markers of enteroendocrine (visualized by anti-chromogranin A staining), goblet (positive for PAS), and Paneth (anti-lysozyme) cell lineages. (F) Expression of endogenous *Nkd1* in cell populations sorted from the intestinal crypts is confined to the cell types localized at the crypt bottom. Left, diagram of the sorting procedure using crypt cells isolated from the proximal half of the small intestine of three Lgr5-EGFP-IRES-CreERT2 mice. Four cell populations were obtained representing ISCs (GFP$^+$), putative precursors of Paneth and enteroendocrine cell lineages (GFP$^+$UEA$^+$), mature Paneth cells (GFP$^-$UEA$^+$), TA cells (GFP$^-$UEA$^-$). Right, qRT-PCR of sorted crypt cell populations. Cp values were normalized to *Ubb*. Means relative to values obtained in GFP$^-$UEA$^-$ cells are presented with corresponding SDs. *Crypt, cryptidins 1/3/6 – 12/14/15*. (G) Distribution of LacZ-positive cells in the crypts of Nkd1-CreERT2$^+$/Rosa26R mice one day after tamoxifen administration. Four hundred crypts in proximal parts of the small intestine in two mice were counted. Results are depicted as means with SDs. The cell positions are indicated in the scheme in the inset: Paneth cells ("P") are depicted in red, CBC stem cells occupy crypt positions "0" and "1", and putative Paneth cell progenitors position "2". Scale bar: 2 mm (B), 5 mm (C), 0.1 mm (D), 5 μM (E).

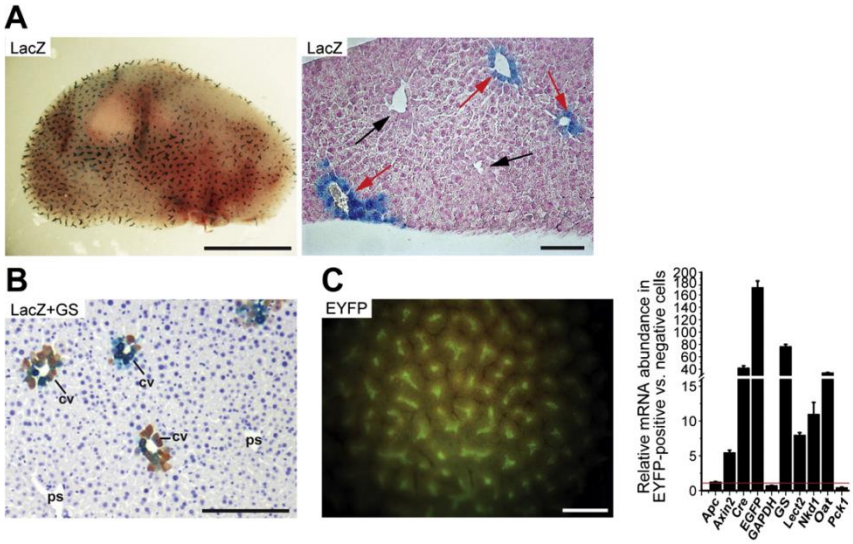


**Fig. 3.** *Nkd1* transcription is zonated to the perivenous hepatocytes. (A) Left, whole-mount staining of LacZ in the adult liver of Nkd1-CreERT2$^{+}$/Rosa26R mice one day after tamoxifen administration. Right, histochemical staining detects the LacZ activity in hepatocytes surrounding the putative centrilobular veins [(cv); red arrow]; periportal hepatocytes in close proximity to the portal space [(ps); black arrow] are LacZ negative. The specimen was counterstained with nuclear red. Scale bar: 4 mm (left image), 0.3 mm (right image). (B) Immunohistochemical co-localization of LacZ (blue color) and anti-GS (brown color) staining. The specimen was counterstained with hematoxylin. Scale bar: 0.3 mm. (C) Left, whole-mount fluorescent image of the Nkd1-CreERT2$^{+}$/Rosa26R-EYFP liver taken four days upon tamoxifen administration. Scale bar: 0.4 mm. Right, qRT-PCR analysis of EYFP$^{+}$ and EYFP$^{-}$ cells sorted from the Nkd1-CreERT2$^{+}$/Rosa26R-EYFP liver. The results were normalized to *Ubb* mRNA levels. The expression level of a given gene in EYFP$^{-}$ cells was arbitrarily set to 1 (red line). Error bar: SD. Notice the enrichment of *Nkd1* mRNA along with other pericentral hepatocyte genes *Axin2*, *GS*, *Lect2*, and *Oat*. In contrast, *Apc* and *GAPDH* genes are not zonated and portal-specific *Pck1* displays a complementary expression pattern to the perivenous hepatocyte genes.

was hypomethylated in the majority of CRCs, the distal CpG island was heavily methylated. In concordance with previously published data [44], differential methylation of the CpG island and adjacent "shores" (for terminology see Materials and Methods) situated within 2 kb of the transcription start site was strongly associated with transcription of the *NKD1* gene. Interestingly, the highest *NKD1* mRNA levels were

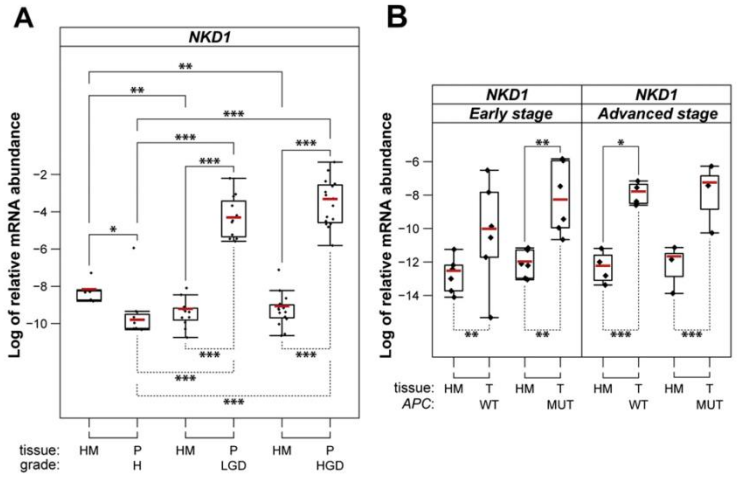


**Fig. 4.** NKD1 expression is increased during colorectal cancerogenesis. (A) Relative expression levels of *NKD1* in colorectal polyps. Log of relative expression levels (-ΔCp) were obtained following normalization of Cp values by geometric average of internal housekeeping genes *ACTB*, *UBB* and *AXIN1*. Predominant histological appearance stratified the lesions to hyperplasia (H), low-grade dysplasia (LGD) and high-grade dysplasia (HGD) subgroups. (B) Relative levels of *NKD1* transcript in CRCs. Cp values were normalized using *ACTB* as a reference gene to obtain ΔCp's. Malignant lesions were subdivided to distinct subgroups with respect to the *APC* mutation status (WT, wild-type *APC*; MUT, *APC* mutated) and disease progression. Statistical significance of differential expression in the given groups was examined by nonparametric Wilcoxon's rank-sum test (solid line). Moreover, the linear model (REML; dashed line), which accounted for the individual background of the patients, tissue type, histopathology, *APC* mutation status (CRC specimens only), was applied. The boxed areas correspond to the second and third quartiles; the range of the values is given by "whiskers" above and below each box. Median of ΔCp values for individual categories is depicted as the red line. Statistical data accompanying Fig. 4A and B can be found in Supplementary Table S5 and S6, respectively. *P < 0.05, **P < 0.01, and ***P < 0.001. HM, matching healthy mucosa; P, polyp; T, tumor.

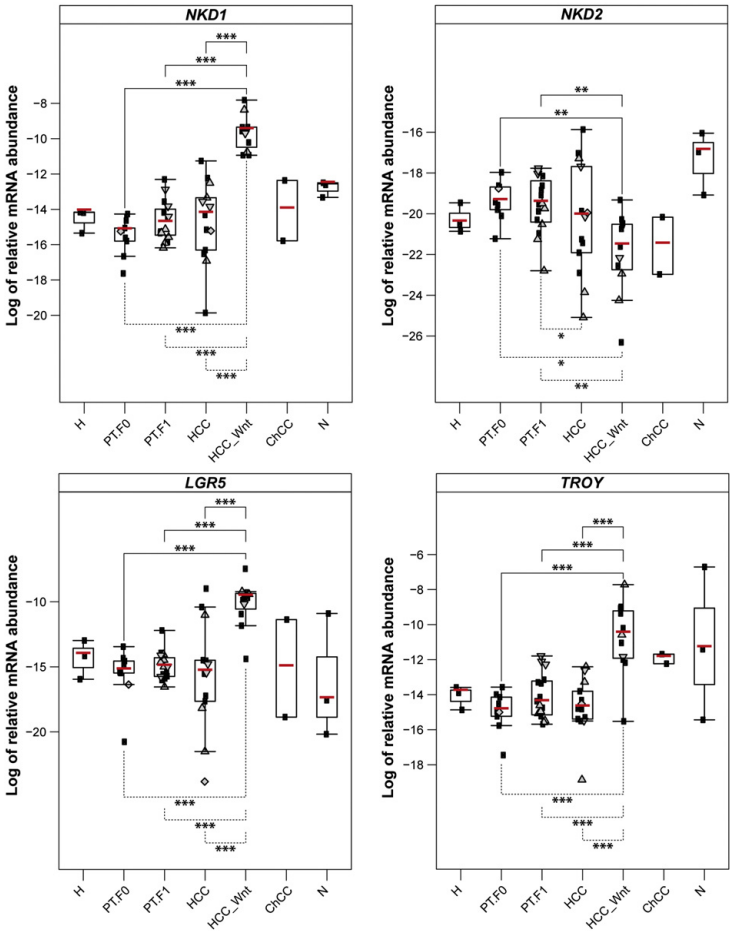


**Fig. 5.** NKD1 transcription is elevated in the Wnt class of HCCs. Relative mRNA abundance of the indicated genes in liver tumors and matched surrounding tissue. For each gene, Cp values were normalized by geometric average of the housekeeping genes *ACTB* and *UBB* (−ΔCp). The Wnt class (HCC_Wnt) was defined by expression levels of *AXIN2*, *EPBH2*, and *GS* genes (details are given in Supplementary Fig. S2). Two cases of cholangiocellular carcinoma constitute a separate group designated as ChCC. Additional types of liver neoplasia (adenolipoma, focal nodular hyperplasia and metastasis of colorectal carcinoma) were merged to a single group (N). Specimens of matched surrounding parenchyma were assessed according to the degree of fibrosis as healthy (H), precancerous tissue displaying mild to moderate fibrosis (PT.F0), or precancerous tissue exhibiting severe fibrosis to cirrhosis (PT.F1) [73]. Statistical significance of differential expression in the given groups was examined by nonparametric Wilcoxon's rank-sum test (solid line). Moreover, the linear model (REML; dashed line), which accounted for the individual background of the patients, tissue type and fibrosis score, was applied. The presence of viral infection is indicated by graphical symbols [circle: virus not detected; triangle: HBV positive; down-pointing triangle: HCV positive; lozenge: HBV + HCV positive]. Statistical analysis of ChCC samples was omitted from the image due to the small group size. Median of ΔCp values for individual categories is depicted as the red line. Numeric values accompanying this figure are given in Supplementary Table S7. *$P < 0.05$, **$P < 0.01$, and ***$P < 0.001$.

detected in CRC specimens that showed hypomethylation in the intron 3 S-shore region (Supplementary Figure S5).

## 4. Discussion

The activity of the Wnt pathway undergoes complex regulation to ensure proper functioning of signaling during development and in adult tissue homeostasis. The regulation may occur at several levels and includes both positive and negative feedback loops. In the intestinal crypt, a well-established cellular system depending on Wnt signaling, the pathway up-regulates Lgr5, a receptor for Rspos, and consequently, the Lgr5-Rspo interaction augments the Wnt/β-catenin signaling output [53]. In addition, Axin2 and Troy, two inhibitors of the Wnt pathway, are also induced by Wnt signaling [6,55]. Interestingly, mRNA levels encoding these genes display some variations among different cellular types located in the crypt. Troy appears to be exclusively expressed in ISCs [6,56]. However, Lgr5 – originally sought to be a unique stem cell marker – is also produced in non-dividing progenitors of the Paneth cells lineage [46]. Moreover, Axin2 expression is confined to the majority of cellular types located in the lower part of the crypts, i.e. ISCs, Paneth cells and their progenitors, and TA cells [46]. According to our lineage tracing experiments and expression analysis (Fig. 2), *Nkd1* represents another negative feedback regulator of Wnt signaling displaying relatively broad expression in the mouse crypt. Currently, it is not clear whether the observed differences in expression profiles of these Wnt pathway genes have any functional consequences. It is possible that these differences contribute to the fine-tuning of Wnt signaling. However, since targeted inactivation of any of the genes described above has no obvious phenotype, such explanation seems unlikely. More probably, random fluctuations in gene transcription might account for

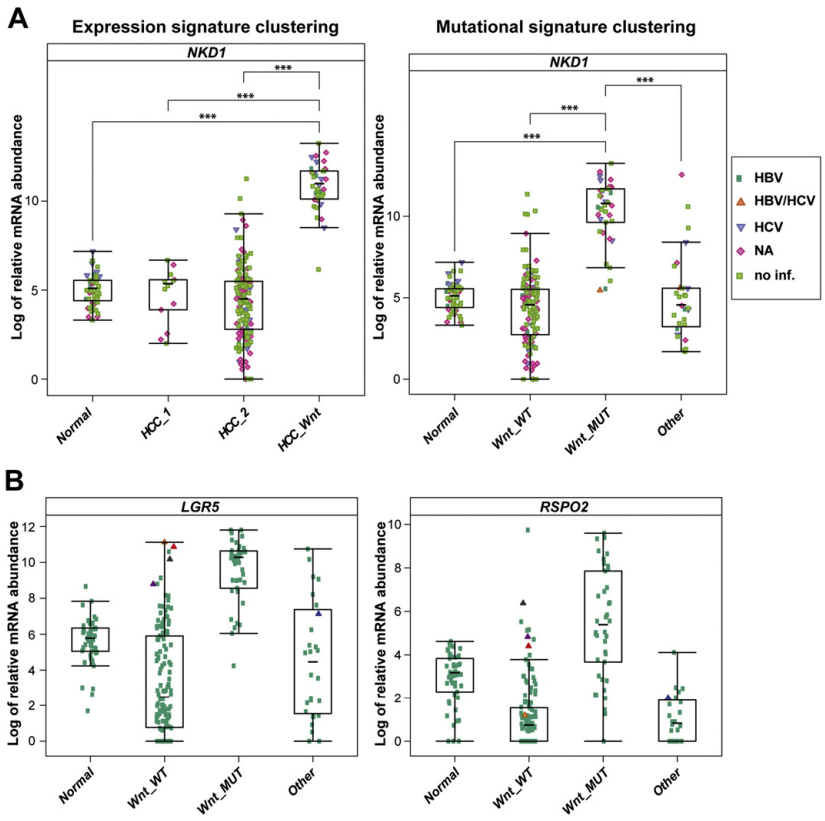


**Fig. 6.** NKD1 defines HCC displaying aberrant Wnt signaling. (A) Left panel, expression of *NKD1* in three gene expression classes of HCCs. The TCGA HCC specimens were stratified using transcription levels of the *AXIN2*, *EPHB2*, and *GS* (details are given in Supplementary Fig. S3). Right panel, relative expression of *NKD1* in HCC samples assigned to the individual mutation groups. Classification of the TCGA HCC specimens according to mutational changes in *APC*, *AXIN1/2*, and *CNNB1* is given in Supplementary Fig. S4. (B) Expression of *LGR5* and *RSPO2* in the HCC mutation groups. Samples assigned to the HCC_Wnt class that do not fall to the Wnt_MUT group are indicated by triangles of matched color. Black lines indicate median of expression levels for individual categories. Numerical values accompanying this figure are given in Supplementary Tables S7 and S8. *$P < 0.05$, **$P < 0.01$, and ***$P < 0.001$.

the observed variations in mRNA levels of a given gene in crypt cells [57]. In the mouse liver, *Nkd1* represents, together with *Axin2* and *Troy* (BF and VK, unpublished data), a robust marker of perivenous hepatocytes. Although the involvement of Wnt signaling in liver zonation is well established, the liver-specific *Nkd1* function has not been – similarly as in gut tissue – documented.

In a collection of human intestinal neoplasia the *NKD* mRNA levels were upregulated in nearly all of the tumors irrespective of the *APC* status (Fig. 4). This was seemingly surprising, since in mouse hyperplastic crypts *Nkd1* overexpression was directly linked to *Apc* loss. Nevertheless, the mutational status of *APC* in the panel of CRCs was based on sequencing of the exon 19 (NCBI nomenclature) that contains the mutational "hot spot", but it likely does not cover all *APC* mutations [6]. Moreover, recent studies employing massive parallel sequencing of tumor DNA indicated that gene alterations resulting in hyperactive Wnt signaling can be found in more than 90% of CRCs [18]. Therefore, limited knowledge of the status of the Wnt pathway in (our) CRC collection can be attributed to the discrepancy between *Nkd1* expression data obtained in the mouse and in clinical samples. This explanation may interpret the observed decrease in the *NKD1* mRNA levels in hyperplastic polyps (Fig. 4A). According to the recent concept of the "serrated neoplasia pathway", precancerous hyperplasia is linked to the development of a separate subclass of gut tumors [58]. Serrated CRC lesions are predominantly initiated by oncogenic *BRAF* mutations and do not harbor genetic changes that would compromise control over Wnt signaling [59].

Relevant CRC datasets obtained from TCGA did not include paired samples of the healthy mucosa, and thus we could not directly compare the *NKD1* mRNA levels in tumors and normal (matched) tissue. Nevertheless, in APC-deficient CRCs at early stage of progression, *NKD1* transcription was higher in MSS lesions than in tumors displaying increased levels of microsatellite instability. Furthermore, upon subdivision of CRCs according to their expression signature, *NKD1* mRNA was significantly increased in the TA (progenitor) type of the tumors (Supplementary Fig. S1). Whether the extent of *NKD1* upregulation reflects a particular mechanism of tumor initiation or mirrors the variability of *NKD1* expression in the cellular types present in the healthy colon remains to be determined.

Although in the majority of CRCs the aberrant Wnt activity is attributable to mutations affecting intracellular components of the Wnt pathway [18], the signaling output can be augmented by epigenetic silencing of genes encoding secreted Wnt antagonists, such as secreted frizzled-related proteins (SFRPs) and dickkopf WNT signaling pathway inhibitors (DKKs) [60–63]. Thus, integration of genetic and epigenetic changes that affect multiple steps of the Wnt signal transduction likely confers a selective advantage to tumor cells. In line with these "multiple-hit"

concepts and given that methylation of *NKD1* regulatory elements was observed in ovarian and gastric cancer [64,65], we investigated the methylation status in 366 CRC samples of the TCGA dataset and examined its relation to *NKD1* transcription. In contrast to other neoplasia, loci proximal to the *NKD1* promoter were unmethylated. Moreover, *NKD1* mRNA was more abundant in colorectal tumors displaying hypomethylation in the S-shore region located in the third intron of the *NKD1* gene (Supplementary Figure S5). Strikingly, the CRC "methylome" analysis by Irizarry and colleagues identified an identical inverse relationship between intron 3 S-shore methylation and *NKD1* expression [44]. In summary, dysregulation of *NKD1* in tumors is possibly driven by as yet undescribed epigenetic mechanisms.

The etiology of HCC is mainly associated with alcohol abuse and HBV and HCV infection. Consequently, HCC is rather a heterogeneous disease and the link between aberrant Wnt signaling and HCC is less obvious than in the cancer of the colon and rectum. Although there is no generally accepted molecular classification of the disease, several recent studies identified (sub)classes of HCC. Importantly, the Wnt-associated class of HCC (approximately 20–40% of all cases) is predominantly defined by the presence of activating mutations in the *CTNNB1* gene. In contrast, alterations in *APC*, so dominant in CRC, are less frequent in HCC (2–3%) [66]. This is rather peculiar since the *APC* gene represents a substantially larger "target" than the exon 3 in the *CTNNB1* gene. Of note, in hepatoblastoma, the most frequent malignant pediatric tumor of the liver, approximately 50% of neoplastic lesions harbor activating mutation in *CTNNB1* [67] and display elevated expression of *NKD1* [68]. Nevertheless, since *APC* and *CTNNB1* mutations are mutually exclusive, the high frequency of the changes in the latter gene possibly reflects a combination of the locus accessibility and/or presence of liver-specific mutagens rather than any unique β-catenin-dependent role in HCC initiation or progression.

The gene expression signature of three Wnt signaling target genes, *AXIN2*, *EPHB2*, and *GS*, was used to stratify HCCs to the β-catenin-dependent "HCC_Wnt" class. Although we were unable (probably due to the limited number of specimens in our experimental collection) to separate the rest of the samples to other classes as described previously [25], the *NKD1* expression profile fitted well to the "HCC_Wnt" class. In agreement with these results, bioinformatic analysis of the HCC datasets obtained from TCGA confirmed that *AXIN2*, *EPHB2*, *GS*, and *NKD1* represent robust markers of the HCC_Wnt class. Interestingly, not all specimens from this class harbored mutations in the *APC*, *AXIN1/2*, and *CTNNB1* genes. Interestingly, we observed amplification of the *RSPO2* locus in two of the samples (out of four in total). This is in accordance with recent data indicating that the amplification of the *RSPO* genes represents a frequent event in HCC (up to 25%) [51–66]. Increased production of *RSPO* ligands has been observed in CRC as an oncogenic "by-pass" mechanism that circumvents intact *APC* [69]. Collectively, the membranous inputs may contribute to liver tumorigenesis in a manner analogous to signaling circuits described in CRC. Finally, seven samples assigned to the Wnt_MUT group did not display the Wnt-dependent expression signature. Since all these samples carried "likely oncogenic mutations" (LOMs) in exon 3 of the *CTNNB1* (Supplementary Table S4) that do not change the regulatory serine/threonine residue, we presume that these mutations are "passenger" without any effect on the β-catenin stability.

Simultaneous inactivation of *APC* and *AXIN2* or *APC* and *NKD1* occurs in exceptional cases only. Since sustained expression of *AXIN2* and *NKD1* is typical of APC-deficient tumors, we speculate that the function of these Wnt pathway inhibitors might be strongly favored to keep the Wnt pathway activity "optimal" for tumor growth [70,71]. This conclusion is in accordance with recent results of Barrry and colleagues demonstrating that another DVL interacting partner, yes-associated protein 1 (YAP1), limits aberrant Wnt signaling and that YAP1-deficiency leads to highly aggressive undifferentiated CRCs or results in Wnt hypersensitivity during intestinal regeneration [72]. Interestingly, YAP1 restricts Wnt signaling independently of the β-catenin destruction complex by suppressing nuclear translocation of Dvl. Thus, we propose that in concordance with the "passive antagonist" model [32], Nkd1 might directly influence the nuclear Dvl function in cells displaying hyperactive Wnt signaling.

In summary, despite its unclear molecular function, *NKD1* can serve as a reliable marker of intestinal and liver tumors that display aberrant Wnt/β-catenin signaling.

## 5. Conclusion

Mutations in genes encoding components of the Wnt/β-catenin pathway that result in aberrant activation of the signaling are undoubtedly linked to the onset of intestinal cancer. In contrast, the etiology of liver cancer is heterogeneous and frequently linked to viral infection. Although several recent studies aimed to identify subclasses of HCC, there is no generally accepted molecular classification of the disease. In the present study we employed a negative feedback regulator of Wnt signaling, Nkd1, as a marker of active Wnt signaling in the intestine and liver and in tumors originating from these organs. Our results provide evidence that *NKD1* can be utilized to distinguish a class of HCC linked to aberrant Wnt signaling.

## Conflicts of interest

There are no conflicts of interest to disclose.

## Acknowledgements

We thank S. Takacova for critically reading the manuscript. We also thank M. Cepko and S. Robine for reagents and Villin-CreERT2 mice. This work was supported by the Grant Agency of the Czech Republic (Grant No. P305/11/1780), institutional grant from the Academy of Sciences of the Czech Republic (RVO 68378050), project BIOCEV – Biotechnology and Biomedicine Centre of the Academy of Sciences and Charles University (CZ.1.05/1.1.00/02.0109) from the European Regional Development Fund to V.K. and R.S., Ministry of Education, Youth and Sports of the Czech Republic (LM2011032) to R.S., Institutional support from the Ministry of Health of the Czech Republic for development of research organization (00023001) to M.O., M.N., and M.J., Grant Agency of Charles University in Prague (1400-243-253470) to J.St., Charles University in Prague Research Project PRVOUK - Oncology P27 to J.Sv.

The results shown here are in part based upon data generated by the TCGA Research (http://cancergenome.nih.gov/). We are deeply grateful to all specimen donors and research groups that have made the data publicly available. We also express our special thanks to the employees of the Transgenic and Archiving Module, the Czech Centre for Phenogenomics, IMG, Prague for their excellent effort in generation of transgenic mice.

## Appendix A. Supplementary data

Supplementary data to this article can be found online at http://dx.doi.org/10.1016/j.cellsig.2014.11.008.

## References

[1] K.M. Cadigan, Cold Spring Harb. Perspect. Biol. 1 (2009) a002881.
[2] T. Valenta, G. Hausmann, K. Basler, EMBO J. 31 (2012) 2714–2736.
[3] A. Schepers, H. Clevers, Cold Spring Harb. Perspect. Biol. 4 (2012) a007989.
[4] H.C. Clevers, C.L. Bevins, Annu. Rev. Physiol. 75 (2013) 289–311.
[5] N. Barker, J.H. van Es, J. Kuipers, P. Kujala, M. van den Born, M. Cozijnsen, A. Haegebarth, J. Korving, H. Begthel, P.J. Peters, H. Clevers, Nature 449 (2007) 1003–1007.
[6] B. Fafilek, M. Krausova, M. Vojtechova, V. Pospichalova, L. Tumova, E. Sloncova, M. Huranova, J. Stancikova, A. Hlavata, J. Svec, R. Sedlacek, O. Luksan, M. Oliverius, L. Voska, M. Jirsa, J. Paces, M. Kolar, M. Krivjanska, K. Klimesova, H. Tlaskalova-Hogenova, V. Korinek, Gastroenterology 144 (2013) 381–391.

[7] L.G. van der Flier, M.E. van Gijn, P. Hatzis, P. Kujala, A. Haegebarth, D.E. Stange, H. Begthel, M. van den Born, V. Guryev, I. Oving, J.H. van Es, N. Barker, P.J. Peters, M. van de Wetering, H. Clevers, Cell 136 (2009) 903–912.
[8] E. Batlle, J.T. Henderson, H. Beghtel, M.M. van den Born, E. Sancho, G. Huls, J. Meeldijk, J. Robertson, M. van de Wetering, T. Pawson, H. Clevers, Cell 111 (2002) 251–263.
[9] M. Krausova, V. Korinek, Cell. Signal. 26 (2014) 570–579.
[10] V. Korinek, N. Barker, P. Moerer, E. van Donselaar, G. Huls, P.J. Peters, H. Clevers, Nat. Genet. 19 (1998) 379–383.
[11] J.H. van Es, A. Haegebarth, P. Kujala, S. Itzkovitz, B.K. Koo, S.F. Boj, J. Korving, M. van den Born, A. van Oudenaarden, S. Robine, H. Clevers, Mol. Cell. Biol. 32 (2012) 1918–1927.
[12] T. Fevr, S. Robine, D. Louvard, J. Huelsken, Mol. Cell. Biol. 27 (2007) 7551–7559.
[13] H. Ireland, R. Kemp, C. Houghton, L. Howard, A.R. Clarke, O.J. Sansom, D.J. Winton, Gastroenterology 126 (2004) 1236–1246.
[14] S.P. Monga, Gene Expr. 16 (2014) 51–62.
[15] S. Benhamouche, T. Decaens, C. Godard, R. Chambrey, D.S. Rickman, C. Moinard, M. Vasseur-Cognet, C.J. Kuo, A. Kahn, C. Perret, S. Colnot, Dev. Cell 10 (2006) 759–770.
[16] P. Polakis, Cold Spring Harb. Perspect. Biol. 4 (2012).
[17] K.W. Kinzler, B. Vogelstein, Cell 87 (1996) 159–170.
[18] Nature 487 (2012) 330–337.
[19] D.P. Minde, Z. Anvarian, S.G. Rudiger, M.M. Maurice, Mol. Cancer 10 (2011) 101.
[20] Y. Shimizu, S. Ikeda, M. Fujimori, S. Kodama, M. Nakahara, M. Okajima, T. Asahara, Genes Chromosom. Cancer 33 (2002) 73–81.
[21] W. Liu, X. Dong, M. Mai, R.S. Seelan, K. Taniguchi, K.K. Krishnadath, K.C. Halling, J.M. Cunningham, L.A. Boardman, C. Qian, E. Christensen, S.S. Schmidt, P.C. Roche, D.I. Smith, S.N. Thibodeau, Nat. Genet. 26 (2000) 146–147.
[22] P.J. Morin, A.B. Sparks, V. Korinek, N. Barker, H. Clevers, B. Vogelstein, K.W. Kinzler, Science 275 (1997) 1787–1790.
[23] H.B. El-Serag, K.L. Rudolph, Gastroenterology 132 (2007) 2557–2576.
[24] Y. Hoshida, S.M. Nijman, M. Kobayashi, J.A. Chan, J.P. Brunet, D.Y. Chiang, A. Villanueva, P. Newell, K. Ikeda, M. Hashimoto, G. Watanabe, S. Gabriel, S.L. Friedman, H. Kumada, J.M. Llovet, T.R. Golub, Cancer Res. 69 (2009) 7385–7392.
[25] A. Lachenmayer, C. Alsinet, R. Savic, L. Cabellos, S. Toffanin, Y. Hoshida, A. Villanueva, B. Minguez, P. Newell, H.W. Tsai, J. Barretina, S. Thung, S.C. Ward, J. Bruix, V. Mazzaferro, M. Schwartz, S.L. Friedman, J.M. Llovet, Clin. Cancer Res. 18 (2012) 4997–5007.
[26] S. Li, M. Mao, Cancer Lett. 340 (2013) 247–253.
[27] R. Rousset, J.A. Mack, K.A. Wharton Jr., J.D. Axelrod, K.M. Cadigan, M.P. Fish, R. Nusse, M.P. Scott, Genes Dev. 15 (2001) 658–671.
[28] I. Schneider, P.N. Schneider, S.W. Derry, S. Lin, L.J. Barton, T. Westfall, D.C. Slusarski, Dev. Biol. 348 (2010) 22–33.
[29] T.J. Van Raay, R.J. Coffey, L. Solnica-Krezel, Dev. Biol. 309 (2007) 151–168.
[30] T.J. Van Raay, N.J. Fortino, B.W. Miller, H. Ma, G. Lau, C. Li, J.L. Franklin, L. Attisano, L. Solnica-Krezel, R.J. Coffey, PLoS One 6 (2011) e18650.
[31] S. Zhang, T. Cagatay, M. Amanai, M. Zhang, J. Kline, D.H. Castrillon, R. Ashfaq, O.K. Oz, K.A. Wharton Jr., Mol. Cell. Biol. 27 (2007) 4454–4464.
[32] D. Angonin, T.J. Van Raay, PLoS One 8 (2013) e74666.
[33] A.R. Moser, H.C. Pitot, W.F. Dove, Science 247 (1990) 322–324.
[34] L.K. Su, K.W. Kinzler, B. Vogelstein, A.C. Preisinger, A.R. Moser, C. Luongo, K.A. Gould, W.F. Dove, Science 256 (1992) 668–670.
[35] P. Soriano, Nat. Genet. 21 (1999) 70–71.
[36] S. Srinivas, T. Watanabe, C.S. Lin, C.M. William, Y. Tanabe, T.M. Jessell, F. Costantini, BMC Dev. Biol. 1 (4) (2001).
[37] M. Kuraguchi, X.P. Wang, R.T. Bronson, R. Rothenberg, N.Y. Ohene-Baah, J.J. Lund, M. Kucherlapati, R.L. Maas, R. Kucherlapati, PLoS Genet. 2 (2006) e146.
[38] F. el Marjou, K.P. Janssen, B.H. Chang, M. Li, V. Hindie, L. Chan, D. Louvard, P. Chambon, D. Metzger, S. Robine, Genesis 39 (2004) 186–193.
[39] T. Shimosato, M. Tohno, T. Sato, J. Nishimura, Y. Kawai, T. Saito, H. Kitazawa, Anim. Sci. J. 80 (2009) 597–604.
[40] O. Machon, C.J. van den Bout, M. Backman, O. Rosok, X. Caubit, S.H. Fromm, B. Geronimo, S. Krauss, Neuroscience 112 (2002) 951–966.
[41] T. Sato, J.H. van Es, H.J. Snippert, D.E. Stange, R.G. Vries, M. van den Born, N. Barker, N.F. Shroyer, M. van de Wetering, H. Clevers, Nature 469 (2011) 415–418.
[42] Y. Ohashi, S. Kansal, M. Schreiber Jr., Advances in peritoneal dialysis, Conference on peritoneal dialysis282012. 131–133.
[43] H. Wu, B. Caffo, H.A. Jaffee, R.A. Irizarry, A.P. Feinberg, Biostatistics 11 (2010) 499–514.
[44] R.A. Irizarry, C. Ladd-Acosta, B. Wen, Z. Wu, C. Montano, P. Onyango, H. Cui, K. Gabo, M. Rongione, M. Webster, H. Ji, J.B. Potash, S. Sabunciyan, A.P. Feinberg, Nat. Genet. 41 (2009) 178–186.
[45] A.E. Powell, Y. Wang, Y. Li, E.J. Poulin, A.L. Means, M.K. Washington, J.N. Higginbotham, A. Juchheim, N. Prasad, S.E. Levy, Y. Guo, Y. Shyr, B.J. Aronow, K.M. Haigis, J.L. Franklin, R.J. Coffey, Cell 149 (2012) 146–158.
[46] S.J. Buczacki, H.I. Zecchini, A.M. Nicholson, R. Russell, L. Vermeulen, R. Kemp, D.J. Winton, Nature 495 (2013) 65–69.
[47] A. Sadanandam, C.A. Lyssiotis, K. Homicsko, E.A. Collisson, W.J. Gibb, S. Wullschleger, L.C. Ostos, W.A. Lannon, C. Grotzinger, M. Del Rio, B. Lhermitte, A.B. Olshen, B. Wiedenmann, L.C. Cantley, J.W. Gray, D. Hanahan, Nat. Med. 19 (2013) 619–625.
[48] C. Fraley, A.E. Raftery, J. Classif. 20 (2003) 263–286.
[49] O.N. Ikediobi, H. Davies, G. Bignell, S. Edkins, C. Stevens, S. O'Meara, T. Santarius, T. Avis, S. Barthorpe, L. Brackenbury, G. Buck, A. Butler, J. Clements, J. Cole, E. Dicks, S. Forbes, K. Gray, K. Halliday, R. Harrison, K. Hills, J. Hinton, C. Hunter, A. Jenkinson, D. Jones, V. Kosmidou, R. Lugg, A. Menzies, T. Mironenko, A. Parker, J. Perry, K. Raine, D. Richardson, R. Shepherd, A. Small, R. Smith, H. Solomon, P. Stephens, J. Teague, C. Tofts, J. Varian, T. Webb, S. West, S. Widaa, A. Yates, W. Reinhold, J.N. Weinstein, M.R. Stratton, P.A. Futreal, R. Wooster, Mol. Cancer Ther. 5 (2006) 2606–2612.
[50] G.R. Bignell, C.D. Greenman, H. Davies, A.P. Butler, S. Edkins, J.M. Andrews, G. Buck, L. Chen, D. Beare, C. Latimer, S. Widaa, J. Hinton, C. Fahey, B. Fu, S. Swamy, G.L. Dalgliesh, B.T. Teh, P. Deloukas, F. Yang, P.J. Campbell, P.A. Futreal, M.R. Stratton, Nature 463 (2010) 893–898.
[51] C. Guichard, G. Amaddeo, S. Imbeaud, Y. Ladeiro, L. Pelletier, I.B. Maad, J. Calderaro, P. Bioulac-Sage, M. Letexier, F. Degos, B. Clement, C. Balabaud, E. Chevet, A. Laurent, G. Couchy, E. Letouze, F. Calvo, J. Zucman-Rossi, Nat. Genet. 44 (2012) 694–698.
[52] V.H. Bustos, A. Ferrarese, A. Venerando, O. Marin, J.E. Allende, L.A. Pinna, Proc. Natl. Acad. Sci. U. S. A. 103 (2006) 19725–19730.
[53] W. de Lau, N. Barker, T.Y. Low, B.K. Koo, V.S. Li, H. Teunissen, P. Kujala, A. Haegebarth, P.J. Peters, M. van de Wetering, D.E. Stange, J.E. van Es, D. Guardavaccaro, R.B. Schasfoort, Y. Mohri, K. Nishimori, S. Mohammed, A.J. Heck, H. Clevers, Nature 476 (2011) 293–297.
[54] J. Guo, T. Cagatay, G. Zhou, C.C. Chan, S. Blythe, K. Suyama, L. Zheng, K. Pan, C. Qian, R. Hamelin, S.N. Thibodeau, P.S. Klein, K.A. Wharton, W. Liu, PLoS One 4 (2009) e7982.
[55] B. Lustig, B. Jerchow, M. Sachs, S. Weiler, T. Pietsch, U. Karsten, M. van de Wetering, H. Clevers, P.M. Schlag, W. Birchmeier, J. Behrens, Mol. Cell. Biol. 22 (2002) 1184–1193.
[56] D.E. Stange, B.K. Koo, M. Huch, G. Sibbel, O. Basak, A. Lyubimova, P. Kujala, S. Bartfeld, J. Koster, J.H. Geahlen, P.J. Peters, J.H. van Es, M. van de Wetering, J.C. Mills, H. Clevers, Cell 155 (2013) 357–368.
[57] S. Itzkovitz, A. Lyubimova, I.C. Blat, M. Maynard, J. van Es, J. Lees, T. Jacks, H. Clevers, A. van Oudenaarden, Nat. Cell Biol. 14 (2012) 106–114.
[58] E.M.F. De Sousa, X. Wang, M. Jansen, E. Fessler, A. Trinh, L.P. de Rooij, J.H. de Jong, O.J. de Boer, R. van Leersum, M.F. Bijlsma, H. Rodermond, M. van der Heijden, C.J. van Noesel, J.B. Tuynman, E. Dekker, F. Markowetz, J.P. Medema, L. Vermeulen, Nat. Med. 19 (2013) 614–618.
[59] K.S. Boparai, E. Dekker, M.M. Polak, A.R. Musler, S. van Eeden, C.J. van Noesel, Am. J. Pathol. 178 (2011) 2700–2707.
[60] H. Suzuki, E. Gabrielson, W. Chen, R. Anbazhagan, M. van Engeland, M.P. Weijenberg, J.G. Herman, S.B. Baylin, Nat. Genet. 31 (2002) 141–149.
[61] A. Bafico, G. Liu, L. Goldin, V. Harris, S.A. Aaronson, Cancer Cell 6 (2004) 497–506.
[62] H. Suzuki, D.N. Watkins, K.W. Jair, K.E. Schuebel, S.D. Markowitz, W.D. Chen, T.P. Pretlow, B. Yang, Y. Akiyama, M. Van Engeland, M. Toyota, T. Tokino, Y. Hinoda, K. Imai, J.G. Herman, S.B. Baylin, Nat. Genet. 36 (2004) 417–422.
[63] Q.J. Voorham, J. Janssen, M. Tijssen, S. Snellenberg, S. Mongera, N.C. van Grieken, H. Grabsch, M. Kliment, B.J. Rembacken, C.J. Mulder, M. van Engeland, G.A. Meijer, R.D. Steenbergen, B. Carvalho, BMC Cancer 13 (2013) 603.
[64] W. Dai, J.M. Teodoridis, C. Zeller, J. Graham, J. Hersey, J.M. Flanagan, E. Stronach, D.W. Millan, N. Siddiqui, J. Paul, R. Brown, Clin. Cancer Res. 17 (2011) 4052–4062.
[65] Y. Yoda, H. Takeshima, T. Niwa, J.G. Kim, T. Ando, R. Kushima, T. Sugiyama, H. Katai, H. Noshiro, T. Ushijima, Gastric Cancer (2014), http://dx.doi.org/10.1007/s10120-014-0348-0.
[66] Z. Kan, H. Zheng, X. Liu, S. Li, T.D. Barber, Z. Gong, H. Gao, K. Hao, M.D. Willard, J. Xu, R. Hauptschein, P.A. Rejto, J. Fernandez, G. Wang, Q. Zhang, B. Wang, R. Chen, J. Wang, N.P. Lee, W. Zhou, Z. Lin, Z. Peng, K. Yi, S. Chen, L. Li, X. Fan, J. Yang, R. Ye, J. Ju, K. Wang, H. Estrella, S. Deng, P. Wei, M. Qiu, I.H. Wulur, J. Liu, M.E. Ehsani, C. Zhang, A. Loboda, W.K. Sung, A. Aggarwal, R.T. Poon, S.T. Fan, J. Wang, J. Hardwick, C. Reinhard, H. Dai, Y. Li, J.M. Luk, M. Mao, Genome Res. 23 (2013) 1422–1433.
[67] A. Koch, D. Denkhaus, S. Albrecht, I. Leuschner, D. von Schweinitz, T. Pietsch, Cancer Res. 59 (1999) 269–273.
[68] A. Koch, A. Waha, W. Hartmann, A. Hrychyk, U. Schuller, K.A. Wharton Jr., S.Y. Fuchs, D. von Schweinitz, T. Pietsch, Clin. Cancer Res. 11 (2005) 4295–4304.
[69] S. Seshagiri, E.W. Stawiski, S. Durinck, Z. Modrusan, E.E. Storm, C.B. Conboy, S. Chaudhuri, Y. Guan, V. Janakiraman, B.S. Jaiswal, J. Guillory, C. Ha, G.J. Dijkgraaf, J. Stinson, F. Gnad, M.A. Huntley, J.D. Degenhardt, P.M. Haverty, R. Bourgon, W. Wang, H. Koeppen, R. Gentleman, T.K. Starr, Z. Zhang, D.A. Largaespada, T.D. Wu, F.J. de Sauvage, Nature 488 (2012) 660–664.
[70] A. Lewis, S. Segditsas, M. Deheragoda, P. Pollard, R. Jeffery, E. Nye, H. Lockstone, H. Davis, S. Clark, G. Stamp, R. Poulsom, N. Wright, I. Tomlinson, Gut 59 (2010) 1680–1686.
[71] S.H. Chandra, I. Wacker, U.K. Appelt, J. Behrens, J. Schneikert, PLoS One 7 (2012) e34479.
[72] E.R. Barry, T. Morikawa, B.L. Butler, K. Shrestha, R. de la Rosa, K.S. Yan, C.S. Fuchs, S.T. Magness, R. Smits, S. Ogino, C.J. Kuo, F.D. Camargo, Nature 493 (2013) 106–110.
[73] K. Ishak, A. Baptista, L. Bianchi, F. Callea, J. De Groote, F. Gudat, H. Denk, V. Desmet, G. Korb, R.N. MacSween, et al., J. Hepatol. 22 (1995) 696–699.

# GENERAL DISCUSSION AND CONCLUSIONS

The novelty of our study mainly pertains to the demonstration that the expression of enteric α-defensins in the thymus is exclusively restricted to mTECs in Aire-dependent fashion. Thus, enteric α-defensin thymic expression prevents the occurrence of self-reactive T-cells of this specificity in the immune periphery. Conversely, the presence of enteric α-defensin-specific T-cells in the immune periphery leads to the diminishment or absence of enteric α-defensin-producing PCs in the gut of APECED patients and Nude mice transferred with T-cells derived from enteric defensin-immunized Aire-deficient mice. This suggests that defensin-specific T-cells can mediate a direct autoimmune attack on PCs and consequently cause gastrointestinal symptoms that parallel those observed in APECED patients (Dobeš et al., 2015).

These critical findings not only provide important mechanistic insights and at least partly explained the presence of gastrointestinal symptoms in APECED patients, but also serve as an impetus for a plethora of new questions, some of them are discussed below.

First, which signals and which cells are responsible for defensin-specific T-cell activation in the gut? This seems to be a quite intriguing question as enteric α-defensins are secreted by PCs directly into the gut lumen, and thus to act as an antigen, they must be initially somehow translocated back to immune periphery through the intestine lining. As defensins can opsonize and tightly associate with bacteria, viruses and fungi, we can speculate that they can become "guilty by association" with intestinal microbes and the immune response can be triggered against them. Notably, the microbicidal mode of action used by defensins includes their binding to microbial membrane by a pore forming mechanism and subsequent binding to intracellular components (White et al., 1995). During the process of intestinal lumen sampling, intestinal APCs (iAPCs) might uptake microbial antigens opsonized with defensins and present them in the context of their MHC molecules. As some bacterial components, in parallel, function as potent "danger signals" able to engage Pattern Recognition Receptors on iAPCs and upregulate the costimulatory molecules, enteric defensins could be mispresented on activated iAPCs as bacterial antigens and trigger autoimmune responses. The second possibility is that the occurrence of local intestinal damage would lead to the disruption of intestinal homeostasis resulting in the presentation of several intestinal autoantigens in the immune activatory context. Current data accumulated over several years suggest the involvement of the first mechanism. Specifically, while human PCs express only two enteric α-defensin – DEFA5 and DEFA6 (Jones and Bevins, 1992, 1993) the presence of autoantibodies against DEFA5, but not DEFA6, was observed in sera of APECED patients (Dobeš et al., 2015). These two members of human defensin family strikingly differ by their mode of action. While DEFA5 is able to directly kill several pathogenic as well as non-pathogenic bacterial strains (Porter et al., 1997; Salzman et

al., 2003b; Salzman et al., 2010), DEFA6 mainly forms large nanonets scaffolds that entrap bacteria (Chu et al., 2012) and its direct killing activity is quite low and dependent on redox potential of the environment. Moreover, DEFA6 was shown to be able to directly kill only commensal microbes, such as Bifidobacterium adolescentis, but not pathogenic one, like Salmonella typhimurium (Schroeder et al., 2015). This suggests that DEFA5 presentation on iAPCs could be linked to the presentation of bacterial antigens in comparison to DEFA6, which preferentially forms large nanonet traps subjected to the extrusion to the gut lumen. Alternatively, DEFA6 might be presented in association with commensal-derived antigens and thus potentially not recognised in immune activatory context.

Second, how is the diminishment or loss of PCs achieved? In mice, we demonstrated the capacity of $CD8^+$ defensin-specific T-cells to increase cell death of PCs by their direct cytotoxic activity in a co-culture experiment. In addition, and along the same experimental lines, lymphocytic infiltrates were detected in the gut of Nude mice transferred with defensin-specific T-cells from defensin-immunized Aire-deficient animals. Moreover, much higher proportion of both activated $CD4^+$ and $CD8^+$ T-cells was observed in the mesenteric lymph nodes of these animals (Dobeš et al., 2015). All these data suggests that cytotoxic T-cells are responsible for the diminished number of PCs, however a direct in vivo proof of this notion is still missing and the involvement of other cell types and mechanisms cannot be excluded. For instance, high IFN-γ levels are promoting degranulation and extrusion of PCs (Farin et al., 2014) leading to their depletion in the gut (Raetz et al., 2013). Speculatively, the initial diminishment of PCs by $CD8^+$ T-cells mediated attack might lead to intestinal dysbiosis, which might, at least partly, induce IFN-γ production with a devastating potential to impact PC numbers. Also a potential physiological disbalance in PC differentiation program due to their initial loss and lower supply of iSCs niche by vitally needed factors, or imbalance in PC-differentiation promoting factors, might further exacerbate the observed phenomenon. These potential scenarios remain to be tested experimentally. It might be also interesting to test whether in case of IBD, defensin expression can decrease as the consequence of PC-targeted autoimmune attack.

Third, are increased SFB numbers, associated with higher frequencies of IL-17 producing pathogenic $CD4^+$ T-cells observed in animal models, also relevant for APECED patients? Recent reports documented the induction of Th17 cells in the gut by SFB (Ivanov et al., 2009). We reported that the transfer of defensin-specific T-cells from defensin-immunized Aire-deficient mice caused the diminishment of PCs and concomitantly the increase in SFB in the gut and frequency of IL-17 producing cells (Dobeš et al., 2015). These T-cells might exert a pathogenic role as they express IL-23R, previously associated with pathogenic proinflammatory Th17 cells signature (Lee et al., 2012). In the cohort of 150 APECED patients, 91% of them have autoantibodies directed against IL-22, IL-17A (41%) and IL-17F (75%). All of these autoantibodies display blocking function to their cognate cytokines (Kisand et al., 2010). These cytokines are needed for Th17-mediated role in neutrophil recruitment and activation,

further promotion of inflammatory responses or production of AMPs (Korn et al., 2009). The inability of APECED patients to mount Th17-polarized immune response was correlated with their incompetence to fight Candida infection (Kisand et al., 2010). This indicates that higher levels of gut SFB detected in a fraction of APECED patients might not be able to promote Th17 polarization events. In contrast, Aire-deficient mice on C57Bl/6 background did not develop autoantibodies directed against IL-17A/F and IL-22, and Aire-deficient mice on Balb/c background develop autoantibodies directed against IL-17A only later in life (1.5-2 year old). This suggests that young and adolescent Aire-deficient mice can normally mount Th17 responses (Karner et al., 2013). Such differences point to potentially significant but not the only examples when animal model of human disease fails to recapitulate the same immunophenotype. To underline this notion, it should be emphasized that APECED patients, with obviously variable and different genetic background, accumulate various disease components over their lifetime. It is just not surprising that our effort to find parallels in the mechanism of pathophysiological immune processes between synchronized sequential events induced artificially in animal models carrying the identical genetic background and those occurring in their human counterparts provides sometimes opposite and/or heterogeneous results.

In aggregate, the Aire-regulated expression of thymic enteric α-defensin prevents and protects human and mice from deleterious autoimmunity which attack gut-resident PCs. In case of Aire-deficiency, the loss of PCs occurs, leading to changes in the composition of gut microbia and occurrence of IL-17 producing cells. The PC loss was associated with diarrhea disease component in APECED patients. In order to gain a more comprehensive and detail insight into this process, the generation of transgenic mouse strains with enteric α-defensin specific TCRs, which bear different affinities to this self-antigen-MHC complex, is currently underway in our laboratory. This will allow to test various parameters of thymic selection of defensin-specific T-cells, e.g. direct mTEC presentation leading presumably to the deletion of defensin-specific T-cells or their conversion into Tregs lineage, or contribution of other thymic cell types to negative selection process, and many others. Moreover, this newly established mouse model will also allow to experimentally dissect the process leading to PC diminishment under autoimmune conditions.

Interestingly, the situation described in the second attached paper is quite opposite to the previous one which describes autoimmunity-mediated PC diminishment, since higher frequency of PCs was observed in animals that are deficient in Hic1 in the intestinal tissue (Janeckova et al., 2015). Moreover, Hic1 deficiency leads to the upregulation of Tlr2 receptor in the intestinal tissue. Unfortunately, the composition of intestinal microbiota was not determined in this report. We can just speculate what is the impact of much higher frequencies of PCs and Tlr2 upregulation on intestinal homeostasis. Intuitively, one can suggests that higher PC numbers would result in more efficient elimination of potential pathogenic intruders as it was previously shown for murine intestinal system with transgenic expression of human enteric α-defensin

(Salzman et al., 2010). In contrast, an aberrant increase in Tlr2 expression (Janeckova et al., 2015) could lead to excessive and rapid degranulation of PCs (Ayabe et al., 2000) potentially leading to intestinal dysbiosis caused by the overload of enteric α-defensin in the gut lumen. The enhanced Tlr2 expression by mucine secreting GCs and their higher proportion in the gut (Janeckova et al., 2015) might also force GCs to secrete higher levels of mucin which, at least transiently, can slow down the uptake of nutrients from the gut lumen. These predictions are fully testable and might be the topic of future experiments focused on the role of Hic1 in the intestine physiology in health and disease.

Lastly, the Nkd1 expression and its involvement in intestinal homeostasis were determined. Nkd1 was expressed in all cells with active Wnt signaling residing in the base of intestinal crypts (Stancikova et al., 2015). Given its regulatory role in Wnt cascade (Angonin and Van Raay, 2013), it is quite surprising that the double knock-out of both murine paralogs Nkd1 and Nkd2, leads only to a very mild phenotype associated with morphological changes of bones and slightly lower body weight. However, as the authors do not analyze the frequency and status of main cell types of the intestine, it is not clear how much these genetic ablations perturbed the physiology of gut (Zhang et al., 2007). The resolution of these questions awaits further experimentation. Interestingly, the association of high Nkd1 expression levels with neoplastic transformation could be potentially utilized as a useful diagnostic molecular marker in clinics.

In summary, presented thesis describes numerous discoveries and observations that extend the current view on the process of immune tolerance and maintenance of gut homeostasis. As these results invite for numerous, so far, unanswered questions, they at the same time pave the road for exciting research activities in the very near future.

# REFERENCES

Abramson, J., Giraud, M., Benoist, C., and Mathis, D. (2010). Aire's partners in the molecular control of immunological tolerance. Cell *140*, 123-135.

Anderson, M.S., Venanzi, E.S., Klein, L., Chen, Z., Berzins, S.P., Turley, S.J., von Boehmer, H., Bronson, R., Dierich, A., Benoist, C., *et al.* (2002). Projection of an immunological self shadow within the thymus by the aire protein. Science *298*, 1395-1401.

Andreu, P., Colnot, S., Godard, C., Gad, S., Chafey, P., Niwa-Kawakita, M., Laurent-Puig, P., Kahn, A., Robine, S., Perret, C., *et al.* (2005). Crypt-restricted proliferation and commitment to the Paneth cell lineage following Apc loss in the mouse intestine. Development *132*, 1443-1451.

Angonin, D., and Van Raay, T.J. (2013). Nkd1 functions as a passive antagonist of Wnt signaling. PLoS One *8*, e74666.

Apter, F.M., Lencer, W.I., Finkelstein, R.A., Mekalanos, J.J., and Neutra, M.R. (1993). Monoclonal immunoglobulin A antibodies directed against cholera toxin prevent the toxin-induced chloride secretory response and block toxin binding to intestinal epithelial cells in vitro. Infect Immun *61*, 5271-5278.

Aschenbrenner, K., D'Cruz, L.M., Vollmann, E.H., Hinterberger, M., Emmerich, J., Swee, L.K., Rolink, A., and Klein, L. (2007). Selection of Foxp3+ regulatory T cells specific for self antigen expressed and presented by Aire+ medullary thymic epithelial cells. Nat Immunol *8*, 351-358.

Atarashi, K., Nishimura, J., Shima, T., Umesaki, Y., Yamamoto, M., Onoue, M., Yagita, H., Ishii, N., Evans, R., Honda, K., *et al.* (2008). ATP drives lamina propria T(H)17 cell differentiation. Nature *455*, 808-812.

Atarashi, K., Tanoue, T., Oshima, K., Suda, W., Nagano, Y., Nishikawa, H., Fukuda, S., Saito, T., Narushima, S., Hase, K., *et al.* (2013). Treg induction by a rationally selected mixture of Clostridia strains from the human microbiota. Nature *500*, 232-236.

Atarashi, K., Tanoue, T., Shima, T., Imaoka, A., Kuwahara, T., Momose, Y., Cheng, G., Yamasaki, S., Saito, T., Ohba, Y., *et al.* (2011). Induction of colonic regulatory T cells by indigenous Clostridium species. Science *331*, 337-341.

Atibalentja, D.F., Byersdorfer, C.A., and Unanue, E.R. (2009). Thymus-blood protein interactions are highly effective in negative selection and regulatory T cell induction. J Immunol *183*, 7909-7918.

Ayabe, T., Satchell, D.P., Pesendorfer, P., Tanabe, H., Wilson, C.L., Hagen, S.J., and Ouellette, A.J. (2002a). Activation of Paneth cell alpha-defensins in mouse small intestine. J Biol Chem *277*, 5219-5228.

Ayabe, T., Satchell, D.P., Wilson, C.L., Parks, W.C., Selsted, M.E., and Ouellette, A.J. (2000). Secretion of microbicidal alpha-defensins by intestinal Paneth cells in response to bacteria. Nat Immunol *1*, 113-118.

Ayabe, T., Wulff, H., Darmoul, D., Cahalan, M.D., Chandy, K.G., and Ouellette, A.J. (2002b). Modulation of mouse Paneth cell alpha-defensin secretion by mIKCa1, a Ca2+-activated, intermediate conductance potassium channel. J Biol Chem *277*, 3793-3800.

Baba, T., Badr Mel, S., Tomaru, U., Ishizu, A., and Mukaida, N. (2012). Novel process of intrathymic tumor-immune tolerance through CCR2-mediated recruitment of Sirpalpha+ dendritic cells: a murine model. PLoS One *7*, e41154.

Baba, T., Nakamoto, Y., and Mukaida, N. (2009). Crucial contribution of thymic Sirp alpha+ conventional dendritic cells to central tolerance against blood-borne antigens in a CCR2-dependent manner. J Immunol *183*, 3053-3063.

Barker, N., van Es, J.H., Kuipers, J., Kujala, P., van den Born, M., Cozijnsen, M., Haegebarth, A., Korving, J., Begthel, H., Peters, P.J., *et al.* (2007). Identification of stem cells in small intestine and colon by marker gene Lgr5. Nature *449*, 1003-1007.

Bernatik, O., Ganji, R.S., Dijksterhuis, J.P., Konik, P., Cervenka, I., Polonio, T., Krejci, P., Schulte, G., and Bryja, V. (2011). Sequential activation and inactivation of Dishevelled in the Wnt/beta-catenin pathway by casein kinases. J Biol Chem *286*, 10396-10410.

Bonasio, R., Scimone, M.L., Schaerli, P., Grabie, N., Lichtman, A.H., and von Andrian, U.H. (2006). Clonal deletion of thymocytes by circulating dendritic cells homing to the thymus. Nat Immunol *7*, 1092-1100.

Brandtzaeg, P. (1998). Development and basic mechanisms of human gut immunity. Nutr Rev *56*, S5-18.

Briggs, K.J., Eberhart, C.G., and Watkins, D.N. (2008). Just say no to ATOH: how HIC1 methylation might predispose medulloblastoma to lineage addiction. Cancer Res *68*, 8654-8656.

Broderick, N.A. (2015). A common origin for immunity and digestion. Front Immunol *6*, 72.

Buczacki, S.J., Zecchini, H.I., Nicholson, A.M., Russell, R., Vermeulen, L., Kemp, R., and Winton, D.J. (2013). Intestinal label-retaining cells are secretory precursors expressing Lgr5. Nature *495*, 65-69.

Buras, J.A., Holzmann, B., and Sitkovsky, M. (2005). Animal models of sepsis: setting the stage. Nat Rev Drug Discov *4*, 854-865.

Cadigan, K.M., and Peifer, M. (2009). Wnt signaling from development to disease: insights from model systems. Cold Spring Harb Perspect Biol *1*, a002881.

Carter, P.B., and Collins, F.M. (1974). The route of enteric infection in normal mice. J Exp Med *139*, 1189-1203.

Cebula, A., Seweryn, M., Rempala, G.A., Pabla, S.S., McIndoe, R.A., Denning, T.L., Bry, L., Kraj, P., Kisielow, P., and Ignatowicz, L. (2013). Thymus-derived regulatory T cells contribute to tolerance to commensal microbiota. Nature *497*, 258-262.

Chen, G., Zhuchenko, O., and Kuspa, A. (2007). Immune-like phagocyte activity in the social amoeba. Science *317*, 678-681.

Chen, W.Y., Zeng, X., Carter, M.G., Morrell, C.N., Chiu Yen, R.W., Esteller, M., Watkins, D.N., Herman, J.G., Mankowski, J.L., and Baylin, S.B. (2003). Heterozygous disruption of Hic1 predisposes mice to a gender-dependent spectrum of malignant tumors. Nat Genet *33*, 197-202.

Cheng, H., and Leblond, C.P. (1974). Origin, differentiation and renewal of the four main epithelial cell types in the mouse small intestine. I. Columnar cell. Am J Anat *141*, 461-479.

Chu, H., Pazgier, M., Jung, G., Nuccio, S.P., Castillo, P.A., de Jong, M.F., Winter, M.G., Winter, S.E., Wehkamp, J., Shen, B., *et al.* (2012). Human alpha-defensin 6 promotes mucosal innate immunity through self-assembled peptide nanonets. Science *337*, 477-481.

Clevers, H.C., and Bevins, C.L. (2013). Paneth cells: maestros of the small intestinal crypts. Annu Rev Physiol *75*, 289-311.

Consortium, F.-G.A. (1997). An autoimmune disease, APECED, caused by mutations in a novel gene featuring two PHD-type zinc-finger domains. Nat Genet *17*, 399-403.

de Lau, W., Barker, N., Low, T.Y., Koo, B.K., Li, V.S., Teunissen, H., Kujala, P., Haegebarth, A., Peters, P.J., van de Wetering, M., *et al.* (2011). Lgr5 homologues associate with Wnt receptors and mediate R-spondin signalling. Nature *476*, 293-297.

Deaglio, S., Dwyer, K.M., Gao, W., Friedman, D., Usheva, A., Erat, A., Chen, J.F., Enjyoji, K., Linden, J., Oukka, M., *et al.* (2007). Adenosine generation catalyzed by CD39 and CD73 expressed on regulatory T cells mediates immune suppression. J Exp Med *204*, 1257-1265.

Deckx, R.J., Vantrappen, G.R., and Parein, M.M. (1967). Localization of lysozyme activity in a Paneth cell granule fraction. Biochim Biophys Acta *139*, 204-207.

Derbinski, J., Gabler, J., Brors, B., Tierling, S., Jonnakuty, S., Hergenhahn, M., Peltonen, L., Walter, J., and Kyewski, B. (2005). Promiscuous gene expression in thymic epithelial cells is regulated at multiple levels. J Exp Med *202*, 33-45.

Derbinski, J., Pinto, S., Rosch, S., Hexel, K., and Kyewski, B. (2008). Promiscuous gene expression patterns in single medullary thymic epithelial cells argue for a stochastic mechanism. Proc Natl Acad Sci U S A *105*, 657-662.

Derbinski, J., Schulte, A., Kyewski, B., and Klein, L. (2001). Promiscuous gene expression in medullary thymic epithelial cells mirrors the peripheral self. Nat Immunol *2*, 1032-1039.

DeVoss, J., Hou, Y., Johannes, K., Lu, W., Liou, G.I., Rinn, J., Chang, H., Caspi, R.R., Fong, L., and Anderson, M.S. (2006). Spontaneous autoimmunity prevented by thymic expression of a single self-antigen. J Exp Med *203*, 2727-2735.

Dharmani, P., Srivastava, V., Kissoon-Singh, V., and Chadee, K. (2009). Role of intestinal mucins in innate host defense mechanisms against pathogens. J Innate Immun *1*, 123-135.

Dobeš, J., Neuwirth, A., Dobešová, M., Vobořil, M., Balounová, J., Ballek, O., Lebl, J., Meloni, A., Krohn, K., Kluger, N., *et al.* (2015). Gastrointestinal Autoimmunity Associated With Loss of Central Tolerance to Enteric alpha-Defensins. Gastroenterology *149*, 139-150.

Dubrot, J., Duraes, F.V., Potin, L., Capotosti, F., Brighouse, D., Suter, T., LeibundGut-Landmann, S., Garbi, N., Reith, W., Swartz, M.A., *et al.* (2014). Lymph node stromal cells acquire peptide-MHCII complexes from dendritic cells and induce antigen-specific CD4(+) T cell tolerance. J Exp Med *211*, 1153-1166.

Durand, A., Donahue, B., Peignon, G., Letourneur, F., Cagnard, N., Slomianny, C., Perret, C., Shroyer, N.F., and Romagnolo, B. (2012). Functional intestinal stem cells after Paneth cell ablation induced by the loss of transcription factor Math1 (Atoh1). Proc Natl Acad Sci U S A *109*, 8965-8970.

Ekwall, O., Hedstrand, H., Grimelius, L., Haavik, J., Perheentupa, J., Gustafsson, J., Husebye, E., Kampe, O., and Rorsman, F. (1998). Identification of tryptophan hydroxylase as an intestinal autoantigen. Lancet *352*, 279-283.

Ermund, A., Schutte, A., Johansson, M.E., Gustafsson, J.K., and Hansson, G.C. (2013). Studies of mucus in mouse stomach, small intestine, and colon. I. Gastrointestinal mucus layers have different properties depending on location as well as over the Peyer's patches. Am J Physiol Gastrointest Liver Physiol *305*, G341-347.

Farin, H.F., Karthaus, W.R., Kujala, P., Rakhshandehroo, M., Schwank, G., Vries, R.G., Kalkhoven, E., Nieuwenhuis, E.E., and Clevers, H. (2014). Paneth cell extrusion and release of antimicrobial products is directly controlled by immune cell-derived IFN-gamma. J Exp Med *211*, 1393-1405.

Farin, H.F., Van Es, J.H., and Clevers, H. (2012). Redundant sources of Wnt regulate intestinal stem cells and promote formation of Paneth cells. Gastroenterology *143*, 1518-1529 e1517.

Ferrero, I., Anjuere, F., Martin, P., Martinez del Hoyo, G., Fraga, M.L., Wright, N., Varona, R., Marquez, G., and Ardavin, C. (1999). Functional and phenotypic analysis of thymic B cells: role in the induction of T cell negative selection. Eur J Immunol *29*, 1598-1609.

Flanagan, D.J., Phesse, T.J., Barker, N., Schwab, R.H., Amin, N., Malaterre, J., Stange, D.E., Nowell, C.J., Currie, S.A., Saw, J.T., *et al.* (2015). Frizzled7 functions as a Wnt receptor in intestinal epithelial Lgr5(+) stem cells. Stem Cell Reports *4*, 759-767.

Fletcher, A.L., Lukacs-Kornek, V., Reynoso, E.D., Pinner, S.E., Bellemare-Pelletier, A., Curry, M.S., Collier, A.R., Boyd, R.L., and Turley, S.J. (2010). Lymph node fibroblastic reticular cells directly present peripheral tissue antigen under steady-state and inflammatory conditions. J Exp Med *207*, 689-697.

Fletcher, A.L., Malhotra, D., and Turley, S.J. (2011). Lymph node stroma broaden the peripheral tolerance paradigm. Trends Immunol *32*, 12-18.

Florea, B.I., Verdoes, M., Li, N., van der Linden, W.A., Geurink, P.P., van den Elst, H., Hofmann, T., de Ru, A., van Veelen, P.A., Tanaka, K., *et al.* (2010). Activity-based profiling reveals reactivity of the murine thymoproteasome-specific subunit beta5t. Chem Biol *17*, 795-801.

Fontenot, J.D., Rasmussen, J.P., Gavin, M.A., and Rudensky, A.Y. (2005). A function for interleukin 2 in Foxp3-expressing regulatory T cells. Nat Immunol *6*, 1142-1151.

Forrester, J.V., Xu, H., Lambe, T., and Cornall, R. (2008). Immune privilege or privileged immunity? Mucosal Immunol *1*, 372-381.

Fre, S., Huyghe, M., Mourikis, P., Robine, S., Louvard, D., and Artavanis-Tsakonas, S. (2005). Notch signals control the fate of immature progenitor cells in the intestine. Nature *435*, 964-968.

Frommer, F., and Waisman, A. (2010). B cells participate in thymic negative selection of murine auto-reactive CD4+ T cells. PLoS One *5*, e15372.

Ganz, T., Selsted, M.E., Szklarek, D., Harwig, S.S., Daher, K., Bainton, D.F., and Lehrer, R.I. (1985). Defensins. Natural peptide antibiotics of human neutrophils. J Clin Invest *76*, 1427-1435.

Garabedian, E.M., Roberts, L.J., McNevin, M.S., and Gordon, J.I. (1997). Examining the role of Paneth cells in the small intestine by lineage ablation in transgenic mice. J Biol Chem *272*, 23729-23740.

Gardner, J.M., Devoss, J.J., Friedman, R.S., Wong, D.J., Tan, Y.X., Zhou, X., Johannes, K.P., Su, M.A., Chang, H.Y., Krummel, M.F., *et al.* (2008). Deletional tolerance mediated by extrathymic Aire-expressing cells. Science *321*, 843-847.

Gardner, J.M., Metzger, T.C., McMahon, E.J., Au-Yeung, B.B., Krawisz, A.K., Lu, W., Price, J.D., Johannes, K.P., Satpathy, A.T., Murphy, K.M., *et al.* (2013). Extrathymic Aire-expressing cells are a distinct bone marrow-derived population that induce functional inactivation of CD4(+) T cells. Immunity *39*, 560-572.

Gavanescu, I., Kessler, B., Ploegh, H., Benoist, C., and Mathis, D. (2007). Loss of Aire-dependent thymic expression of a peripheral tissue antigen renders it a target of autoimmunity. Proc Natl Acad Sci U S A *104*, 4583-4587.

Ghosh, D., Porter, E., Shen, B., Lee, S.K., Wilk, D., Drazba, J., Yadav, S.P., Crabb, J.W., Ganz, T., and Bevins, C.L. (2002). Paneth cell trypsin is the processing enzyme for human defensin-5. Nat Immunol *3*, 583-590.

Giraud, M., Yoshida, H., Abramson, J., Rahl, P.B., Young, R.A., Mathis, D., and Benoist, C. (2012). Aire unleashes stalled RNA polymerase to induce ectopic gene expression in thymic epithelial cells. Proc Natl Acad Sci U S A *109*, 535-540.

Godl, K., Johansson, M.E., Lidell, M.E., Morgelin, M., Karlsson, H., Olson, F.J., Gum, J.R., Jr., Kim, Y.S., and Hansson, G.C. (2002). The N terminus of the MUC2 mucin forms trimers that are held together within a trypsin-resistant core fragment. J Biol Chem *277*, 47248-47256.

Gommeaux, J., Gregoire, C., Nguessan, P., Richelme, M., Malissen, M., Guerder, S., Malissen, B., and Carrier, A. (2009). Thymus-specific serine protease regulates positive selection of a subset of CD4+ thymocytes. Eur J Immunol *39*, 956-964.

Goto, Y., Panea, C., Nakato, G., Cebula, A., Lee, C., Diez, M.G., Laufer, T.M., Ignatowicz, L., and Ivanov, II (2014). Segmented Filamentous Bacteria Antigens Presented by Intestinal Dendritic Cells Drive Mucosal Th17 Cell Differentiation. Immunity.

Greter, M., Heppner, F.L., Lemos, M.P., Odermatt, B.M., Goebels, N., Laufer, T., Noelle, R.J., and Becher, B. (2005). Dendritic cells permit immune invasion of the CNS in an animal model of multiple sclerosis. Nat Med *11*, 328-334.

Hadeiba, H., Lahl, K., Edalati, A., Oderup, C., Habtezion, A., Pachynski, R., Nguyen, L., Ghodsi, A., Adler, S., and Butcher, E.C. (2012). Plasmacytoid dendritic cells transport peripheral antigens to the thymus to promote central tolerance. Immunity *36*, 438-450.

Hao, H.X., Xie, Y., Zhang, Y., Charlat, O., Oster, E., Avello, M., Lei, H., Mickanin, C., Liu, D., Ruffner, H., *et al.* (2012). ZNRF3 promotes Wnt receptor turnover in an R-spondin-sensitive manner. Nature *485*, 195-200.

Hawiger, D., Inaba, K., Dorsett, Y., Guo, M., Mahnke, K., Rivera, M., Ravetch, J.V., Steinman, R.M., and Nussenzweig, M.C. (2001). Dendritic cells induce peripheral T cell unresponsiveness under steady state conditions in vivo. J Exp Med *194*, 769-779.

He, T.C., Sparks, A.B., Rago, C., Hermeking, H., Zawel, L., da Costa, L.T., Morin, P.J., Vogelstein, B., and Kinzler, K.W. (1998). Identification of c-MYC as a target of the APC pathway. Science *281*, 1509-1512.

Helander, A., Miller, C.L., Myers, K.S., Neutra, M.R., and Nibert, M.L. (2004). Protective immunoglobulin A and G antibodies bind to overlapping intersubunit epitopes in the head domain of type 1 reovirus adhesin sigma1. J Virol *78*, 10695-10705.

Helander, A., Silvey, K.J., Mantis, N.J., Hutchings, A.B., Chandran, K., Lucas, W.T., Nibert, M.L., and Neutra, M.R. (2003). The viral sigma1 protein and glycoconjugates

containing alpha2-3-linked sialic acid are involved in type 1 reovirus adherence to M cell apical surfaces. J Virol *77*, 7964-7977.

Hepworth, M.R., Fung, T.C., Masur, S.H., Kelsen, J.R., McConnell, F.M., Dubrot, J., Withers, D.R., Hugues, S., Farrar, M.A., Reith, W., *et al.* (2015). Immune tolerance. Group 3 innate lymphoid cells mediate intestinal selection of commensal bacteria-specific CD4(+) T cells. Science *348*, 1031-1035.

Hepworth, M.R., Monticelli, L.A., Fung, T.C., Ziegler, C.G., Grunberg, S., Sinha, R., Mantegazza, A.R., Ma, H.L., Crawford, A., Angelosanto, J.M., *et al.* (2013). Innate lymphoid cells regulate CD4+ T-cell responses to intestinal commensal bacteria. Nature *498*, 113-117.

Higgins, P.J., and Weiner, H.L. (1988). Suppression of experimental autoimmune encephalomyelitis by oral administration of myelin basic protein and its fragments. J Immunol *140*, 440-445.

Hooper, L.V., Stappenbeck, T.S., Hong, C.V., and Gordon, J.I. (2003). Angiogenins: a new class of microbicidal proteins involved in innate immunity. Nat Immunol *4*, 269-273.

Huang, C.T., Workman, C.J., Flies, D., Pan, X., Marson, A.L., Zhou, G., Hipkiss, E.L., Ravi, S., Kowalski, J., Levitsky, H.I., *et al.* (2004). Role of LAG-3 in regulatory T cells. Immunity *21*, 503-513.

Hubert, F.X., Kinkel, S.A., Crewther, P.E., Cannon, P.Z., Webster, K.E., Link, M., Uibo, R., O'Bryan, M.K., Meager, A., Forehan, S.P., *et al.* (2009). Aire-deficient C57BL/6 mice mimicking the common human 13-base pair deletion mutation present with only a mild autoimmune phenotype. J Immunol *182*, 3902-3918.

Hugot, J.P., Chamaillard, M., Zouali, H., Lesage, S., Cezard, J.P., Belaiche, J., Almer, S., Tysk, C., O'Morain, C.A., Gassull, M., *et al.* (2001). Association of NOD2 leucine-rich repeat variants with susceptibility to Crohn's disease. Nature *411*, 599-603.

Ikeda, S., Kishida, S., Yamamoto, H., Murai, H., Koyama, S., and Kikuchi, A. (1998). Axin, a negative regulator of the Wnt signaling pathway, forms a complex with GSK-3beta and beta-catenin and promotes GSK-3beta-dependent phosphorylation of beta-catenin. EMBO J *17*, 1371-1384.

Ireland, H., Kemp, R., Houghton, C., Howard, L., Clarke, A.R., Sansom, O.J., and Winton, D.J. (2004). Inducible Cre-mediated control of gene expression in the murine gastrointestinal tract: effect of loss of beta-catenin. Gastroenterology *126*, 1236-1246.

Ivanov, II, Atarashi, K., Manel, N., Brodie, E.L., Shima, T., Karaoz, U., Wei, D., Goldfarb, K.C., Santee, C.A., Lynch, S.V., *et al.* (2009). Induction of intestinal Th17 cells by segmented filamentous bacteria. Cell *139*, 485-498.

Ivanov, II, Frutos Rde, L., Manel, N., Yoshinaga, K., Rifkin, D.B., Sartor, R.B., Finlay, B.B., and Littman, D.R. (2008). Specific microbiota direct the differentiation of IL-17-producing T-helper cells in the mucosa of the small intestine. Cell Host Microbe *4*, 337-349.

Iwata, M., Hirakiyama, A., Eshima, Y., Kagechika, H., Kato, C., and Song, S.Y. (2004). Retinoic acid imprints gut-homing specificity on T cells. Immunity *21*, 527-538.

Jaensson, E., Uronen-Hansson, H., Pabst, O., Eksteen, B., Tian, J., Coombes, J.L., Berg, P.L., Davidsson, T., Powrie, F., Johansson-Lindbom, B., *et al.* (2008). Small intestinal CD103+ dendritic cells display unique functional properties that are conserved between mice and humans. J Exp Med *205*, 2139-2149.

Janda, C.Y., Waghray, D., Levin, A.M., Thomas, C., and Garcia, K.C. (2012). Structural basis of Wnt recognition by Frizzled. Science *337*, 59-64.

Janeckova, L., Pospichalova, V., Fafilek, B., Vojtechova, M., Tureckova, J., Dobes, J., Dubuissez, M., Leprince, D., Baloghova, N., Horazna, M., *et al.* (2015). HIC1 Tumor Suppressor Loss Potentiates TLR2/NF-kappaB Signaling and Promotes Tissue Damage-Associated Tumorigenesis. Mol Cancer Res *13*, 1139-1148.

Johansson, M.E., Ambort, D., Pelaseyed, T., Schutte, A., Gustafsson, J.K., Ermund, A., Subramani, D.B., Holmen-Larsson, J.M., Thomsson, K.A., Bergstrom, J.H., *et al.* (2011). Composition and functional role of the mucus layers in the intestine. Cell Mol Life Sci *68*, 3635-3641.

Jones, D.E., and Bevins, C.L. (1992). Paneth cells of the human small intestine express an antimicrobial peptide gene. J Biol Chem *267*, 23216-23225.

Jones, D.E., and Bevins, C.L. (1993). Defensin-6 mRNA in human Paneth cells: implications for antimicrobial peptides in host defense of the human bowel. FEBS Lett *315*, 187-192.

Joo, M., Shahsafaei, A., and Odze, R.D. (2009). Paneth cell differentiation in colonic epithelial neoplasms: evidence for the role of the Apc/beta-catenin/Tcf pathway. Hum Pathol *40*, 872-880.

Josefowicz, S.Z., Lu, L.F., and Rudensky, A.Y. (2012). Regulatory T cells: mechanisms of differentiation and function. Annu Rev Immunol *30*, 531-564.

Karam, S.M. (1999). Lineage commitment and maturation of epithelial cells in the gut. Front Biosci *4*, D286-298.

Karner, J., Meager, A., Laan, M., Maslovskaja, J., Pihlap, M., Remm, A., Juronen, E., Wolff, A.S., Husebye, E.S., Podkrajsek, K.T., *et al.* (2013). Anti-cytokine autoantibodies suggest pathogenetic links with autoimmune regulator deficiency in humans and mice. Clin Exp Immunol *171*, 263-272.

Kim, J.M., Rasmussen, J.P., and Rudensky, A.Y. (2007). Regulatory T cells prevent catastrophic autoimmunity throughout the lifespan of mice. Nat Immunol *8*, 191-197.

Kim, K.A., Kakitani, M., Zhao, J., Oshima, T., Tang, T., Binnerts, M., Liu, Y., Boyle, B., Park, E., Emtage, P., *et al.* (2005). Mitogenic influence of human R-spondin1 on the intestinal epithelium. Science *309*, 1256-1259.

Kim, S.E., Huang, H., Zhao, M., Zhang, X., Zhang, A., Semonov, M.V., MacDonald, B.T., Garcia Abreu, J., Peng, L., and He, X. (2013). Wnt stabilization of beta-catenin reveals principles for morphogen receptor-scaffold assemblies. Science *340*, 867-870.

Kim, Y.S., and Ho, S.B. (2010). Intestinal goblet cells and mucins in health and disease: recent insights and progress. Curr Gastroenterol Rep *12*, 319-330.

Kisand, K., Boe Wolff, A.S., Podkrajsek, K.T., Tserel, L., Link, M., Kisand, K.V., Ersvaer, E., Perheentupa, J., Erichsen, M.M., Bratanic, N., *et al.* (2010). Chronic mucocutaneous candidiasis in APECED or thymoma patients correlates with autoimmunity to Th17-associated cytokines. J Exp Med *207*, 299-308.

Kisand, K., and Peterson, P. (2015). Autoimmune Polyendocrinopathy Candidiasis Ectodermal Dystrophy. J Clin Immunol *35*, 463-478.

Klein, L. (2009). Dead man walking: how thymocytes scan the medulla. Nat Immunol *10*, 809-811.

Klein, L., Hinterberger, M., Wirnsberger, G., and Kyewski, B. (2009). Antigen presentation in the thymus for positive selection and central tolerance induction. Nat Rev Immunol *9*, 833-844.

Klein, L., Kyewski, B., Allen, P.M., and Hogquist, K.A. (2014). Positive and negative selection of the T cell repertoire: what thymocytes see (and don't see). Nat Rev Immunol *14*, 377-391.

Kluger, N., Jokinen, M., Krohn, K., and Ranki, A. (2013). Gastrointestinal manifestations in APECED syndrome. J Clin Gastroenterol *47*, 112-120.

Kluger, N., Jokinen, M., Lintulahti, A., Krohn, K., and Ranki, A. (2015). Gastrointestinal immunity against tryptophan hydroxylase-1, aromatic L-amino-acid decarboxylase, AIE-75, villin and Paneth cells in APECED. Clin Immunol *158*, 212-220.

Kobayashi, K.S., Chamaillard, M., Ogura, Y., Henegariu, O., Inohara, N., Nunez, G., and Flavell, R.A. (2005). Nod2-dependent regulation of innate and adaptive immunity in the intestinal tract. Science *307*, 731-734.

Koh, A.S., Kuo, A.J., Park, S.Y., Cheung, P., Abramson, J., Bua, D., Carney, D., Shoelson, S.E., Gozani, O., Kingston, R.E., *et al.* (2008). Aire employs a histone-binding module to mediate immunological tolerance, linking chromatin regulation with organ-specific autoimmunity. Proc Natl Acad Sci U S A *105*, 15878-15883.

Korinek, V., Barker, N., Willert, K., Molenaar, M., Roose, J., Wagenaar, G., Markman, M., Lamers, W., Destree, O., and Clevers, H. (1998). Two members of the Tcf family implicated in Wnt/beta-catenin signaling during embryogenesis in the mouse. Mol Cell Biol *18*, 1248-1256.

Korn, T., Bettelli, E., Oukka, M., and Kuchroo, V.K. (2009). IL-17 and Th17 Cells. Annu Rev Immunol *27*, 485-517.

Koslowski, M.J., Kubler, I., Chamaillard, M., Schaeffeler, E., Reinisch, W., Wang, G., Beisner, J., Teml, A., Peyrin-Biroulet, L., Winter, S., *et al.* (2009). Genetic variants of Wnt transcription factor TCF-4 (TCF7L2) putative promoter region are associated with small intestinal Crohn's disease. PLoS One *4*, e4496.

Krausova, M., and Korinek, V. (2014). Wnt signaling in adult intestinal stem cells and cancer. Cell Signal *26*, 570-579.

Kretschmer, K., Apostolou, I., Hawiger, D., Khazaie, K., Nussenzweig, M.C., and von Boehmer, H. (2005). Inducing and expanding regulatory T cell populations by foreign antigen. Nat Immunol *6*, 1219-1227.

Kudryashova, E., Quintyn, R., Seveau, S., Lu, W., Wysocki, V.H., and Kudryashov, D.S. (2014). Human defensins facilitate local unfolding of thermodynamically unstable regions of bacterial protein toxins. Immunity *41*, 709-721.

Kyewski, B., Derbinski, J., Gotter, J., and Klein, L. (2002). Promiscuous gene expression and central T-cell tolerance: more than meets the eye. Trends Immunol *23*, 364-371.

Lala, S., Ogura, Y., Osborne, C., Hor, S.Y., Bromfield, A., Davies, S., Ogunbiyi, O., Nunez, G., and Keshav, S. (2003). Crohn's disease and the NOD2 gene: a role for paneth cells. Gastroenterology *125*, 47-57.

Lathrop, S.K., Bloom, S.M., Rao, S.M., Nutsch, K., Lio, C.W., Santacruz, N., Peterson, D.A., Stappenbeck, T.S., and Hsieh, C.S. (2011). Peripheral education of the immune system by colonic commensal microbiota. Nature *478*, 250-254.

Lecuyer, E., Rakotobe, S., Lengline-Garnier, H., Lebreton, C., Picard, M., Juste, C., Fritzen, R., Eberl, G., McCoy, K.D., Macpherson, A.J., *et al.* (2014). Segmented filamentous bacterium uses secondary and tertiary lymphoid tissues to induce gut IgA and specific T helper 17 cell responses. Immunity *40*, 608-620.

Lee, J.W., Epardaud, M., Sun, J., Becker, J.E., Cheng, A.C., Yonekura, A.R., Heath, J.K., and Turley, S.J. (2007). Peripheral antigen display by lymph node stroma promotes T cell tolerance to intestinal self. Nat Immunol *8*, 181-190.

Lee, Y., Awasthi, A., Yosef, N., Quintana, F.J., Xiao, S., Peters, A., Wu, C., Kleinewietfeld, M., Kunder, S., Hafler, D.A., *et al.* (2012). Induction and molecular signature of pathogenic TH17 cells. Nat Immunol *13*, 991-999.

Lei, Y., Ripen, A.M., Ishimaru, N., Ohigashi, I., Nagasawa, T., Jeker, L.T., Bosl, M.R., Hollander, G.A., Hayashi, Y., Malefyt Rde, W., *et al.* (2011). Aire-dependent production of XCL1 mediates medullary accumulation of thymic dendritic cells and contributes to regulatory T cell development. J Exp Med *208*, 383-394.

Li, J., Park, J., Foss, D., and Goldschneider, I. (2009). Thymus-homing peripheral dendritic cells constitute two of the three major subsets of dendritic cells in the steady-state thymus. J Exp Med *206*, 607-622.

Liston, A., Lesage, S., Wilson, J., Peltonen, L., and Goodnow, C.C. (2003). Aire regulates negative selection of organ-specific T cells. Nat Immunol *4*, 350-354.

Liu, K., Iyoda, T., Saternus, M., Kimura, Y., Inaba, K., and Steinman, R.M. (2002). Immune tolerance after delivery of dying cells to dendritic cells in situ. J Exp Med *196*, 1091-1097.

Maassen, C.B., and Claassen, E. (2008). Strain-dependent effects of probiotic lactobacilli on EAE autoimmunity. Vaccine *26*, 2056-2057.

Macfarlane, G.T., and Macfarlane, S. (1997). Human colonic microbiota: ecology, physiology and metabolic potential of intestinal bacteria. Scand J Gastroenterol Suppl *222*, 3-9.

Magnusson, F.C., Liblau, R.S., von Boehmer, H., Pittet, M.J., Lee, J.W., Turley, S.J., and Khazaie, K. (2008). Direct presentation of antigen by lymph node stromal cells protects against CD8 T-cell-mediated intestinal autoimmunity. Gastroenterology *134*, 1028-1037.

Malchow, S., Leventhal, D.S., Nishi, S., Fischer, B.I., Shen, L., Paner, G.P., Amit, A.S., Kang, C., Geddes, J.E., Allison, J.P., *et al.* (2013). Aire-dependent thymic development of tumor-associated regulatory T cells. Science *339*, 1219-1224.

Mallow, E.B., Harris, A., Salzman, N., Russell, J.P., DeBerardinis, R.J., Ruchelli, E., and Bevins, C.L. (1996). Human enteric defensins. Gene structure and developmental expression. J Biol Chem *271*, 4038-4045.

Maloy, K.J., and Powrie, F. (2011). Intestinal homeostasis and its breakdown in inflammatory bowel disease. Nature *474*, 298-306.

Mantis, N.J., Rol, N., and Corthesy, B. (2011). Secretory IgA's complex roles in immunity and mucosal homeostasis in the gut. Mucosal Immunol *4*, 603-611.

Martinez Rodriguez, N.R., Eloi, M.D., Huynh, A., Dominguez, T., Lam, A.H., Carcamo-Molina, D., Naser, Z., Desharnais, R., Salzman, N.H., and Porter, E. (2012). Expansion of Paneth cell population in response to enteric Salmonella enterica serovar Typhimurium infection. Infect Immun *80*, 266-275.

Maynard, C.L., Harrington, L.E., Janowski, K.M., Oliver, J.R., Zindl, C.L., Rudensky, A.Y., and Weaver, C.T. (2007). Regulatory T cells expressing interleukin 10 develop from Foxp3+ and Foxp3- precursor cells in the absence of interleukin 10. Nat Immunol *8*, 931-941.

McDole, J.R., Wheeler, L.W., McDonald, K.G., Wang, B., Konjufca, V., Knoop, K.A., Newberry, R.D., and Miller, M.J. (2012). Goblet cells deliver luminal antigen to CD103+ dendritic cells in the small intestine. Nature *483*, 345-349.

Moog, F. (1981). The lining of the small intestine. Sci Am *245*, 154-158, 160, 162 et passiom.

Mowat, A.M., and Agace, W.W. (2014). Regional specialization within the intestinal immune system. Nat Rev Immunol *14*, 667-685.

Murata, S., Sasaki, K., Kishimoto, T., Niwa, S., Hayashi, H., Takahama, Y., and Tanaka, K. (2007). Regulation of CD8+ T cell development by thymus-specific proteasomes. Science *316*, 1349-1353.

Nagamine, K., Peterson, P., Scott, H.S., Kudoh, J., Minoshima, S., Heino, M., Krohn, K.J., Lalioti, M.D., Mullis, P.E., Antonarakis, S.E., *et al.* (1997). Positional cloning of the APECED gene. Nat Genet *17*, 393-398.

Nakagawa, T., Roth, W., Wong, P., Nelson, A., Farr, A., Deussing, J., Villadangos, J.A., Ploegh, H., Peters, C., and Rudensky, A.Y. (1998). Cathepsin L: critical role in Ii degradation and CD4 T cell selection in the thymus. Science *280*, 450-453.

Nedjic, J., Aichinger, M., Emmerich, J., Mizushima, N., and Klein, L. (2008). Autophagy in thymic epithelium shapes the T-cell repertoire and is essential for tolerance. Nature *455*, 396-400.

Niederkorn, J.Y. (2006). See no evil, hear no evil, do no evil: the lessons of immune privilege. Nat Immunol *7*, 354-359.

Nusse, R. (2012). Wnt signaling. Cold Spring Harb Perspect Biol *4*.

Oftedal, B.E., Hellesen, A., Erichsen, M.M., Bratland, E., Vardi, A., Perheentupa, J., Kemp, E.H., Fiskerstrand, T., Viken, M.K., Weetman, A.P., *et al.* (2015). Dominant Mutations in the Autoimmune Regulator AIRE Are Associated with Common Organ-Specific Autoimmune Diseases. Immunity *42*, 1185-1196.

Ogura, Y., Bonen, D.K., Inohara, N., Nicolae, D.L., Chen, F.F., Ramos, R., Britton, H., Moran, T., Karaliuskas, R., Duerr, R.H., *et al.* (2001). A frameshift mutation in NOD2 associated with susceptibility to Crohn's disease. Nature *411*, 603-606.

Ogura, Y., Lala, S., Xin, W., Smith, E., Dowds, T.A., Chen, F.F., Zimmermann, E., Tretiakova, M., Cho, J.H., Hart, J., *et al.* (2003). Expression of NOD2 in Paneth cells: a possible link to Crohn's ileitis. Gut *52*, 1591-1597.

Ouellette, A.J., Greco, R.M., James, M., Frederick, D., Naftilan, J., and Fallon, J.T. (1989). Developmental regulation of cryptdin, a corticostatin/defensin precursor mRNA in mouse small intestinal crypt epithelium. J Cell Biol *108*, 1687-1695.

Ouellette, A.J., and Lualdi, J.C. (1990). A novel mouse gene family coding for cationic, cysteine-rich peptides. Regulation in small intestine and cells of myeloid origin. J Biol Chem *265*, 9831-9837.

Ouellette, A.J., Miller, S.I., Henschen, A.H., and Selsted, M.E. (1992). Purification and primary structure of murine cryptdin-1, a Paneth cell defensin. FEBS Lett *304*, 146-148.

Ozawa, M., Baribault, H., and Kemler, R. (1989). The cytoplasmic domain of the cell adhesion molecule uvomorulin associates with three independent proteins structurally related in different species. EMBO J *8*, 1711-1717.

Pabst, O., and Mowat, A.M. (2012). Oral tolerance to food protein. Mucosal Immunol *5*, 232-239.

Perheentupa, J. (2006). Autoimmune polyendocrinopathy-candidiasis-ectodermal dystrophy. J Clin Endocrinol Metab *91*, 2843-2850.

Petnicki-Ocwieja, T., Hrncir, T., Liu, Y.J., Biswas, A., Hudcovic, T., Tlaskalova-Hogenova, H., and Kobayashi, K.S. (2009). Nod2 is required for the regulation of commensal microbiota in the intestine. Proc Natl Acad Sci U S A *106*, 15813-15818.

Porter, E.M., van Dam, E., Valore, E.V., and Ganz, T. (1997). Broad-spectrum antimicrobial activity of human intestinal defensin 5. Infect Immun *65*, 2396-2401.

Posovszky, C., Lahr, G., von Schnurbein, J., Buderus, S., Findeisen, A., Schroder, C., Schutz, C., Schulz, A., Debatin, K.M., Wabitsch, M., *et al.* (2012). Loss of enteroendocrine cells in autoimmune-polyendocrine-candidiasis-ectodermal-dystrophy (APECED) syndrome with gastrointestinal dysfunction. J Clin Endocrinol Metab *97*, E292-300.

Potten, C.S. (1977). Extreme sensitivity of some intestinal crypt cells to X and gamma irradiation. Nature *269*, 518-521.

Potten, C.S., Kovacs, L., and Hamilton, E. (1974). Continuous labelling studies on mouse skin and intestine. Cell Tissue Kinet *7*, 271-283.

Proietto, A.I., Lahoud, M.H., and Wu, L. (2008). Distinct functional capacities of mouse thymic and splenic dendritic cell populations. Immunol Cell Biol *86*, 700-708.

Putsep, K., Axelsson, L.G., Boman, A., Midtvedt, T., Normark, S., Boman, H.G., and Andersson, M. (2000). Germ-free and colonized mice generate the same products from enteric prodefensins. J Biol Chem *275*, 40478-40482.

Radeva, M.Y., Jahns, F., Wilhelm, A., Glei, M., Settmacher, U., Greulich, K.O., and Mothes, H. (2010). Defensin alpha 6 (DEFA 6) overexpression threshold of over 60 fold can distinguish between adenoma and fully blown colon carcinoma in individual patients. BMC Cancer *10*, 588.

Raetz, M., Hwang, S.H., Wilhelm, C.L., Kirkland, D., Benson, A., Sturge, C.R., Mirpuri, J., Vaishnava, S., Hou, B., Defranco, A.L., *et al.* (2013). Parasite-induced TH1 cells and intestinal dysbiosis cooperate in IFN-gamma-dependent elimination of Paneth cells. Nat Immunol *14*, 136-142.

Ramsey, C., Winqvist, O., Puhakka, L., Halonen, M., Moro, A., Kampe, O., Eskelin, P., Pelto-Huikko, M., and Peltonen, L. (2002). Aire deficient mice develop multiple features of APECED phenotype and show altered immune response. Hum Mol Genet *11*, 397-409.

Reizis, B., Colonna, M., Trinchieri, G., Barrat, F., and Gilliet, M. (2011). Plasmacytoid dendritic cells: one-trick ponies or workhorses of the immune system? Nat Rev Immunol *11*, 558-565.

Riccio, O., van Gijn, M.E., Bezdek, A.C., Pellegrinet, L., van Es, J.H., Zimber-Strobl, U., Strobl, L.J., Honjo, T., Clevers, H., and Radtke, F. (2008). Loss of intestinal crypt progenitor cells owing to inactivation of both Notch1 and Notch2 is accompanied by derepression of CDK inhibitors p27Kip1 and p57Kip2. EMBO Rep *9*, 377-383.

Rochereau, N., Drocourt, D., Perouzel, E., Pavot, V., Redelinghuys, P., Brown, G.D., Tiraby, G., Roblin, X., Verrier, B., Genin, C., *et al.* (2013). Dectin-1 is essential for reverse transcytosis of glycosylated SIgA-antigen complexes by intestinal M cells. PLoS Biol *11*, e1001658.

Rood, B.R., and Leprince, D. (2013). Deciphering HIC1 control pathways to reveal new avenues in cancer therapeutics. Expert Opin Ther Targets *17*, 811-827.

Rosatelli, M.C., Meloni, A., Meloni, A., Devoto, M., Cao, A., Scott, H.S., Peterson, P., Heino, M., Krohn, K.J., Nagamine, K., *et al.* (1998). A common mutation in Sardinian autoimmune polyendocrinopathy-candidiasis-ectodermal dystrophy patients. Hum Genet *103*, 428-434.

Roth, S., Franken, P., Sacchetti, A., Kremer, A., Anderson, K., Sansom, O., and Fodde, R. (2012). Paneth cells in intestinal homeostasis and tissue injury. PLoS One *7*, e38965.

Rothenberg, M.E., Nusse, Y., Kalisky, T., Lee, J.J., Dalerba, P., Scheeren, F., Lobo, N., Kulkarni, S., Sim, S., Qian, D., *et al.* (2012). Identification of a cKit(+) colonic crypt base secretory cell that supports Lgr5(+) stem cells in mice. Gastroenterology *142*, 1195-1205 e1196.

Round, J.L., and Mazmanian, S.K. (2010). Inducible Foxp3+ regulatory T-cell development by a commensal bacterium of the intestinal microbiota. Proc Natl Acad Sci U S A *107*, 12204-12209.

Rousset, R., Mack, J.A., Wharton, K.A., Jr., Axelrod, J.D., Cadigan, K.M., Fish, M.P., Nusse, R., and Scott, M.P. (2001). Naked cuticle targets dishevelled to antagonize Wnt signal transduction. Genes Dev *15*, 658-671.

Rubinfeld, B., Souza, B., Albert, I., Muller, O., Chamberlain, S.H., Masiarz, F.R., Munemitsu, S., and Polakis, P. (1993). Association of the APC gene product with beta-catenin. Science *262*, 1731-1734.

Salzman, N.H., Chou, M.M., de Jong, H., Liu, L., Porter, E.M., and Paterson, Y. (2003a). Enteric salmonella infection inhibits Paneth cell antimicrobial peptide expression. Infect Immun *71*, 1109-1115.

Salzman, N.H., Ghosh, D., Huttner, K.M., Paterson, Y., and Bevins, C.L. (2003b). Protection against enteric salmonellosis in transgenic mice expressing a human intestinal defensin. Nature *422*, 522-526.

Salzman, N.H., Hung, K., Haribhai, D., Chu, H., Karlsson-Sjoberg, J., Amir, E., Teggatz, P., Barman, M., Hayward, M., Eastwood, D., *et al.* (2010). Enteric defensins are essential regulators of intestinal microbial ecology. Nat Immunol *11*, 76-83.

Sartor, R.B. (2008). Microbial influences in inflammatory bowel diseases. Gastroenterology *134*, 577-594.

Sartor, R.B. (2010). Genetics and environmental interactions shape the intestinal microbiome to promote inflammatory bowel disease versus mucosal homeostasis. Gastroenterology *139*, 1816-1819.

Sass, V., Schneider, T., Wilmes, M., Korner, C., Tossi, A., Novikova, N., Shamova, O., and Sahl, H.G. (2010). Human beta-defensin 3 inhibits cell wall biosynthesis in Staphylococci. Infect Immun *78*, 2793-2800.

Sato, T., van Es, J.H., Snippert, H.J., Stange, D.E., Vries, R.G., van den Born, M., Barker, N., Shroyer, N.F., van de Wetering, M., and Clevers, H. (2011). Paneth cells constitute the niche for Lgr5 stem cells in intestinal crypts. Nature *469*, 415-418.

Satoh, Y., Habara, Y., Ono, K., and Kanno, T. (1995). Carbamylcholine- and catecholamine-induced intracellular calcium dynamics of epithelial cells in mouse ileal crypts. Gastroenterology *108*, 1345-1356.

Satoh, Y., Ishikawa, K., Oomori, Y., Takeda, S., and Ono, K. (1992). Bethanechol and a G-protein activator, NaF/AlCl3, induce secretory response in Paneth cells of mouse intestine. Cell Tissue Res *269*, 213-220.

Scarpa, R., Alaggio, R., Norberto, L., Furmaniak, J., Chen, S., Smith, B.R., Masiero, S., Morlin, L., Plebani, M., De Luca, F., *et al.* (2013). Tryptophan hydroxylase autoantibodies as markers of a distinct autoimmune gastrointestinal component of autoimmune polyendocrine syndrome type 1. J Clin Endocrinol Metab *98*, 704-712.

Scheetz, T., Bartlett, J.A., Walters, J.D., Schutte, B.C., Casavant, T.L., and McCray, P.B., Jr. (2002). Genomics-based approaches to gene discovery in innate immunity. Immunol Rev *190*, 137-145.

Schroeder, B.O., Ehmann, D., Precht, J.C., Castillo, P.A., Kuchler, R., Berger, J., Schaller, M., Stange, E.F., and Wehkamp, J. (2015). Paneth cell alpha-defensin 6 (HD-6) is an antimicrobial peptide. Mucosal Immunol *8*, 661-671.

Scott, C.L., Aumeunier, A.M., and Mowat, A.M. (2011). Intestinal CD103+ dendritic cells: master regulators of tolerance? Trends Immunol *32*, 412-419.

Selsted, M.E., Harwig, S.S., Ganz, T., Schilling, J.W., and Lehrer, R.I. (1985). Primary structures of three human neutrophil defensins. J Clin Invest *76*, 1436-1439.

Selsted, M.E., and Ouellette, A.J. (2005). Mammalian defensins in the antimicrobial immune response. Nat Immunol *6*, 551-557.

Shanahan, M.T., Tanabe, H., and Ouellette, A.J. (2011). Strain-specific polymorphisms in Paneth cell alpha-defensins of C57BL/6 mice and evidence of vestigial myeloid alpha-defensin pseudogenes. Infect Immun *79*, 459-473.

Shroyer, N.F., Wallis, D., Venken, K.J., Bellen, H.J., and Zoghbi, H.Y. (2005). Gfi1 functions downstream of Math1 to control intestinal secretory cell subtype allocation and differentiation. Genes Dev *19*, 2412-2417.

Siegfried, E., Wilder, E.L., and Perrimon, N. (1994). Components of wingless signalling in Drosophila. Nature *367*, 76-80.

Skoldberg, F., Portela-Gomes, G.M., Grimelius, L., Nilsson, G., Perheentupa, J., Betterle, C., Husebye, E.S., Gustafsson, J., Ronnblom, A., Rorsman, F., *et al.* (2003). Histidine decarboxylase, a pyridoxal phosphate-dependent enzyme, is an autoantigen of gastric enterochromaffin-like cells. J Clin Endocrinol Metab *88*, 1445-1452.

Snippert, H.J., van der Flier, L.G., Sato, T., van Es, J.H., van den Born, M., Kroon-Veenboer, C., Barker, N., Klein, A.M., van Rheenen, J., Simons, B.D., *et al.* (2010). Intestinal crypt homeostasis results from neutral competition between symmetrically dividing Lgr5 stem cells. Cell *143*, 134-144.

Soderbergh, A., Myhre, A.G., Ekwall, O., Gebre-Medhin, G., Hedstrand, H., Landgren, E., Miettinen, A., Eskelin, P., Halonen, M., Tuomi, T., *et al.* (2004). Prevalence and clinical associations of 10 defined autoantibodies in autoimmune polyendocrine syndrome type I. J Clin Endocrinol Metab *89*, 557-562.

Stancikova, J., Krausova, M., Kolar, M., Fafilek, B., Svec, J., Sedlacek, R., Neroldova, M., Dobes, J., Horazna, M., Janeckova, L., *et al.* (2015). NKD1 marks intestinal and liver tumors linked to aberrant Wnt signaling. Cell Signal *27*, 245-256.

Steinman, R.M., Hawiger, D., and Nussenzweig, M.C. (2003). Tolerogenic dendritic cells. Annu Rev Immunol *21*, 685-711.

Stokes, C.R., Soothill, J.F., and Turner, M.W. (1975). Immune exclusion is a function of IgA. Nature *255*, 745-746.

Stritesky, G.L., Jameson, S.C., and Hogquist, K.A. (2012). Selection of self-reactive T cells in the thymus. Annu Rev Immunol *30*, 95-114.

Stubbe, H., Berdoz, J., Kraehenbuhl, J.P., and Corthesy, B. (2000). Polymeric IgA is superior to monomeric IgA and IgG carrying the same variable domain in preventing Clostridium difficile toxin A damaging of T84 monolayers. J Immunol *164*, 1952-1960.

Sun, C.M., Hall, J.A., Blank, R.B., Bouladoux, N., Oukka, M., Mora, J.R., and Belkaid, Y. (2007). Small intestine lamina propria dendritic cells promote de novo generation of Foxp3 T reg cells via retinoic acid. J Exp Med *204*, 1775-1785.

Suzuki, K., Fukui, H., Kayahara, T., Sawada, M., Seno, H., Hiai, H., Kageyama, R., Okano, H., and Chiba, T. (2005). Hes1-deficient mice show precocious differentiation of Paneth cells in the small intestine. Biochem Biophys Res Commun *328*, 348-352.

Takahashi, T., Tagami, T., Yamazaki, S., Uede, T., Shimizu, J., Sakaguchi, N., Mak, T.W., and Sakaguchi, S. (2000). Immunologic self-tolerance maintained by CD25(+)CD4(+) regulatory T cells constitutively expressing cytotoxic T lymphocyte-associated antigen 4. J Exp Med *192*, 303-310.

Tang, Y.Q., Yuan, J., Osapay, G., Osapay, K., Tran, D., Miller, C.J., Ouellette, A.J., and Selsted, M.E. (1999). A cyclic antimicrobial peptide produced in primate leukocytes by the ligation of two truncated alpha-defensins. Science *286*, 498-502.

Taniguchi, R.T., DeVoss, J.J., Moon, J.J., Sidney, J., Sette, A., Jenkins, M.K., and Anderson, M.S. (2012). Detection of an autoreactive T-cell population within the polyclonal repertoire that undergoes distinct autoimmune regulator (Aire)-mediated selection. Proc Natl Acad Sci U S A *109*, 7847-7852.

Traverso, G. (2015). AIREing out the gut. Sci Transl Med *7*, EC119.

Ueda, Y., Kayama, H., Jeon, S.G., Kusu, T., Isaka, Y., Rakugi, H., Yamamoto, M., and Takeda, K. (2010). Commensal microbiota induce LPS hyporesponsiveness in colonic macrophages via the production of IL-10. Int Immunol *22*, 953-962.

Valenta, T., Lukas, J., Doubravska, L., Fafilek, B., and Korinek, V. (2006). HIC1 attenuates Wnt signaling by recruitment of TCF-4 and beta-catenin to the nuclear bodies. EMBO J *25*, 2326-2337.

van der Flier, L.G., and Clevers, H. (2009). Stem cells, self-renewal, and differentiation in the intestinal epithelium. Annu Rev Physiol *71*, 241-260.

Van der Sluis, M., De Koning, B.A., De Bruijn, A.C., Velcich, A., Meijerink, J.P., Van Goudoever, J.B., Buller, H.A., Dekker, J., Van Seuningen, I., Renes, I.B., *et al.* (2006). Muc2-deficient mice spontaneously develop colitis, indicating that MUC2 is critical for colonic protection. Gastroenterology *131*, 117-129.

van Es, J.H., Jay, P., Gregorieff, A., van Gijn, M.E., Jonkheer, S., Hatzis, P., Thiele, A., van den Born, M., Begthel, H., Brabletz, T., *et al.* (2005). Wnt signalling induces maturation of Paneth cells in intestinal crypts. Nat Cell Biol *7*, 381-386.

Velcich, A., Yang, W., Heyer, J., Fragale, A., Nicholas, C., Viani, S., Kucherlapati, R., Lipkin, M., Yang, K., and Augenlicht, L. (2002). Colorectal cancer in mice genetically deficient in the mucin Muc2. Science *295*, 1726-1729.

Villadangos, J.A., and Young, L. (2008). Antigen-presentation properties of plasmacytoid dendritic cells. Immunity *29*, 352-361.

von Boehmer, H., Teh, H.S., and Kisielow, P. (1989). The thymus selects the useful, neglects the useless and destroys the harmful. Immunol Today *10*, 57-61.

von Herrath, M.G., Dyrberg, T., and Oldstone, M.B. (1996). Oral insulin treatment suppresses virus-induced antigen-specific destruction of beta cells and prevents autoimmune diabetes in transgenic mice. J Clin Invest *98*, 1324-1331.

Wales, M.M., Biel, M.A., el Deiry, W., Nelkin, B.D., Issa, J.P., Cavenee, W.K., Kuerbitz, S.J., and Baylin, S.B. (1995). p53 activates expression of HIC-1, a new candidate tumour suppressor gene on 17p13.3. Nat Med *1*, 570-577.

Wang, F., Scoville, D., He, X.C., Mahe, M.M., Box, A., Perry, J.M., Smith, N.R., Lei, N.Y., Davies, P.S., Fuller, M.K., *et al.* (2013). Isolation and characterization of intestinal stem cells based on surface marker combinations and colony-formation assay. Gastroenterology *145*, 383-395 e381-321.

Wehkamp, J., Harder, J., Weichenthal, M., Schwab, M., Schaffeler, E., Schlee, M., Herrlinger, K.R., Stallmach, A., Noack, F., Fritz, P., *et al.* (2004). NOD2 (CARD15) mutations in Crohn's disease are associated with diminished mucosal alpha-defensin expression. Gut *53*, 1658-1664.

Wehkamp, J., Salzman, N.H., Porter, E., Nuding, S., Weichenthal, M., Petras, R.E., Shen, B., Schaeffeler, E., Schwab, M., Linzmeier, R., *et al.* (2005). Reduced Paneth cell alpha-defensins in ileal Crohn's disease. Proc Natl Acad Sci U S A *102*, 18129-18134.

Wehkamp, J., Wang, G., Kubler, I., Nuding, S., Gregorieff, A., Schnabel, A., Kays, R.J., Fellermann, K., Burk, O., Schwab, M., *et al.* (2007). The Paneth cell alpha-defensin deficiency of ileal Crohn's disease is linked to Wnt/Tcf-4. J Immunol *179*, 3109-3118.

Weiner, H.L., da Cunha, A.P., Quintana, F., and Wu, H. (2011). Oral tolerance. Immunol Rev *241*, 241-259.

White, S.H., Wimley, W.C., and Selsted, M.E. (1995). Structure, function, and membrane integration of defensins. Curr Opin Struct Biol *5*, 521-527.

Wilson, C.L., Ouellette, A.J., Satchell, D.P., Ayabe, T., Lopez-Boado, Y.S., Stratman, J.L., Hultgren, S.J., Matrisian, L.M., and Parks, W.C. (1999). Regulation of intestinal alpha-defensin activation by the metalloproteinase matrilysin in innate host defense. Science *286*, 113-117.

Wing, K., and Sakaguchi, S. (2010). Regulatory T cells exert checks and balances on self tolerance and autoimmunity. Nat Immunol *11*, 7-13.

Wong, G.T., Manfra, D., Poulet, F.M., Zhang, Q., Josien, H., Bara, T., Engstrom, L., Pinzon-Ortiz, M., Fine, J.S., Lee, H.J., *et al.* (2004). Chronic treatment with the gamma-secretase inhibitor LY-411,575 inhibits beta-amyloid peptide production and alters lymphopoiesis and intestinal cell differentiation. J Biol Chem *279*, 12876-12882.

Wu, H.J., Ivanov, II, Darce, J., Hattori, K., Shima, T., Umesaki, Y., Littman, D.R., Benoist, C., and Mathis, D. (2010). Gut-residing segmented filamentous bacteria drive autoimmune arthritis via T helper 17 cells. Immunity *32*, 815-827.

Yamano, T., Nedjic, J., Hinterberger, M., Steinert, M., Koser, S., Pinto, S., Gerdes, N., Lutgens, E., Ishimaru, N., Busslinger, M., *et al.* (2015). Thymic B Cells Are Licensed

to Present Self Antigens for Central T Cell Tolerance Induction. Immunity *42*, 1048-1061.

Yang, Q., Bermingham, N.A., Finegold, M.J., and Zoghbi, H.Y. (2001). Requirement of Math1 for secretory cell lineage commitment in the mouse intestine. Science *294*, 2155-2158.

Yu, X., Harden, K., Gonzalez, L.C., Francesco, M., Chiang, E., Irving, B., Tom, I., Ivelja, S., Refino, C.J., Clark, H., *et al.* (2009). The surface protein TIGIT suppresses T cell activation by promoting the generation of mature immunoregulatory dendritic cells. Nat Immunol *10*, 48-57.

Yusung, S.A., and Martin, M.G. (2015). A Breath of Fresh AIRE Surrounds Paneth Cells and Defensins. Gastroenterology *149*, 22-25.

Zhang, S., Cagatay, T., Amanai, M., Zhang, M., Kline, J., Castrillon, D.H., Ashfaq, R., Oz, O.K., and Wharton, K.A., Jr. (2007). Viable mice with compound mutations in the Wnt/Dvl pathway antagonists nkd1 and nkd2. Mol Cell Biol *27*, 4454-4464.

Zlotogora, J., and Shapiro, M.S. (1992). Polyglandular autoimmune syndrome type I among Iranian Jews. J Med Genet *29*, 824-826.